QUALITY ASSESSMENT OF ANTIMALARIAL MEDICINES SOLD IN THE DEMOCRATIC REPUBLIC OF THE CONGO
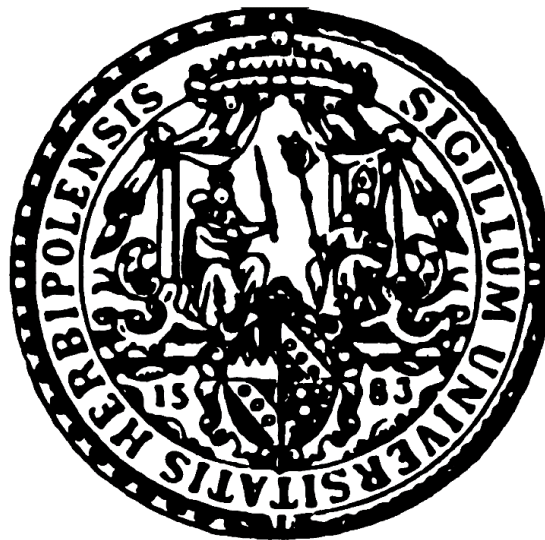
AND

PHYTOCHEMICAL INVESTIGATIONS ON A CONGOLESE *ANCISTROCLADUS* LIANA

DISSERTATION

zur Erlangung des

naturwissenschaftlichen Doktorgrades

der Julius-Maximilians-Universität Würzburg

vorgelegt von

Jean-Pierre Mufusama Koy Sita

aus Kinshasa, Demokratische Republik Kongo

Würzburg 2019

Eingereicht bei der Fakultät für Chemie und Pharmazie am:

…………………………….

Gutachter der schriftlichen Arbeit:

1. Gutachter ……………………………..

2. Gutachter ……………………………..

Prüfer des öffentlichen Promotionskolloquiums:

1. Prüfer ……………………………..

2. Prüfer ……………………………..

3. Prüfer ……………………………..

Datum des öffentlichen Promotionskolloquiums:

…………………………..

Doktorurkunde ausgehändigt am:

Die vorliegende Arbeit wurde in der Zeit von Januar 2014 bis Oktober 2018
am Institut für Organische Chemie der Universität Würzburg angefertigt.

Herrn Prof. Dr. Dr. h.c. mult. Gerhard Bringmann danke ich für
die hervorragende Unterstützung bei dieser Arbeit, die freundliche Atmosphäre und die
exzellenten Arbeitsbedingungen.

Dedicated to my late parents

Contents

Contents

Abbreviations

ACT	artemisinin-based combination therapy
AIDS	acquired immune deficiency syndrome
AL	artemether plus lumefantrine
ANOVA	analysis of variance
API	active pharmaceutical ingredient
ASAQ	artesunate plus amodiaquine
ASSP	artesunate plus sulfadoxine-pyrimethamine
ATR	attenuated total reflection
BGE	background electrolyte
c	concentration
CC	column chromatography
CE	capillary electrophoresis
CGE	capillary gel electrophoresis
CIEF	capillary isoelectric focusing
CITP	capillary isotachophoresis
CQ	chloroquine
CZE	capillary zone electrophoresis
DAD	diode array detection
DC	Dünnschichtchromatographie
DDQ	2,3-dichloro-5,6-dicyano-1,4-benzoquinone
DMEM	Dulbecco's modified Eagle's medium
DMSO	dimethyl sulfoxide
DNA	deoxyribonucleic acid
DRC	Democratic Republic of the Congo
EA	ethyl acetate
ECD	electronic circular dichroism
EOF	electro-osmotic flow
eq.	equivalent
FDA	Food and Drug Administration
FEMA	Flavor and Extract Manufacturers' Association
GC-MSD	gas chromatography in combination with mass-selective detection
GPHF	Global Pharma Health Fund
GRAS	generally recognized as safe

Abbreviations

GSP	general synthetic procedure
HIV	human immunodeficiency virus
HMBC	heteronuclear multiple-bond correlation spectroscopy
HPLC	high-performance liquid chromatography
HRESIMS	high-resolution electrospray ionization mass spectrometry
HSCCC	high-speed countercurrent chromatography
IC_{50}	half maximal inhibitory concentration
ICH	International Council for Harmonization
IR	infrared
λ	wavelength
LC-MS	liquid chromatography coupled to mass spectrometry
LOD	limit of detection
LOQ	limit of quantification
m/z	mass to charge ratio
MEDQUARG	medicine quality assessment reporting guidelines
MEEKC	microemulsion electrokinetic chromatography
MEKC	micellar electrokinetic chromatography
MS	mass spectrometry
MTPA	α-methoxy-α-trifluoromethylphenylacetic acid
MTT	3-(4,5-dimethylthiazol-2-yl)-2,5-diphenyltetrazolium bromide
NDM	nutrient-deprived medium
NIQ	naphthylisoquinoline
NMCP	National Malaria Control Program
NMR	nuclear magnetic resonance
NOESY	nuclear overhauser effect spectroscopy
NRRA	National or Regional Regulatory Authority
OOS	out of specification
PBS	phosphate-buffered saline
PC_{50}	half maximal preferential cytotoxicity
PE	petroleum ether
ROESY	rotating frame nuclear overhauser effect spectroscopy
RSD	relative standard deviation
SD	standard deviation
SDS	sodium dodecyl sulfate

SP	sulfadoxine-pyrimethamine
SSFC	substandard/spurious/falsely-labelled/falsified/counterfeit
TFA	trifluoroacetic acid
TLC	thin-layer chromatography
t_R	retention time
Tris	tris(hydroxymethyl)aminomethane
USA	United States of America
UV	ultraviolet
WHO	World Health Organization

Introduction

Introduction

In the beginning of the 20th century, effective antimicrobial agents became available enabling the control of infectious diseases worldwide.[1] As an example, in 1910 the synthesis of arsphenamine (Salvarsan) by Paul Ehrlich and co-workers led to the successful treatment of syphilis. Later, the development of sulfonamides by Gerhard Domagk and others permitted to enlarge the therapeutic arsenal.[2] Moreover, the discovery of natural products like penicillin and its derivatives opened a new era of antimicrobial chemotherapy and saved thousands of lives during the Second World War.[3,4]

Unfortunately, the effective prevention and treatment of such life-threatening diseases is increasingly impeded by the emergence and spread of resistance (Figure 1).[5,6] When microorganisms are exposed to anti-infective agents, the occurrence of mutations makes them ineffective. As a consequence, the infection may persist, creating prolongation of illness, disability, or even death.[7–9] This leads to increased costs due to longer hospitalization and the need for more intense care.[10,11] Resistance to medicines is inevitable as it appears naturally over time, especially through genetic changes. Moreover, this process is known to be accelerated by the misuse and the overuse of the antimicrobial drugs.[12]
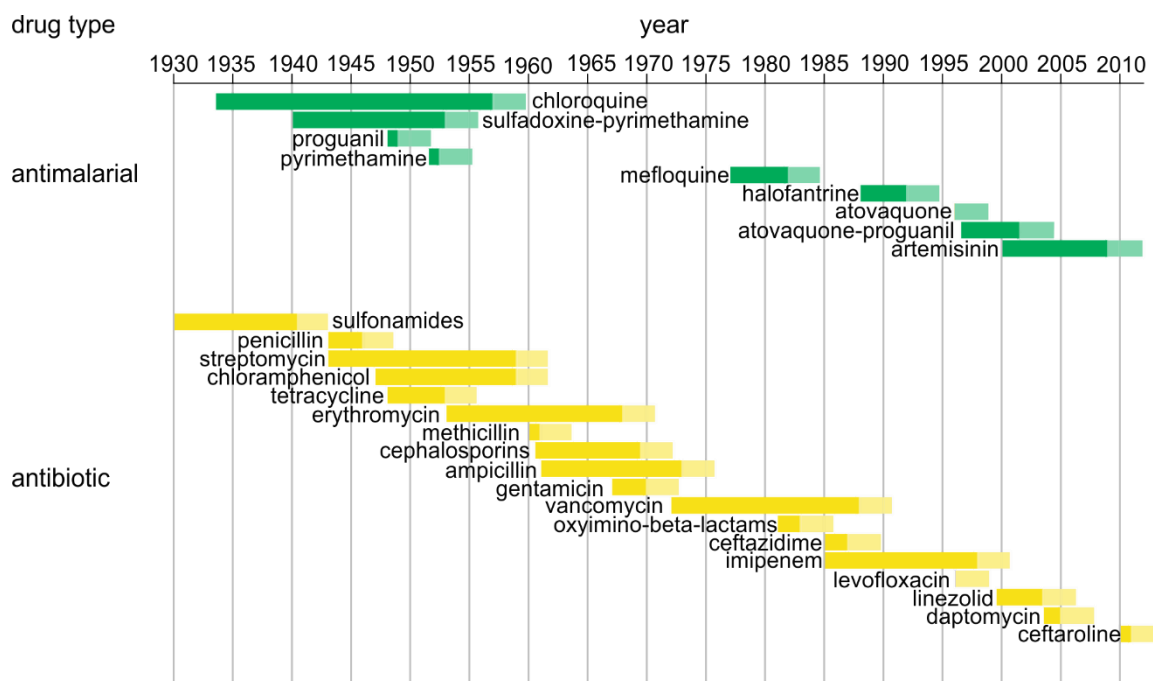
Figure 1. Chronology of the antimalarial and antibiotic discovery and of the subsequent evolution of resistance indicated by the ends of the bars. Reprinted from ref.[6]

For example, carbapenem antibiotics are among the last resorts in the treatment of *Klebsiella pneumoniae* infections. Unfortunately, resistance of *K. pneumoniae* to this useful therapy has meanwhile spread all over the world.[13–17] Likewise, resistance to fluoroquinolone antibiotics

is widespread in *Escherichia coli*, which is responsible for urinary tract infections.[18–20] The failure of the recommended treatment of gonorrhea by using cephalosporin antibiotics of the third generation through resistance has been confirmed in at least ten countries.[21–23] Moreover, likewise widespread is the resistance to first-line drugs to treat infections caused by *Staphylococcus aureus*.[24] Furthermore, the recent detection of resistance to colistin, the last-resort treatment for infections caused by Enterobacteriaceae already resistant to carbapenems, makes diseases caused by such bacteria virtually untreatable.[25]

In the case of tuberculosis, different forms are known, according to the level of drug resistance. One of them is called "multidrug-resistant tuberculosis" as it is resistant to the two most powerful anti-tuberculosis drugs, namely isoniazid and rifampicin. Another form is named "extensively drug-resistant tuberculosis", identified in 105 countries,[26] because it is resistant to at least four compounds of the core anti-tuberculosis therapy, viz. isoniazid and rifampicin, plus any fluoroquinolone and at least one of three injectable second-line drugs (amikacin, kanamycin, or capreomycin).

Increasing levels of resistance of the human immunodeficiency virus (HIV) have important economic implications as second-and third-line regimens are up to 18 times more expensive than first-line drugs.[27] Resistance to antiviral medicines like amantadine and rimantadine (both M2 proton channel blockers) has been reported in Influenza A virus, though the frequency of resistance to oseltamivir, a neuraminidase inhibitor, remains low.[28]

Resistance to previous generations of antimalarial medicines like chloroquine or sulfadoxine-pyrimethamine (Figure 2) in *Plasmodium falciparum* became widespread in the 1950s and 1960s, undermining malaria control efforts and reversing gains in child survival.[29–32] Recently, resistance to artemisinin-based combination therapies (ACTs), the first-line treatment for uncomplicated *P. falciparum malaria*, has been confirmed in the Greater Mekong sub-region in southeast Asia. Patients with artemisinin-resistant infections fully recover after treatment if they received an ACT containing effective partner drug, like lumefantrine and piperaquine. Nevertheless, along the Cambodia-Thailand border, *P. falciparum* has become resistant to almost all available antimalarial medicines.[33–37]

Introduction
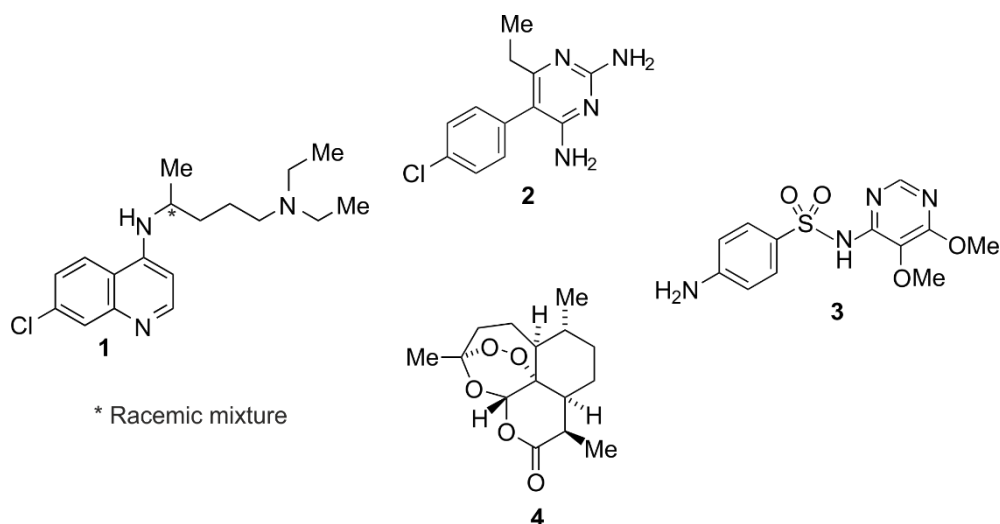
Figure 2. Antimalarial medicines: chloroquine (**1**), pyrimethamine (**2**), sulfadoxine (**3**), and artemisinin (**4**).

On the one hand, greater innovation and investments are required for research and development of new antimicrobial medicines as well as other infectious diseases control tools like vaccines or diagnostic testing systems.[38–41,6] A promising approach to access novel lead structures in the fight against infectious diseases is the analysis of naturally occurring plant-derived compounds, including naphthylisoquinoline alkaloids.[42,43] The latter represent a rapidly growing class of structurally, pharmacologically, and biosynthetically remarkable natural products,[44] exclusively found in lianas of the paleotropical plant families Dioncophyllaceae and Ancistrocladaceae.[45,46] As an example, korupensamine A (**5**) and dioncophylline C (**6**) have shown good to pronounced antiplasmodial activities both in vitro and in vivo (Figure 3).[47,48] Moreover, the Congo Basin has proven to be an important source of *Ancistrocladus* species; among them four have already been taxonomically accepted while others are as yet botanically undescribed.[49,50]
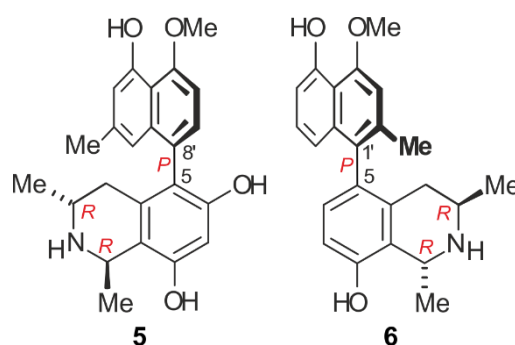
Figure 3. Naphthylisoquinoline alkaloids with antiplasmodial potency *in vitro* and *in vivo*: korupensamine A (**5**), and dioncophylline C (**6**).

On the other hand, it is important to guarantee that existing therapies and products are of assured quality and that the respective medicines are properly used.[51–54] Post-marketing surveillance of medicines does not only comprise the evaluation of the efficacy and safety,[55] but also the compliance to quality standards and specifications, as measured by analytical techniques. In this respect, field studies and surveys help drug regulatory authorities to take evidence-based decisions to improve public health. In the Democratic Republic of the Congo (DRC), data on medicine quality are scarce. In limited settings, there is a real need of developing cost-effective methods like those based on capillary electrophoresis.[56]

Moreover, the safety profile of commonly-used food ingredients like (*R*)-tonkafuranone (**7a**)[57] should be questioned in view of the fact that structurally related compounds such as patulin (**8**) have been found to be both mutagenic and neurotoxic (Figure 4).[58,59] For this purpose, the preparation of **7a** and derivatives and the subsequent determination of their respective toxicities can help to understand whether the shared chemical feature is of concern or not.
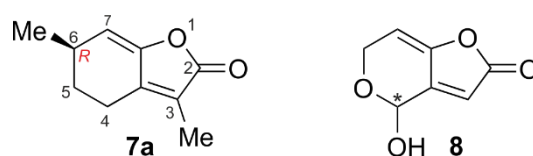
Figure 4. A widely used food ingredient, (*R*)-tonkafuranone (**7a**), and a structurally related compound – but with mutagenic and neurotoxic properties, patulin (**8**).

Introduction

In this context, the aims of the current work were:

- To assess the quality of antimalarial medicines collected in DRC;
- To develop and validate new analytical methods based on capillary electrophoresis (CE) for determining the content and the impurity profile of antimalarial medicines;
- To search for structurally novel compounds with anti-infective potency from a Congolese *Ancistrocladus* plant;
- To isolate and assign the absolute configuration of synthetized (*R*)-tonkafuranone (**7a**) and analogs for the investigation of their structure activity-relationships towards patulin (**8**).

According to these goals, the present work is divided into the following sections:

1) Quality of the antimalarial medicine artemether (**10a**) - lumefantrine (**12**) in eight cities of the Democratic Republic of the Congo;

2) Capillary zone electrophoresis for the determination of amodiaquine (**13**) and three of its synthetic impurities in pharmaceutical formulations;

3) Phytochemical investigations on naphthylisoquinoline alkaloids from the leaves of a botanically yet undescribed Congolese *Ancistrocladus* species;

4) (*R*)-Tonkafuranone (**7a**) and related compounds: Improved synthesis, stereochemical purity in nature, and bioactivities of the pure enantiomers.

I. Specific Background

I.1 Malaria and Poor-Quality Medicines

I.1.1 Malaria

Spread to humans through the bites of infected female *Anopheles* mosquitoes,[60,61] malaria is a tropical disease caused by *Plasmodium* parasites. To date, five species are known, namely *P. falciparum, P. vivax, P. ovale, P. malariae,* and *P. knowlesi*.[62] Two of them are accountable for the majority of malaria cases: Responsible for the majority of malaria-related deaths worldwide*, P. falciparum* is the most prevalent malaria parasite on the African continent,[63] whereas outside this region, *P. vivax* is the leading species.[64,65]

Fever, headache, and chills are the initial symptoms of this acute febrile illness, which, if untreated within 24 h (*P. falciparum*), can progress to a serious disease, often leading to death.[66] Serious anemia, respiratory distress due to metabolic acidosis, cerebral malaria, or multi-organ involvement may occur during severe forms.[67] In endemic areas, the developed partial immunity allows asymptomatic infections to occur.[68] Nearly half of the world's population is at risk of malaria (as per 2016).[69] Although, sub-Saharan Africa hosts most of the cases and deaths, the risk is still present in South-East Asia, Eastern Mediterranean countries, the Western Pacific region, and the Latin and Central Americas (Figure 5).[70,71] Ongoing malaria transmission was reported for 91 countries and areas in 2016.[69] A higher risk of acquiring malaria and developing severe forms of the disease has been reported in infants, children under five years of age, pregnant women, and patients with HIV/AIDS, as well as for non-immune migrants, mobile populations, and travelers.[72,73]

In November 2017, the WHO reported 216 million cases occurring in 2016 and an estimated number of 445,000 deaths.[69] As mentioned above, the African Region, as defined by WHO, carries a high share of the global burden. In 2016, the region was indeed home to 90% of the total number of cases and 91% of the deaths. About 15 countries, including India, account for 80% of the global burden. Approximately 70% of the deaths are related to children under five years of age, particularly in areas with high transmission, although the number of deaths has declined from 440,000 in 2010 to 285,000 in 2016.[69]
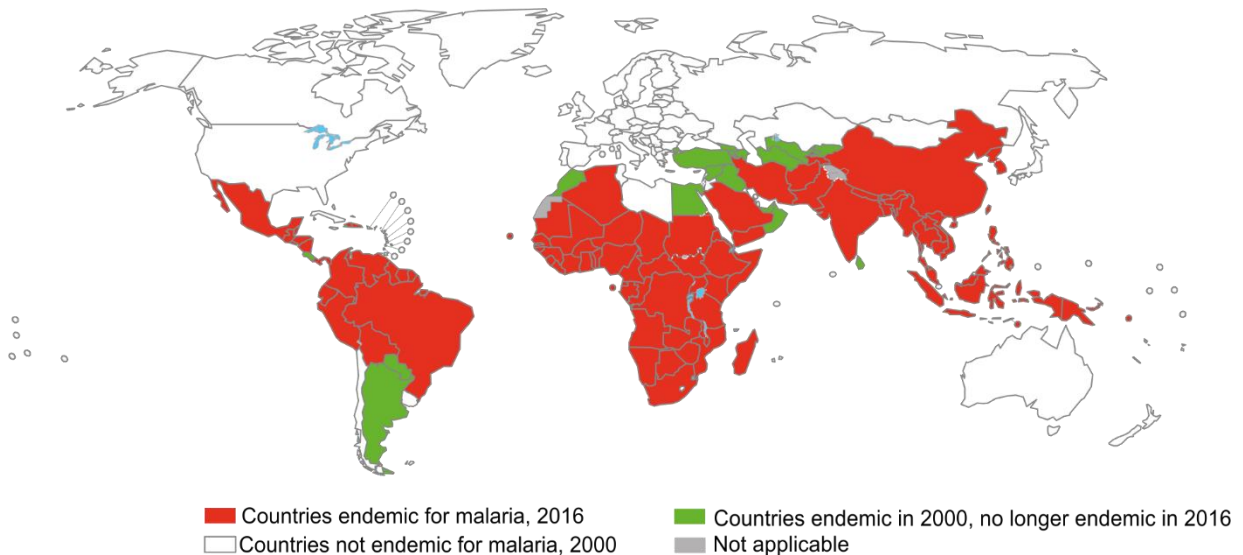
Figure 5. Countries endemic for malaria in 2000 and in 2016. Reprinted from ref.[71]

The most effective way to prevent malaria and to reduce its transmission is through vector control. The WHO recommends protective measures for all population at risk with effective control mechanisms. In a wide range of circumstances, two forms of vector control, namely insecticide-treated mosquito nets and indoor residual spraying, have proven to be efficient.[74] Disease prevention also includes antimalarial medicines: Travelers practice chemoprophylaxis, *e.g.* taking mefloquine, which suppresses the blood stage of the infection.[75] In moderate- to high-transmission areas, pregnant women are recommended to take an intermittent preventive treatment with sulfadoxine-pyrimethamine (SP) at each scheduled antenatal visit after the first trimester,[76] while infants (until one year old) are advised to receive three doses of the same medication during routine vaccinations.[77]

It has been demonstrated that early diagnosis and treatment of the infection do not only allow to reduce the prevalence of the disease and to prevent death, but also to inhibit the transmission.[78,79] The most efficacious treatment available nowadays, for *P. falciparum* malaria, is the artemisinin-based combination therapy (ACT). The WHO recommends that all cases of suspected malaria should be confirmed using parasite-based diagnostic testing, either microscopy or rapid diagnostic test, before administering any treatment.[78] The following ACTs (Figure 6) are recommended by the WHO to treat uncomplicated *P. falciparum* malaria: artemether plus lumefantrine (AL), artesunate plus amodiaquine (ASAQ), artesunate plus mefloquine, dihydroartemisinin plus piperaquine, and artesunate plus sulfadoxine-pyrimethamine (ASSP).

I.1 Malaria and Poor-Quality Medicines

During the first trimester of pregnancy, the treatment recommended by the WHO for uncomplicated *P. falciparum* is the combination of quinine and clindamycin, while uncomplicated *P. vivax*, *P. ovale*, *P. malariae*, or *P. knowlesi* malaria should be treated either with an ACT or with chloroquine in areas with chloroquine-susceptible infections, and only with an ACT in areas with chloroquine-resistant infections.[78] Primaquine, SP, and amodiaquine plus SP are recommended to be used for preventive purposes only.[80,81] For severe malaria, the WHO recommends intravenous or intramuscular artesunate followed by an ACT.[82] If artesunate is not available, artemether is to be preferred to quinine.[83]
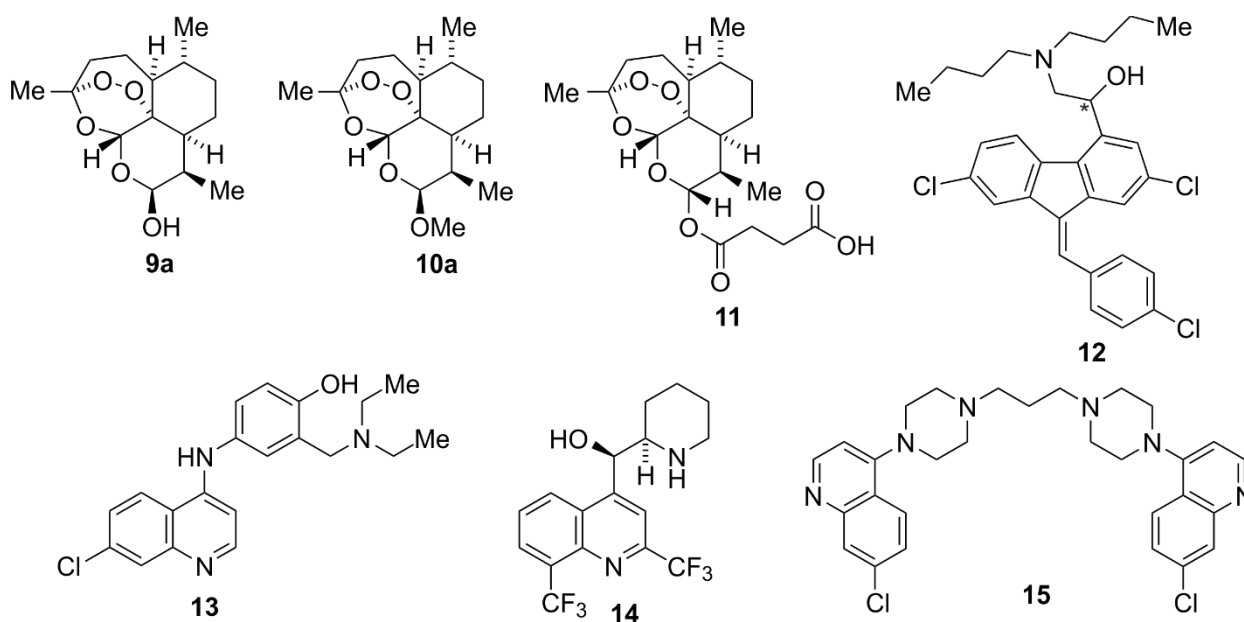
Figure 6. ACT components: dihydroartemisinin (**9a**), artemether (**10a**), artesunate (**11**), lumefantrine (**12**), amodiaquine (**13**), mefloquine (**14**), and piperaquine (**15**).

I.1.2 Poor-Quality Medicines

During the past two decades, different concepts have been utilized to address the threat caused by poor-quality medicines to public health.[84–87] To reflect this complexity, the term *substandard/spurious/falsely-labelled/falsified/counterfeit* (SSFFC) medical products was used by the WHO for a long time. At the 70th World Health Assembly held in 2017, the following definitions were adopted:[88,89]

- *Substandard* medical products (*out of specification*, OOS): "are authorized medical products that fail to meet either their quality standards or specifications, or both".[88] If the lack of compliance by an authorized manufacturer to the quality standards or

specifications due to misrepresentation of identity, composition, or source is deliberate, then the medical product should be considered as *falsified;*[89]

- *Unregistered* (*unlicensed*) medical products: "are those that have not undergone evaluation and/or approval by the National or Regional Regulatory Authority (NRRA) for the market in which they are marketed/distributed or used, subject to permitted conditions under national or regional regulation and legislation".[88]

- *Falsified* medical products: "are those that deliberately/fraudulently misrepresent their identity, composition or source".[88]

The quality of falsified medicines is unpredictable as they may contain an incorrect amount of the active pharmaceutical ingredients (APIs), incorrect ingredients, or even no active ingredients,[90] while substandard medicines often result from poor manufacturing practices or incorrect storage: They may contain the wrong amount of APIs (too much or too little), degraded products, or fail dissolution testing due to wrong formulation, ensuing in a poor oral bioavailability, and, thus, reduced efficacy.[91]

The presence of poor-quality medicines and other medical products in countries and their use by patients undermine the progress towards meeting the *United Nations Sustainable Development Goals*.[92,93] Low-quality products represent a real threat for public health as they may increase the mortality and morbidity of potentially fatal diseases, induce drug resistance and loss of medicine efficacy; patients taking them may also suffer from adverse effects due to unexpected ingredients or components.[87] This problem continues to increase as globalized manufacturing and distribution systems are becoming ever more complex.[94,95] Therefore, the risk of quality deficiencies due to different production processes or incorrect storage during distribution may occur.

Opportunities for poor-quality medicines to be introduced into the supply chain are also triggered by an increasing demand for medicines, vaccines, or other medical products, by poor management of the supply chain, and by the growth of e-commerce.[96,87] According to a recent WHO literature review that included a total of 100 publications reporting on the testing of 48,218 samples of medicines collected from 88 countries, the observed failure rate of tested samples of substandard and falsified medicines in low- and middle-income countries is approximately 10.5%.[95]

I.1 Malaria and Poor-Quality Medicines

A variety of methods from analytical chemistry and other scientific fields have been used to detect poor-quality medicines:[97,98] This includes inexpensive field assays as well as sophisticated laboratory instruments and technologies; detection methods may differ in the type of data (qualitative or quantitative) provided about a medicine sample; methods also vary in the amount of training required for technicians to use them. This comprises the following techniques which are widely used in the field of pharmaceutical quality analysis:[99–110] visual inspection of packaging, colorimetric tests, disintegration and dissolution testing, thin-layer chromatography (TLC), Raman and near-infrared spectroscopy, high-performance liquid chromatography (HPLC), mass spectrometry (MS), nuclear magnetic resonance (NMR) spectroscopy and using capillary electrophoresis (CE).

During visual inspection, the sample under investigation is compared with an authentic product with respect to its packaging and/or its physical characteristics.[111] TLC, by contrast, is a separation technique, in which a mixture is resolved into its constituents by partition between a stationary phase (usually silica gel, alumina, or cellulose) and a mobile phase made up with a solvent or a solvent mixture. Because different analytes migrate the TLC plate at different rates and thus, different distances, the separation is achieved. Thus, TLC is used for the identification of compounds and the determination of their purity. Due to its cost-effectiveness and its applicability in field studies, TLC has widely been used in the detection of falsified and substandard medicines.[97] Infrared (IR) and Raman spectroscopy, on the contrary, measure vibrational energy levels associated with the chemical bonds in a sample. Their potential for rapid, on-site and non-destructive identification of falsified and substandard medicines has been demonstrated.[112,113] Despite the high cost of its equipment and the need for skilled operators, HPLC is still the gold standard in pharmaceutical analysis, due to its high reproducibility, sensitivity, and accuracy for both qualitative and quantitative purposes.[114]

I.2 Capillary Electrophoresis

Introduced in the 1980s, capillary electrophoresis (CE) is an electrophoretic technique with high-speed and high-resolution abilities.[115,116] The instrumentation generally comprises a buffer-filled fused-silica capillary with two buffer reservoirs each equipped with platinum electrodes (Figure 7).[117–120] The outside walls of the fused-silica capillary tube are usually coated with polyimide to assure durability, flexibility, and stability.[121] The sample is introduced at one end and detection arises at the other. A voltage of 5 to 30 kV is applied across the two electrodes; its polarity can be reversed to permit a fast separation of anions.[122–125] An electro-osmotic flow (EOF) is usually created when a high voltage is applied across a fused-silica capillary tube containing a buffer solution; as a result, the migration is toward the cathode. The rate of the EOF is generally greater than the electrophoretic migration velocities of the individual ions and effectively becomes the "mobile-phase pump" of CE. Owing to electro-osmosis, the order of migration is cations, neutrals, and anions.[126]
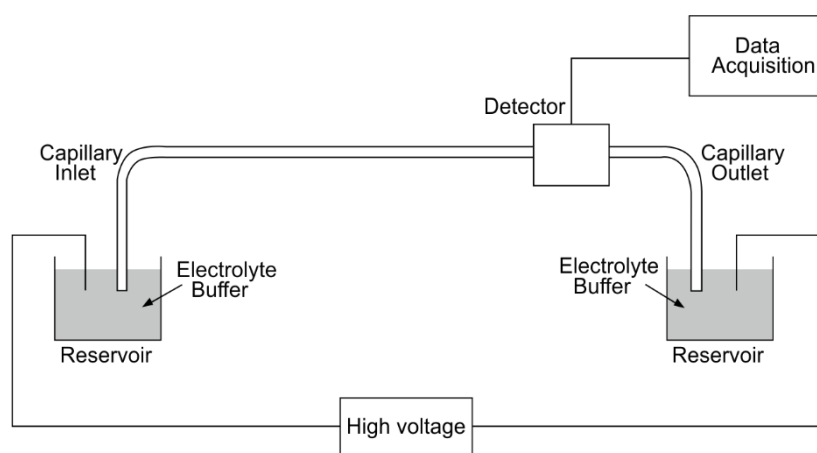
Figure 7. Simplified CE instrumentation. Reprinted from ref.[117]

There are two common sample application techniques, namely the electrokinetic injection and the pressure injection. The first technique uses voltage and the second one vacuum. In both cases, the injected volume is controlled by the duration of the injection.[127,128] Several types of detectors have been reported in the literature:[129–133] spectrometric detection (*i.a.*, by absorption, fluorescence, thermal lens, Raman, chemiluminescence, mass spectrometry), or electrochemical detection (*i.a.*, by conductivity, potentiometry, amperometry). To keep the detection volume on the nanoliter scale or even smaller, detection takes place on-capillary. In this case a small section of the protective polyimide coating is detached from the exterior of the capillary by burning or scratching.[129,130] This section of the capillary then serves as the

detection window. This small path length restricts detection limits. However, the use of small volumes can be beneficial for mass spectrometry detection when compared to HPLC.[134,135]

For analytes that exhibit a low molar absorptivity and that are, thus, difficult to detect without previous derivatization, indirect absorbance detection has been utilized:[136,137] An ionic chromophore is added to the buffer and the detector records a constant signal because of the presence of that substance; it decreases during the passage of an analyte band through the detection window; the analyte is determined from the decrease in absorbance.

Several modes of CE have been reported:[117,138] capillary zone electrophoresis (CZE), micellar electrokinetic chromatography (MEKC), microemulsion electrokinetic chromatography (MEEKC), capillary gel electrophoresis (CGE), capillary isoelectric focusing (CIEF), and capillary isotachophoresis (CITP). In CZE, the separation mechanism is based on differences in the charge-to-mass ratio. It has been applied to the separation of both large and small molecules, including inorganic ions. In CIEF, analytes are separated according to their isoelectric point (pI), using a pH gradient. Its applications comprise the determination of the pI of a protein and the separation of proteins such as immunoglobulins and hemoglobin variants. With respect to CGE, it uses physical or chemical gels to separate macromolecules like DNA and oligonucleotides. In CITP, leading and terminating electrolytes are utilized to resolve ionic compounds. MEKC, by contrast, it employs micelles (surfactants) to separate charged and neutral small molecules, while MEEKC uses microemulsions for the same purpose.

A variety of difficult analytical separation problems have been solved by CE techniques including those regarding inorganic anions and cations, amino acids, catecholamines, drugs, vitamins, carbohydrates, peptides, proteins, nucleic acids, nucleotides, and polynucleotides.[139–141] In pharmaceutical analysis, CE applications cover both achiral and chiral separations, the latter being possible by adding chiral selectors like cyclodextrins.[142,143]

I.3 Naphthylisoquinoline Alkaloids

Naphthylisoquinoline (NIQ) alkaloids represent a class of structurally, pharmacologically, and biosynthetically remarkable natural products with a lot of fascinating facets.[144,44] So far, they have been exclusively found in lianas of the small paleotropical plant families Dioncophyllaceae and Ancistrocladaceae.[45,46] The Dioncophyllaceae family, which only grows in West Africa, consists of three monotypic genera, *Dioncophyllum* (with the only species *D. thollonii*), *Habropetalum* (only *H. dawei*), and *Triphyophyllum* (only *T. peltatum*),[145] whereas the closely related Ancistrocladaceae family has only one genus, *Ancistrocladus*, being present in West, East, and Central Africa as well as in India and Sri Lanka, and in South-East Asia, comprising about twenty accepted species so far (Figure 8).[49]
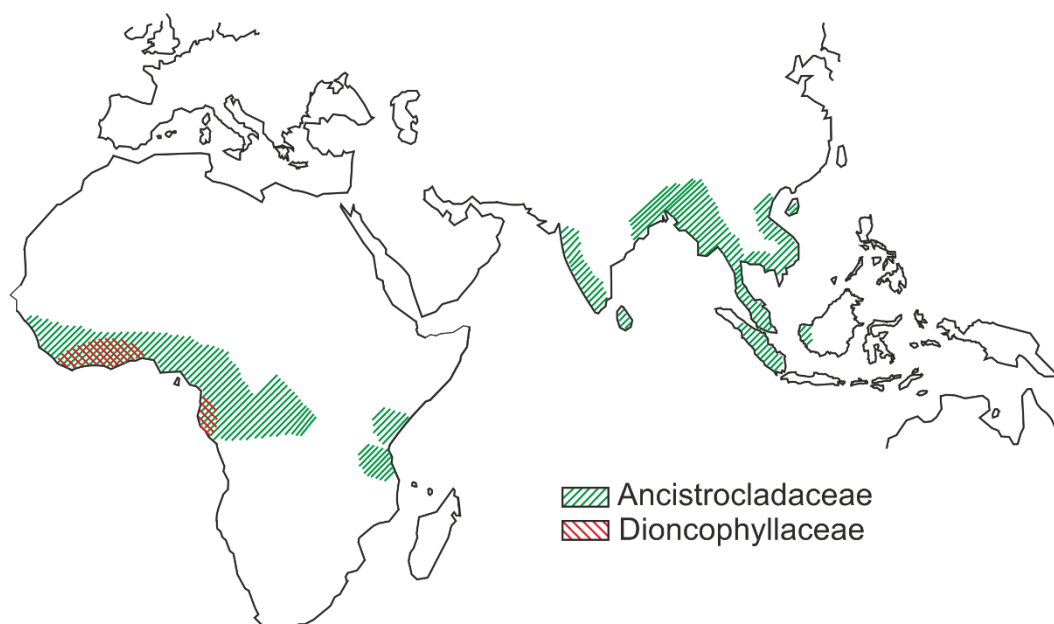
Figure 8. Geographic distribution of Ancistrocladaceae and Dioncophyllaceae plants.[49,145]

As suggested by biomimetic polyketide cyclization reactions and firmly proven by feeding experiments,[146,147] NIQs are exclusively formed from acetate/malonate units and not from aromatic amino acids as described for other isoquinoline alkaloids.[148] Both molecular halves, i.e. the naphthalene and the isoquinoline portions, are formed from joint polyketide precursors.[146,147]

Despite their structural variety, all NIQs have a 4,5-dioxy-2-methylnaphthalene and a 1,3-dimethyl-8-oxy- or -6,8-dioxyisoquinoline (or -di- or -tetrahydroisoquinoline) moiety in common, which may additionally have stereocenters.

18

I.3 Naphthylisoquinoline Alkaloids

In the Dioncophyllaceae plants, NIQs have (*R*)-configuration at C-3, lacking an oxygen function at C-6,[149] while in the South-East Asian and East African Ancistrocladaceae, the respective carbon atoms are (3*S*)-configured and the alkaloids are 6-oxygenated.[84] The West and Central African *Ancistrocladus* species, by contrast, have been found to contain both Dioncophyllaceae and Ancistrocladaceae-type alkaloids, including all possible hybrid forms.[150] Moreover, due to the oxygenation pattern of the two molecular halves, the isoquinoline moiety has three (C-5, C-7, N) and the naphthalene part even four possible coupling positions (C-1', C3', C-6', and C-8'). Thus, twelve different coupling types between the naphthalene and isoquinoline halves are imaginable, of which nine have been found in nature, (Figure 9).[151–159] Also, the steric hindrance next to the axis may drastically vary, resulting in a broad range of different atropisomerization barriers. Furthermore, some of the monomeric NIQs described above were found to be oxidatively coupled to form the corresponding dimers via their naphthalene portion, giving rise to the presence of up to three consecutive stereogenic axes.[160–164]
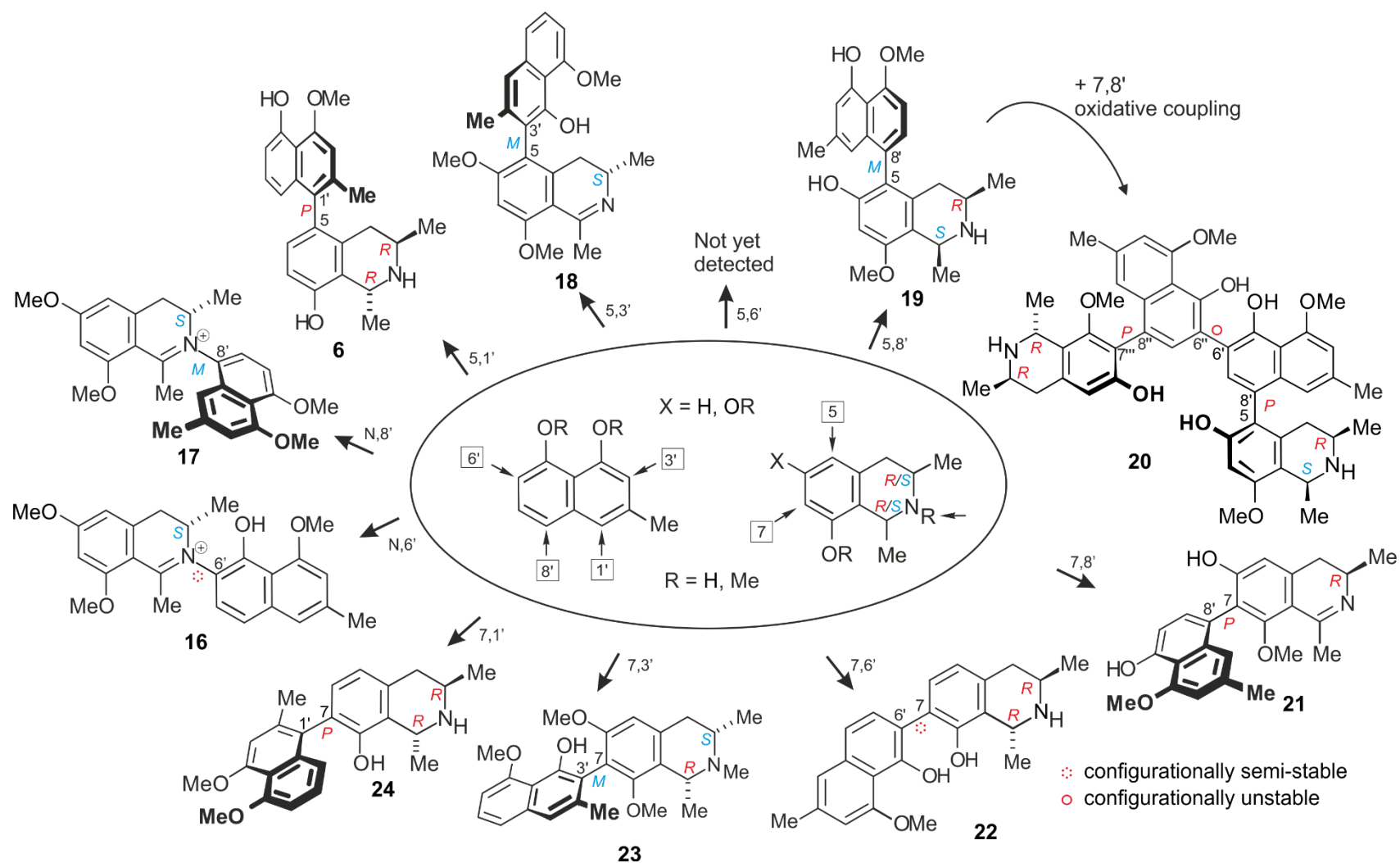
Figure 9. Structural variability of naphthylisoquinoline alkaloids: ancistrocladinium B (**16**), ancistrocladinium A (**17**), dioncophylline C (**6**), ancistrotanzanine A (**18**), ancistrolikokine B (**19**), ealapasamine A (**20**), yaoundamine A (**21**), dioncophylline B (**22**), ancistrotectorine (**23**), and dioncophylline A (**24**).

I.3 Naphthylisoquinoline Alkaloids

For the isolation and structural elucidation of NIQs, a wide diversity of strategies and techniques have been developed.[165,166] Among them, the analytical 'triad' – HPLC coupled to NMR, to tandem mass spectrometry (MS/MS), and to electronic circular dichroism (ECD) – has allowed to establish the steorostructures of novel naphthylisoquinoline alkaloids directly, right from crude extracts.[167–169] Besides conventional chromatography on normal and reversed-phase silica gel, other techniques like high-speed countercurrent chromatography (HSCCC) or ion-exchange chromatography have been reported to be most useful for the preparative isolation of promising alkaloids.[170,171]

The absolute configuration at the stereocenters in the tetrahydroisoquinoline part of NIQs has been assigned by a ruthenium-mediated oxidative degradation procedure, which smoothly transforms the stereocenters at C-1 and C-3 into the amino acids alanine and 3-aminobutyric acid:[172,173] After conversion to the methyl esters and Mosher-type derivatization with the acid chloride of (S)-α-trifluormethylphenylacetic acid, the absolute configuration can be determined by gas chromatography in combination with mass-selective detection (GC-MSD) and comparison with the corresponding derivatives of the authentic amino acids of known configuration. The stereoinformation at C-1 needs to be additionally confirmed by an assignment of the relative configuration at C-1 versus at C-3 by NMR.

The axial configuration relative to stereocenters can be established by optimized long-range NOE and ROE investigations as well as by X-ray structure analysis,[174,175] while the absolute configuration at the axis is usually determined by NOE interactions over the axis in conjunction with the results of the oxidative degradation. Additional proof of this absolute configuration is provided by electronic circular dichroism (ECD) investigations. Furthermore, quantum-chemical calculation of ECD spectra, both for the (M)- and the (P)-atropisomers and comparison of the predicted spectra with the experimental one, has proven to be an efficient alternative to the Exciton Chirality method.[176,177] Moreover, the total synthesis may still provide further valuable information for the structural elucidation; it can also be used to obtain more material of the sometimes scarcely occurring natural products and their structural analogs for biological investigations.[178,179]

The use of several species of the Ancistrocladaceae and Dioncophyllaceae families in folk medicine has motivated further pharmacological studies. The biological evaluations have been focused on the molluscicidal,[180,181] insect larvicidal,[182] antifeedant, and growth-retarding activities,[183,184] and, in recent years, mainly on the antiprotozoal,[48,185–187] antitumoral,[188,189] and antiviral potencies.[190,191]

II. Results and Discussion

II.1 Quality of the Antimalarial Medicine Artemether - Lumefantrine in Eight Cities of the Democratic Republic of the Congo

II.1.1 Introduction

In 2016, the Democratic Republic of the Congo (DRC) and Nigeria together accounted for 35% of the global total of estimated malaria deaths.[69] In the course of that year, malaria was responsible for 38% of morbidity and 35% of mortality in DRC.[192] For the management of uncomplicated *Plasmodium falciparum* malaria, the Congolese National Malaria Control Program (NMCP) has approved both combinations of artesunate-amodiaquine (ASAQ) (since 2005) and artemether-lumefantrine (AL) (since 2012).[193] ASAQ containing products are mainly found in the public sector, while AL pharmaceuticals are mostly distributed by private outlets, which represent the principal suppliers of antimalarial medicines[194] either being produced locally or imported from other African countries, or originating from Asia, Europe, or America.

Because of the central role of antimalarial medicines in the effective reduction of morbidity and mortality related to malaria, their quality must be assured by the manufacturers, under the control of regulatory authorities.[195] Unfortunately, facts on the quality of antimalarial drugs circulating in the pharmaceutical market of DRC were scarce when the present study[196] was designed: One study inspected the quality of chloroquine (CQ), quinine, sulfadoxine-pyrimethamine (SP), and proguanil collected in Bukavu and two villages around, revealing the presence of substandard CQ and SP products;[197] a second report was related to artesunate, dihydroartemisinin, and artemether, likewise collected in Bukavu and describing poor-quality medicines for all types of collected samples;[198] a third survey, regarding chloroquine, quinine, sulfadoxine-pyrimethamine, and mefloquine collected in Goma from the informal market, indicated failures during packaging analysis, dissolution testing, and content determination.[199] None of the three above-mentioned studies were related to the quality of ACT containing products.

In other African countries, however, an improvement of medicine quality has been reported: A survey conducted in Tanzania has revealed a failure rate of only 4.8% for antimalarial drugs collected between 2012 and 2015.[200] A likewise low prevalence of substandard and falsified antimalarial medicines has recently been found in Southern Malawi.[201]

As part of post-marketing surveillance, the present survey[196] aimed to assess the quality of the antimalarial medicine artemether-lumefantrine commercialized in the private pharmaceutical outlets in DRC. This is an extended report of the initial pilot study involving only samples from Kinshasa: In 2012, 18 samples of AL tablets were purchased at six sampling sites, in two licensed and two non-licensed drug outlets, and from two street vendors. The results obtained in the pilot phase revealed evidence of substandard medicines with low API contents (66.7%) and failures in a simple disintegration test (33.3%). In view of these alarming preliminary results, the survey has been then enlarged to 150 samples being collected in eight cities to draw a more representative quality map of these essential medicines in DRC. The results of this survey will be presented and discussed in the following subsections. The need of equipping developing countries with modern analytical techniques such as HPLC to fight against the spread of poor-quality medicines, is also underlined.

II.1.2 Sample Collection

In total, 74 powders for preparing an oral suspension and 76 tablet samples were purchased: The highest number of oral suspension samples was purchased in Mbandaka (18.9%), while the largest number of tablet samples came from Goma (22.4%). In general, the total number of samples per city including tablets and powders for oral suspension was between 9 (Mbuji-Mayi) and 28 (Mbandaka).

During the design of the survey, only the *Medicine Quality Assessment Reporting Guidelines* (MEDQUARG) were available as a proposal.[202] The respective WHO guidelines, which include most of the recommendations of the initial guidelines,[203] were not yet existing. However, many aspects of these guidelines were considered in the methodology, for example conducting the sample collection based on a sampling plan adapted to the respective city; thus, eight out of eleven provincial capital cities were selected as representatives of the northern, southern, eastern, and western parts of the country. In each selected city, the outlets were chosen from the private sector, where the target medicine could mainly be found as stated by a study conducted in Kinshasa and Katanga.[194] In many cities of the country, pharmacies and drug stores are not equally distributed but are concentrated in certain areas where most people purchase medicines. The number of outlets within the city was not reported because the whole city was considered as a single sampling site; nevertheless, samples were obtained from as many outlets as possible.

From the study mentioned above,[194] unlicensed outlets were reported to be the predominant suppliers of the target medicine. Moreover, the pilot study conducted only in Kinshasa in 2012 showed that there was no significant difference in medicine quality between the type of outlets within the private sector. Therefore, this parameter was not considered during the current study. The medications were acquired by a mystery shopper approach, i.e., medicines were requested as being used for patient treatment and not for quality control issues. If different brands were available in an outlet, the seller was asked to give the most commanded one.

II.1.3 Visual Inspection

Based on the information available on the labels, 52.7% of the collected samples were manufactured in India and 28.7% were produced locally (DRC); of the latter, 17.3% were from a single manufacturer, namely New Cesamex from Kinshasa, DRC (Figure 10). The examination also showed that 68% of the samples had shelf-lives of two years and 30% of the samples of three years. Only three Coartem® samples had longer shelf-lives of four (two samples) and five years (one sample) and were labeled as originating from the USA or from China, having the following batch numbers: F2929, F2153, and X1341 (Figure 11). Their unusually long shelf-lives made these three samples suspicious. Thus, they were the first ones to be chemically investigated.
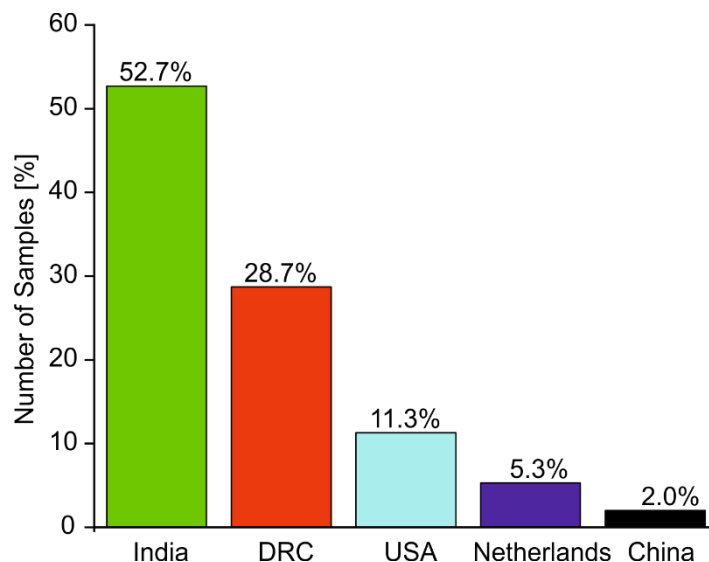
Figure 10. Countries of origin as indicated on the collected samples.
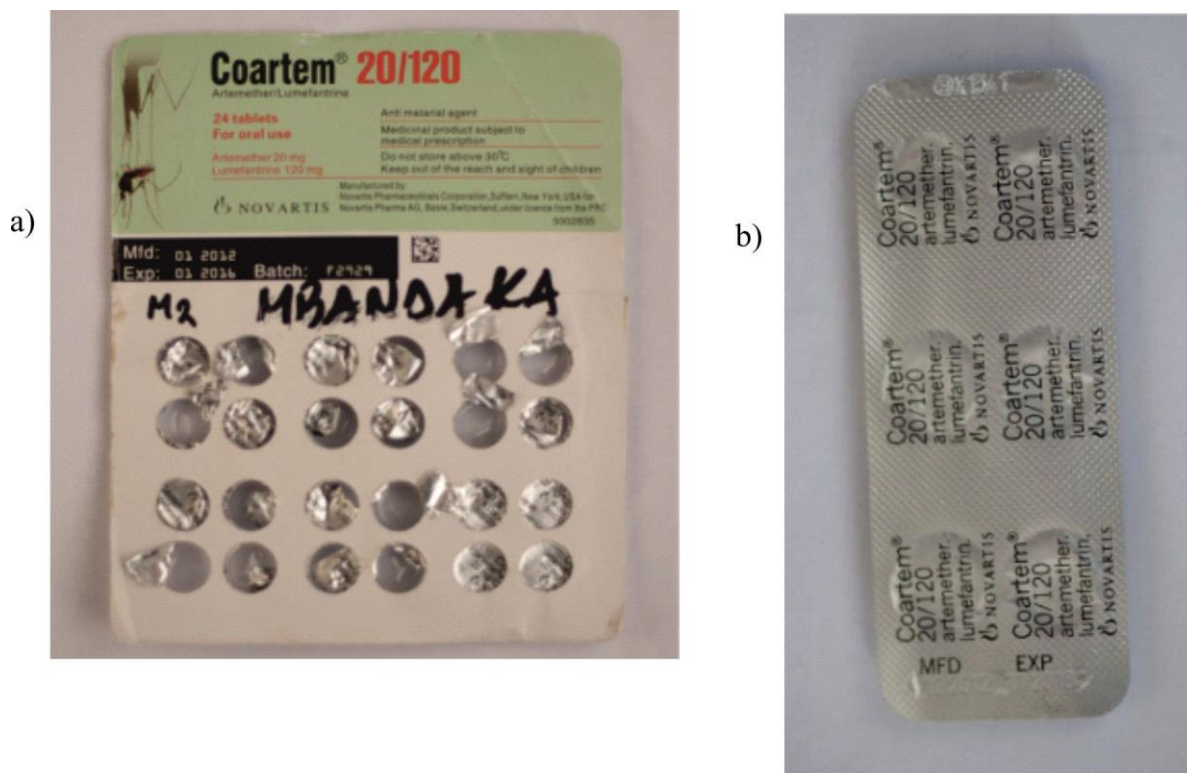
Figure 11. Photos of suspicious samples after visual inspection: a) from Mbandaka, labeled as "Coartem® from the USA"; and b) from Mbuji-Mayi, denoted as "Coartem® from China".

Visual inspection can be a useful screening tool for the detection of poor-quality medicines, particularly when the sample under investigation presents some obvious differences in the packaging or appearance. One of the limitations is that an original specimen from the manufacturer or the regulatory authority is required to allow comparing the suspicious sample with the reference sample. In this study, samples having the same commercial name but collected in different pharmaceutical outlets were compared for inconsistencies.[98,204] As mentioned above, this strategy helped to suspect three Coartem® samples as possibly falsified products. During visual inspection, a sample collected in Matadi was found to already have expired. Still, all collected samples were further investigated as they might hypothetically be procured by a patient with no knowledge of the expiry date.

II.1.4 Analysis by Thin-Layer Chromatography

All 150 samples were subjected to a rapid TLC screening. Table 1 shows that the three suspicious Coartem® samples were the only ones that contained none of the declared APIs; in view of the results from the packaging analysis, they were considered falsified.

II.1 Quality of the Antimalarial Medicine Artemether - Lumefantrine

These samples had been collected in two cities geographically very distant from each other: Mbandaka (north-west) and Mbuji-Mayi (central); they were labeled as produced by the same manufacturer but originated from different manufacturing plants. A sample collected in Matadi showed only one spot corresponding to lumefantrine (**12**). This sample was also considered to be a falsified product.[195]

Table 1. Summary of the TLC results

Town of collection	N° samples	Pass	Fail
Goma	20	20	-
Kikwit	18	18	-
Kinshasa	19	19	-
Kisangani	18	18	-
Lubumbashi	20	20	-
Matadi	18	17	1[a]
Mbandaka	28	26	2[b]
Mbuji-Mayi	9	8	1[b]
Total	150	146	4
Frequency [%]		97.3	2.7

[a] only lumefantrine (**12**) detected.

[b] no active ingredient detected.

Falsified Coartem® samples had previously been discovered in Angola, Ghana, Cameroon, Benin, and Nigeria.[205–208,105] It should be noted that at the end of the year 2013, which corresponds to our sampling period, the WHO published an updated list of four falsified batches of Coartem® circulating in Cameroon.[209] Additionally, as stated by local media in Yaoundé (Cameroon), four batches were concerned by this reported falsification, mainly found in the informal market.[210] They were labeled as manufactured by Novartis Pharmaceuticals Corporation, Suffern, New York, USA for Novartis Pharma AG, Switzerland, with expiry dates between 2011 and 2016. Two of the cited falsified medicines (F2153, F2929) had the same visual characteristics as those collected in Mbandaka.

In general, TLC is a widely used technique for the identification of poor-quality pharmaceutical compounds and finished products and has been applied in numerous quality surveys worldwide.[211]

It is cost-effective, simple, and rapid. In most of the studies conducted in Africa and Asia, the Global Pharma Health Fund (GPHF) Minilab® protocols were used as a semi-quantitative assessment tool.[205,212–214] During the pilot study conducted only in Kinshasa, the results obtained from the Minilab® kit were comparable to those obtained using the assay method of *The International Pharmacopoeia* TLC monograph for identity control of APIs.[215] The latter was therefore considered during the present survey. It allowed a quick chemical analysis of the collected drug samples and gave further proof that the suspicious Coartem® samples contained none of the declared ingredients. Furthermore, another sample was found to contain no artemether when applying these protocols.

II.1.5 Analysis by High-Performance Liquid Chromatography

All samples under investigation were likewise submitted to an in-depth HPLC analysis. Table 2 gives an overview of the results obtained for both artemether (**10a**) and lumefantrine (**12**): The absence of the two APIs was further confirmed in the three falsified Coartem® samples. The lack of artemether was corroborated in the sample from Matadi; in general, the artemether content of the drug samples varied from 0 to 147.3%: four samples had artemether contents below 50% of the indicated value, ten between 50 and 75%, 32 between 75 and 90%, 87 between 90 and 110%, and 17 above 110%; concerning lumefantrine, the contents ranged between 0 and 142.7%: Five samples had contents below 50%, four between 50 and 75%, 23 between 75 and 90%, 110 between 90 and 110%, and eight above 110%.

During the experiments, it was found that the sonication time used for preparing the sample solutions is a most critical parameter with respect to precision and accuracy of the respective assay results. Using a sonication time shorter than 120 min resulted in a very high intra-individual deviation of the respective contents of more than 20%. Thus, different sonication times were evaluated (30, 60, and 120 min) and a duration of 120 min was eventually chosen to ensure complete extraction of the APIs from the tablet or from the powder for oral suspension matrices.

II.1 Quality of the Antimalarial Medicine Artemether - Lumefantrine

Table 2. Summary of the HPLC-UV assays; contents in %.

Country of origin	Formulation	Artemether (**10a**)			Lumefantrine (**12**)		
		x < 90	x > 110	90 ≥ x ≤ 110	x < 90	x > 110	90 ≥ x ≤ 110
China	T	1	-	2	1	-	2
	P	-	-	-	-	-	-
DRC	T	-	1	11	-	1	11
	P	12	3	16	16	1	14
India	T	7	1	36	-	-	44
	P	18	8	9	12	6	17
Netherlands	T	-	-	-	-	-	-
	P	6	-	2	1	-	7
USA	T	2	4	11	2	-	15
	P	-	-	-	-	-	-
Totals		46	17	87	32	8	110
Frequency [%]		30.7	11.3	58	21.3	5.3	73.3

T: tablet. P: powder for oral suspension. x: the amount of the API determined relative to the amount stated on the packaging.

Moreover, HPLC-UV analysis permitted classifying the samples by their chromatographic impurity profiles: Apart from the peaks corresponding to the APIs, i.e., artemether (**10a**) and lumefantrine (**12**), 15 (10%) and 28 (18.7%) samples had two and three additional peaks, respectively, eluting near the peak of artemether (**10a**) (Figure 12).
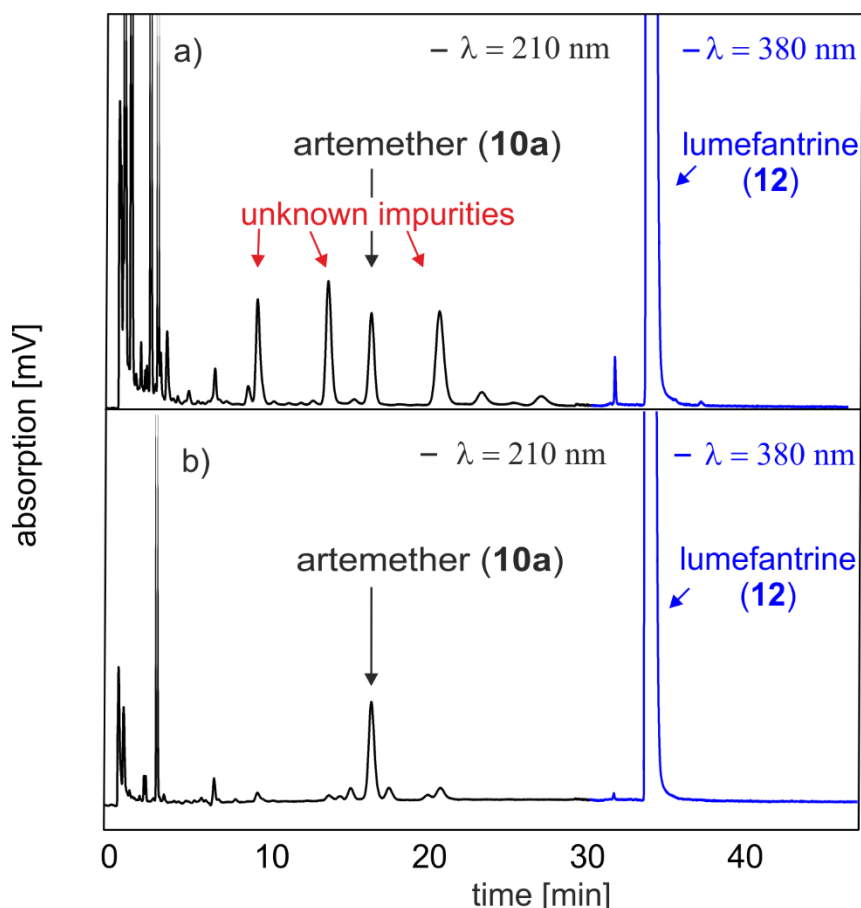
Figure 12. HPLC chromatograms of artemether (**10a**) and lumefantrine (**12**) fixed-dose combination: a) a typical drug sample with unknown impurities; and b) reference substances.

The presence of these peaks might be due to impurities in APIs and/or in the excipients, or because of degradation products formed during the manufacturing process and/or due to inadequate storage conditions. As these impurities can affect efficacy and safety of the pharmaceutical products or, in the case of potentially toxic by-products, might even impose an additional danger, these compounds inevitably must be monitored and chemically identified.[216]

To identify the compounds underlying these additional peaks, two approaches can be considered: (1) spiking experiments or (2) the isolation from the authentic drug sample. The first approach uses commercially or synthetically available reference compounds, which, when added to the authentic drug sample, produce an increase in the peak area or height. Comparison of the ultraviolet and mass spectra gives further evidence of the chemical identity. The second approach, though time consuming and tedious, is often the only option to fully characterize an unknown compound.[217,218]

Considering the first approach, the reference compounds for the putative impurities were chosen based on a study[219] dealing with a stability-indicating HPLC assay for artemether in a powder for oral suspension: The analyzed compounds were α-artemether (**10b**), artemisinin (**4**), dihydroartemisinin (**9**), methyl paraben (**25**), and propyl paraben (**26**). With respect to their relative retention times (Figure 13) in comparison to artemether, α-artemether (**10b**) and artemisinin (**4**) seemed to be good candidates to be responsible for two of three additional peaks representing the impurities in the chromatogram of the AL drug samples. By spiking experiments with an authentic drug sample, only α-artemether (**10b**) co-eluted with one of the three peaks (Figure 14).
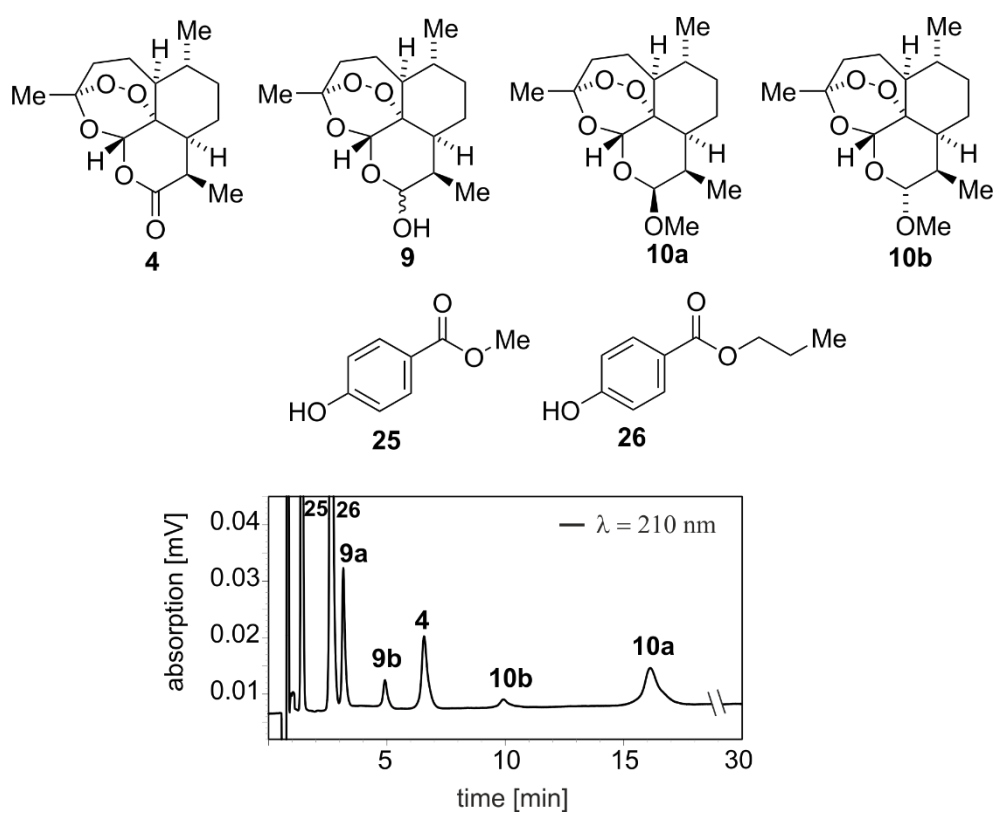
Figure 13. Chromatogram of artemether (**10a**), α-artemether (**10b**), artemisinin (**4**), dihydroartemisinin (**9a** and **9b**), methyl paraben (**25**), and propyl paraben (**26**).
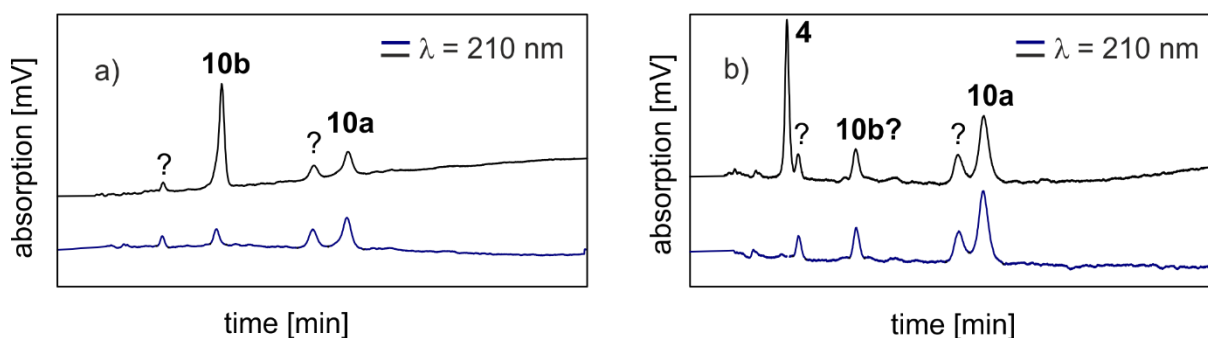
Figure 14. Overlaid chromatograms of an authentic drug sample containing additional peaks (in blue) and the same authentic drug sample (in black) spiked with: a) α-artemether (**10b**); and b) with artemisinin (**4**).

Although HPLC requires a laboratory with sophisticated equipment, which might not always be available in low- and middle-income countries, it is still the gold standard in pharmaceutical analysis[211,220] and offers several advantages such as high selectivity, high sensitivity, high accuracy, and high precision. Using a slightly modified version of the method described in the monograph of *The International Pharmacopoeia*,[215] HPLC-UV analysis permitted to confirm all the suspected cases, i.e., samples with only one or none of the two declared ingredients, and to discriminate substandard from good-quality medicines. Among the substandard products, it was also possible to identify those containing additional undesired unknown impurities.

II.1.6 Analysis by Liquid Chromatography - Mass Spectrometry

HPLC analysis in combination with diode array detection (HPLC-DAD) and MS investigations (LC-MS) clearly revealed that the online ultraviolet and mass spectra of the assumed compound in an authentic drug sample had different profiles compared to the ones of α-artemether (**10b**) in contrast to the above assumption based on the spiking experiment.

Attempts to isolate the additional compounds from a drug sample using preparative HPLC with a gradient elution on a C18 column gave three fractions. LC-MS measurements on the isolated fractions and selected drug samples showed molecular weights correlated to that of lumefantrine (**12**), viz., *m/z* = 406, 420, and 436, which correspond to compounds already reported in the literature (Figure 15).[221] By-products related to the chemical synthesis of lumefantrine (**12**) have also been found in AL drug samples collected in Nigeria.[222]
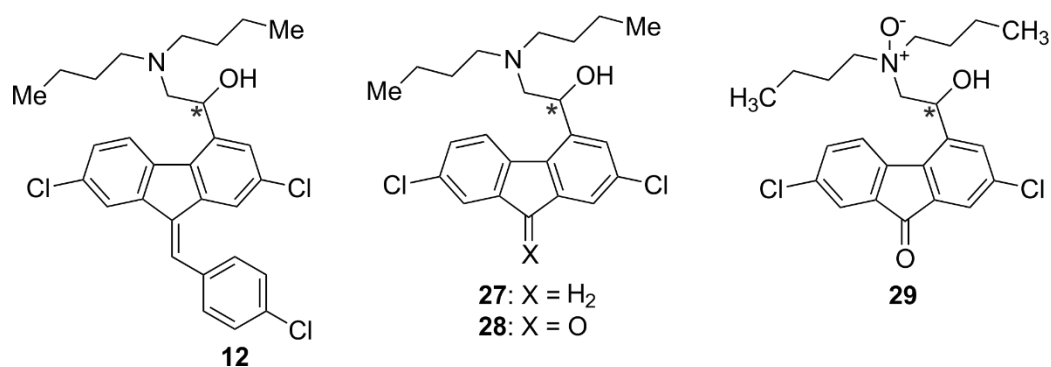
Figure 15. The antimalarial medicine lumefantrine (**12**) and three related compounds **27**, **28**, and **29** found in an authentic drug sample (* probably in a racemic mixture).

II.1.7 Comparison with Other Studies

Although different sampling methodologies and sample sizes have been applied in medicine quality surveys conducted in Africa, the occurrence of falsified products obtained in this study (2.7%) is close only to that from Nigeria (1.2%)[207] or Gabon (0.5%).[214] Some surveys have even revealed a zero rate of falsified ACTs in Ghanaian and Tanzanian markets.[223,224] These low values should encourage health authorities of other countries in Africa and Asia that it is feasible to reinforce the regulatory systems despite the limited settings and infrastructures. However, the failure rates of substandard medicines (42% for artemether (**10a**) and 26.7% for lumefantrine (**12**) and, considering both APIs from the same sample, giving a failure rate of 46.7%) found here were quite high when compared to other medicine quality surveys.[207,224,223] A study in Ghana has reported a rate of 35% of substandard ACTs,[224] whereas other studies have stated rates of 6.8% and 12.1% of substandard ACTs in Nigeria and in Tanzania, respectively.[207,223] A recently published study has shown a failure rate of 62% for AL powders for oral suspension supplied by private pharmaceutical wholesalers in Kinshasa.[225] These dissimilarities could be explained by the sample collection techniques and the analytical procedures used, but also by the drug legislation and the law enforcement policies, which differ from one country to another.[226] An improved quality control system could reduce the number of falsified and substandard medicines as it has recently been shown in Tanzania.[227]

II.1.8 Limitations of the Study

Due to a very restricted number of individual dosage units originating from one distinct batch, evaluations of galenic properties such as dissolution testing or the determination of content uniformity were not performed. Yet, a poor galenic quality of the respective samples regarding dissolution could be anticipated as prolonging the sonication time during sample preparation led to a significantly higher degree of extraction of the respective active ingredients from the matrices. Moreover, the current study is limited to a specific sector of the medicine supply system, viz. only to private outlets in major cities.

II.1.9 Conclusion

In the context of post-marketing surveillance supporting public-health authorities to take evidence-based decisions to fight the spread of poor-quality medicines, the present study was conducted to assess the quality of antimalarial artemether-lumefantrine (AL) medicines circulating in the Democratic Republic of the Congo (DRC). In total, 150 samples of AL-containing products were collected from private pharmaceutical outlets in eight main cities: Goma, Kikwit, Kinshasa, Kisangani, Lubumbashi, Matadi, Mbandaka, and Mbuji-Mayi. These drug samples were successively analyzed by visual inspection, TLC, and HPLC following the protocols described in *The International Pharmacopoeia*.[215] Of the 150 collected samples, three (2%) failed the visual inspection as they had shelf-lives different from those of other samples with the same brand name. Four samples (2.7%) did not pass the TLC test as they contained only one or even none of the two declared active pharmaceutical ingredients (APIs). HPLC assays showed that 46 (30.7%) samples had artemether (**10a**) contents below 90% and 17 (11.3%) above 110% of the content claimed on the label. For lumefantrine (**12**), 32 (21.7%) samples had contents below 90%, and eight (5.3%) had contents above 110% of the indicated content. Although the rate of totally falsified products was quite low (2.7%), found only in two of the eight investigated cities, the prevalence of substandard medical products was unacceptably high in all cities, exhibiting an overall failure rate of 46.7%. These findings should urgently have consequences to control this phenomenon: the training in simple detection techniques for health professionals, i.e., pharmacists, medical doctors, and nurses; the awareness of the population to the danger of poor-quality medicines; the reinforcement of medicine regulation; and the acquisition of laboratory facilities including modern technique equipment, at least at a national level.

II.2 Capillary Zone Electrophoresis for the Determination of Amodiaquine and Three of its Synthetic Impurities in Pharmaceutical Formulations

II.2.1 Introduction

Amodiaquine (**13**), a 4-aminoquinoline derivative, is among others a commonly-used antimalarial medicine in co-formulation with artesunate (**11**) as a first-line treatment of uncomplicated *Plasmodium falciparum* malaria, where it is the major constituent usually present in a ratio of 2.7 to 1 (amodiaquine/artesunate).[228,229,78] Due to the different intensities in UV absorption, it is challenging to simultaneously analyze amodiaquine (**13**) and any artemisinin derivatives, in particular when it comes to impurity profiling. Therefore, most of the available analytical methods have been designed either for the one or for the other agent. As an example, *The International Pharmacopoeia*[215] describes methods both for content determination of the main component and for related compounds in amodiaquine tablets, the first utilizing HPLC and the second one TLC, with a detection limit of 0.5%.

For decades, amodiaquine (**13**) has been obtained by chemical synthesis and consequently can contain organic impurities related to that synthesis, such as 4,7-dichloroquine (**30**), 4-aminophenol (**31**), or 4-[(7-chloroquinolin-4-yl)amino]phenol (**32**), which are starting materials or intermediate products in the production of **13**.[230] Nevertheless, none of the existing compendial protocols[215] describes the separation or the quantitative analysis of specified amodiaquine-related compounds. Reported generic methods have also included *N*-deethylamodiaquine (**33**), which is the pharmacologically active agent being formed by in vivo *N*-deethylation of amodiaquine (**13**) (Figure 16).[231,232]
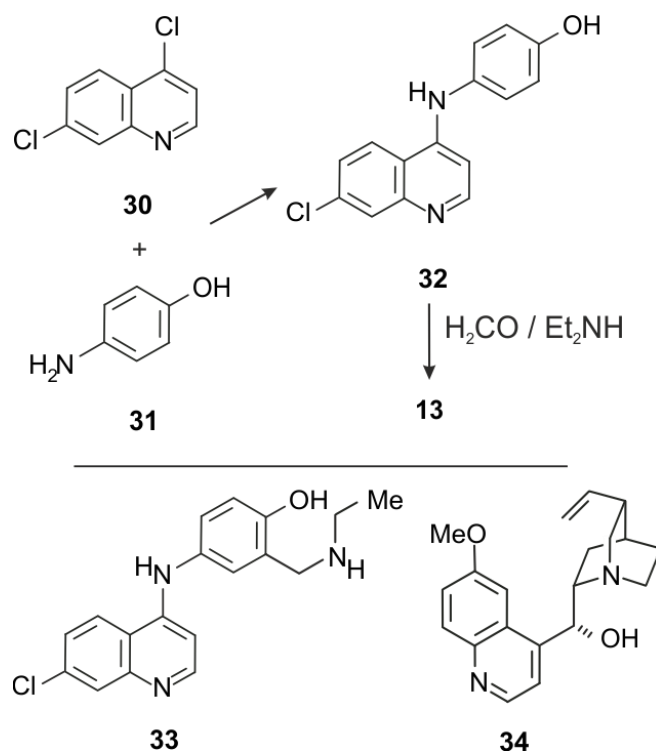
Figure 16. Synthesis of amodiaquine (**13**)[230] and chemical structures of 4,7-dichloroquinoline (**30**), 4-aminophenol (**31**), 4-[(7-chloroquinolin-4-yl)amino]phenol (**32**), *N*-deethylamodiaquine (**33**), and quinine (**34**).

As mentioned earlier, capillary electrophoresis (CE) is an alternative technique, orthogonal to HPLC, providing high efficiency. Furthermore, only small samples are required, there is a low consumption of solvents, and no expensive columns with special modifications of the stationary phase are needed. Given the urgent demand of applying modern analytical techniques in developing countries, the above features render CE an attractive and cost-effective technology for medicine quality assessment and thus, for the fight against the spread of falsified and substandard medical products in laboratories with limited settings.[111,97,227] A low-cost CE instrument has recently been designed and it is suitable of being used in tropical environments.[233,104]

The current chapter will present and discuss the results from the development of a simple electrophoretic method using capillary zone electrophoresis (CZE) for the simultaneous separation of amodiaquine (**13**) and three of its anticipated impurities, **30**–**32**. The new method was validated for both content determination of the main component and impurity profiling following the guideline Q2(R1) of the *International Council for Harmonization* (ICH)[234] and successfully applied to determine the quality of drug samples collected in DRC.

The results of the quantitative analysis for content determination were compared to those obtained with the HPLC method described in *The International Pharmacopoeia*. Of note, this is the first report on a CZE method for the impurity profiling of amodiaquine (**13**) in pharmaceutical formulations.[235]

II.2.2 Method Development

In the recent literature,[236,237] two MEKC methods have been reported for the simultaneous analysis of amodiaquine (**13**) and artesunate (**11**) in pharmaceutical formulations. One uses a 25 mM borate buffer at pH 9 and 30 mM of sodium dodecyl sulfate (SDS);[236] the other one utilizes a 10 mM phosphate buffer at pH 6.6 with 30 mM SDS and 36% of acetonitrile (v/v), operating at a capillary temperature of 29 °C.[237]

Initial experiments showed that none of them was appropriate for concurrently determining **13** and the impurities **30**−**33** since no separation could be attained. Several background electrolytes (BGEs) were tested to accomplish this objective, *e.g.*, phosphoric acid adjusted with NaOH, triethanolamine, Tris[104,238] (all phosphate buffers with pH values ranging from 2 to 7 and buffer concentrations ranging from 25 to 100 mM), or sodium phosphate. The latter provided better resolution values between critical pairs, *viz.*, amodiaquine (**13**) and 4-aminophenol (**31**) or **13** and 4-[(7-chloroquinolin-4-yl)amino]phenol (**32**), within a reasonable analysis time of 20 min. Details on the method development using this buffer system are described in the following subsections. A detection wavelength of 220 nm was chosen because most studied analytes, especially **30** and **31**, displayed a good UV absorption at low concentrations, allowing an appropriate method sensitivity.

II.2.2.1 Influence of Buffer Concentration and pH Value Changes

Four molarities of the sodium phosphate buffer (25, 50, 75, and 100 mM) were evaluated, each at a pH range from 4.6 to 7.0, including 5.0, 5.4, 5.8, 6.2, and 6.6. When an artificial mixture of amodiaquine (**13**), the related compounds **30**−**32**, and the active metabolite of **13**, *N*-deethylamodiaquine (**33**), as well as quinine (**34**) used as internal standard, was analyzed in the ratio of 5:3:1:1:1:1 (w/w), a baseline separation of all analytes at pH values of 4.6 and 5.0 was obtained (Figure 17A). Unfortunately, the resolution values were not high enough for the desired compound ratio (solution containing 1.0 % of each impurity) (Figure 17B). Since *N*-deethylamodiaquine (**33**) does not represent a related compound originating from synthesis (Figure 15), it was excluded from further method development.
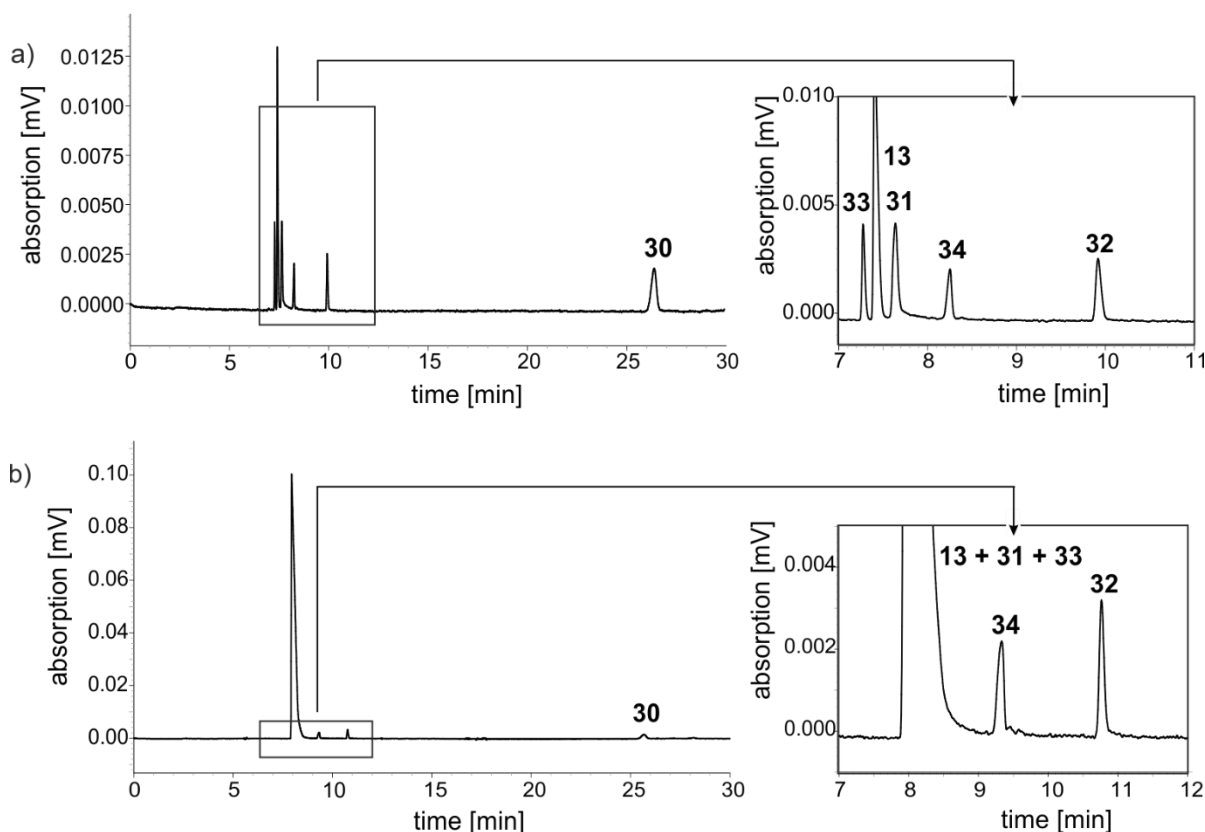
Figure 17. Representative electropherograms of *N*-deethylamodiaquine (**33**), amodiaquine (**13**), 4-aminophenol (**31**), quinine (**34**), 4-[(7-chloroquinolin-4-yl)amino]phenol (**32**), and 4,7-dichloroquinoline (**30**), recorded during initial method development. Ratio of the analytes: 1:5:3:1:1:1 (w/w) in a) and of 1:100:3:1:1:1 in b). Background electrolyte: 50 mM sodium phosphate pH 4.60; applied voltage: +20 kV; temperature: 25 °C.

Yet, a baseline separation of an artificial mixture of amodiaquine (**13**), impurities **30−32**, and the internal standard quinine (**34**) was successfully achieved working at pH values between 5.8 and 6.6. As shown in Table 3, the pH value of 6.2 gave the best resolution values between critical pairs (**13** *versus* **32** and **32** *versus* **34**). As outlined in Table 3, the buffer concentration of 100 mM was the most appropriate one as compared to 25, 50, and 75 mM. Under these conditions (pH 6.2, 100 mM), it was even possible to separate the above-mentioned mixture from chloroquine (**1**), which can thus be used as an alternative internal standard or which might be present in a sample by deliberate substitution of the active ingredient.

II.2 Capillary Zone Electrophoresis for the Determination of Amodiaquine

Table 3. Influence of buffer concentration and pH value [voltage: 20 kV, temperature: 25 °C]

Resolution	Buffer concentration [pH = 6.2]				pH value [buffer conc. = 100 mM]			
	25 mM	50 mM	75 mM	100 mM	5.8	6.2	6.6	7
R_s 1 (cpd. **13/32**)	na	4.8	5.2	6.8	6.2	6.8	4.2	na[a]
R_s 2 (cpd. **32/34**)	na	1.9	2.4	3.4	2.5	3.4	2.2	na
R_s 3 (cpd. **34/31**)	na	12.2	14.1	19.4	5.3	19.4	21.8	na
R_s4 (cpd. **31/30**)	na	9.4	9.4	11.3	18	11.3	3.8	na
Migration time of last peak (min)	10.3	11.7	10.9	13.8	12.1	13.8	10.5	10.7

[a] not applicable due to bad peak shape.

II.2.2.2 Influence of Voltage and Separation Temperature

The above-described tests were performed at a voltage +20 kV and a temperature of 25 °C. Table 4 shows the influences due to changes in these two critical parameters; further experiments were carried out at voltages of 25 and 30 kV and at temperatures of 20 and 30 °C. Considering the resolution values between critical pairs − amodiaquine (**13**) versus 4-[(7-chloroquinolin-4-yl)amino]phenol (**32**) and 4-[(7-chloroquinolin-4-yl)amino]phenol (**32**) versus quinine (**34**) − the analysis times, and the resulting currents, the voltage and the capillary temperature were maintained at the initial values of +20 kV and 25 °C.

Table 4. Influence of temperature and voltage (100 mM sodium phosphate at pH 6.2)

Resolution	Running temperature [voltage = 20 kV]			Running voltage [temperature = 25 °C]		
	20 °C	25 °C	30 °C	20 kV	25 kV	30 kV
Rs 1 (cpd. **13/32**)	8	6.8	6.3	6.8	6.9	na[a]
Rs 2 (cpd. **32/34**)	4.1	3.4	3	3.4	3.5	na
Rs 3 (cpd. **34/31**)	19.6	19.4	20	19.4	20.6	na
Rs 4 (cpd. **31/30**)	15.7	11.3	9.2	11.3	11.6	na
Migration time of the last peak (min)	16.4	13.8	11.7	13.8	11	na

[a] not applicable due to current leakage.

Consequently, the optimal conditions were as follows: a 100 mM sodium phosphate buffer at a pH value of 6.2 as BGE, applying a voltage of +20 kV, a temperature of 25 °C, using a fused-silica capillary, and a detection wavelength of 220 nm. The analysis time was as short as 20 min, with the longest migration time being 13.2 min for the last peak (Figure 18A). Under these conditions, the generated current was 46.8 µA. Moreover, the resolution of 4-[(7-chloroquinolin-4-yl)amino]phenol (**32**) and quinine (**34**) was used as a system suitability criterion because of its lowest value of 3.4 (Figure 18A).
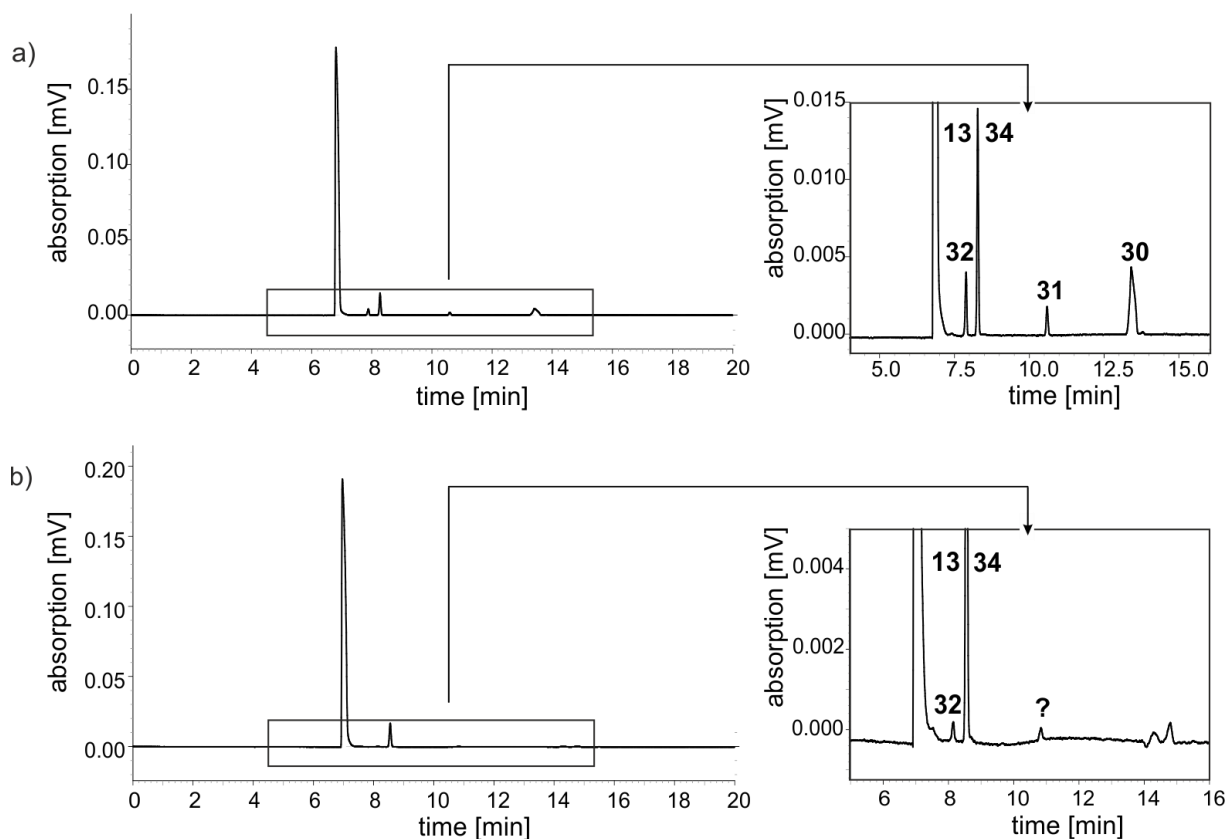
Figure 18. Electropherograms recorded using the optimized method conditions (background electrolyte: 100 mM sodium phosphate pH 6.2; voltage: +20 kV; temperature: 25°C): a) Electropherogram of an artificial mixture of amodiaquine (**13**) containing related compounds 4-[(7-chloroquinolin-4-yl)amino]phenol (**32**), 4-aminophenol (**31**), and 4,7-dichloroquinoline (**30**) at an acceptance limit of 0.5% and quinine (**34**) as the internal standard; resolution mean values (n = 6): **13** *versus* **32** (6.8 ± 0.6), **32** *versus* **34** (3.4 ± 0.4), **34** versus **31** (19.5 ± 1.6), **31** *versus* **30** (11.7 ± 0.9); and b) Electropherogram of a real-drug sample (Sunat-A®) containing 5 mg mL^{-1} of amodiaquine (**9**) with quinine (**34**) as the internal standard; related compound **32** and an unknown impurity (denoted as "?") were found applying a detection wavelength of 220 nm.

II.2.3 Method Validation

II.2.3.1 Content Determination of the Main Component

Specificity of the developed method for the content determination was proven by the fact that no additional signal was found in the real-drug sample solutions (with or without artesunate) when compared to the standard solution. When analyzing samples containing artesunate, a corresponding peak was not detectable. This can probably be attributed to the low amount of the compound, the lack of a suitable chromophore, or incomplete extraction during sample preparation.

Evaluation of linearity for amodiaquine (**13** for the structure, see Table 7) during content determination was performed by plotting the corrected peak area ratios against quinine (**34**) as the internal standard in the concentration range of 0.2–0.6 mg mL^{-1}, yielding a linear relationship. The regression curve followed the equation $y = 0.036x + 0.007$ ($R^2 = 0.9990$). The statistical evaluation using a lack-of-fit ANOVA (analysis of variance) test indicated that the model passed the test with F_{calc} (0.09), which was lower than F_{tab} (3.71) at a 95% significance level.

The percentage values of accuracy for the determination assay of amodiaquine (**13**) by the proposed CZE method are summarized in Table 5. The recovery ranged from 98.1 to 98.4%, indicating that the method was accurate. The intra- and inter-day precision data for **13** are presented in Table 6. The values were calculated by applying the mean corrected peak area ratio to the internal standard (IS), expressed in terms of relative standard deviation (% RSD) and were found to range from about 1.4 to 3.0%, suggesting that the method had an adequate level of precision for the quantitation of **13**.

Table 5. Accuracy data for 4,7-dichloroquinoline (**30**), 4-aminophenol (**31**), 4-[(7-chloroquinolin-4-yl)amino]phenol (**32**), and amodiaquine (**13**)

Studied compound	Level [%]	Added [mg mL^{-1}]	Observed [mg mL^{-1}]	Accuracy [%]	SD	RSD [%]
30	0.5	0.025	0.024	97.78	0.02	1.36
	1.0	0.050	0.050	99.17	0.06	1.89
	1.5	0.075	0.070	92.73	0.23	4.85
31	0.5	0.025	0.019	77.57	0.01	3.52
	1.0	0.050	0.042	83.84	0.03	3.32
	1.5	0.075	0.059	79.08	0.03	2.40
32	0.5	0.025	0.027	108.81	0.01	0.90
	1.0	0.050	0.050	100.15	0.04	1.79
	1.5	0.075	0.072	96.39	0.03	0.94
13	80	0.32	0.31	98.20	2.90	2.95
	100	0.40	0.39	98.11	3.19	3.25
	120	0.48	0.47	98.44	0.42	0.43

To estimate the stability of the real-drug sample and the standard solutions, the difference in content of the standard and real-drug sample solutions over time was determined in relation to the initial assay results. An acceptance limit of ± 2% was considered. Thus, the recovery rate should be between 98 and 102% of the initial concentration to demonstrate stability of the solutions.[239] The results showed that all contents of the standard and sample solutions remained within the acceptance limit of ± 2% from initial observations, revealing that the standard and sample solutions were stable for at least three days. According to the two-sample test for variance at a level of 0.05%, variances of the two data sets were not significantly different.

During robustness studies, no significant change was observed in the resolution between the peak of amodiaquine (**13**) and that of the internal standard (quinine, **34**). The change of the pH value gave the highest standard deviation (SD = 1.0), while the remaining parameters had SD values between 0.3 and 0.5. For all parameters tested, a baseline separation between the API and the internal standard was still ensured. The developed and validated method was used for determining the content of amodiaquine (**13**) in four commercial samples collected in DRC.

II.2 Capillary Zone Electrophoresis for the Determination of Amodiaquine

To obtain reference values, two of them were additionally analyzed using the compendial HPLC method described in *The International Pharmacopoeia*.[215]

Table 6. Intra-day and inter-day precision data for 4,7-dichloroquinoline (**30**), 4-aminophenol (**31**), 4-[(7-chloroquinolin-4-yl)amino]phenol (**32**), and amodiaquine (**13**)

Compound	Level [%]	Point of time	Intra-day precision [a] mean corrected peak area / IS	SD	RSD [%]	Inter-day precision [b] mean corrected peak area / IS	SD	RSD [%]
30	0.5	Day 1	0.59	0.02	3.88	0.53	0.05	8.53
	0.5	Day 2	0.51	0.02	3.43			
	0.5	Day 3	0.49	0.01	1.11			
30	1	Day 1	1.08	0.02	2.30	1.05	0.05	4.74
	1	Day 2	1.08	0.02	1.88			
	1	Day 3	0.99	0.02	2.48			
31	0.5	Day 1	0.12	0.01	4.61	0.13	0.02	15.09
	0.5	Day 2	0.11	0.02	16.72			
	0.5	Day 3	0.15	0.01	9.31			
31	1	Day 1	0.25	0.01	3.92	0.28	0.02	8.99
	1	Day 2	0.27	0.01	2.15			
	1	Day 3	0.30	0.01	4.20			
32	0.5	Day 1	0.40	0.01	3.73	0.37	0.02	5.78
	0.5	Day 2	0.37	0.01	2.98			
	0.5	Day 3	0.35	0.01	2.94			
32	1	Day 1	0.70	0.03	4.50	0.68	0.04	5.37
	1	Day 2	0.70	0.01	1.92			
	1	Day 3	0.63	0.01	1.02			
13	100	Day 1	3.50	0.05	1.42	3.50	0.10	2.98
	100	Day 2	3.40	0.07	2.11			
	100	Day 3	3.59	0.08	2.27			

[a] n = 6 for amodiaquine (**13**), n = 3 for the related substances **30**–**32**. [b] n = 18 for amodiaquine (**13**), n = 9 for the related substances **30**–**32**.

II.2.3.2 Impurity Profiling

The specificity of the method was demonstrated by the fact that the peaks of all three related compounds **30**, **31**, and **32** were well separated from each other and from those of amodiaquine (**13**) and quinine (**34**); the lowest resolution value was observed between 4-[(7-chloroquinolin-4-yl)amino]phenol (**32**) and the internal standard quinine (**34**).

Within the concentration range of 25–75 µg mL^{-1}, the method proved to be linear for impurities **30**−**32** (i.e., 0.5–1.5% of the nominal sample concentration of 5.0 mg mL^{-1} for 4), with R^2 values ranging from 0.9989 to 0.9997. The equations of the individual calibration curves are given in Table 7.
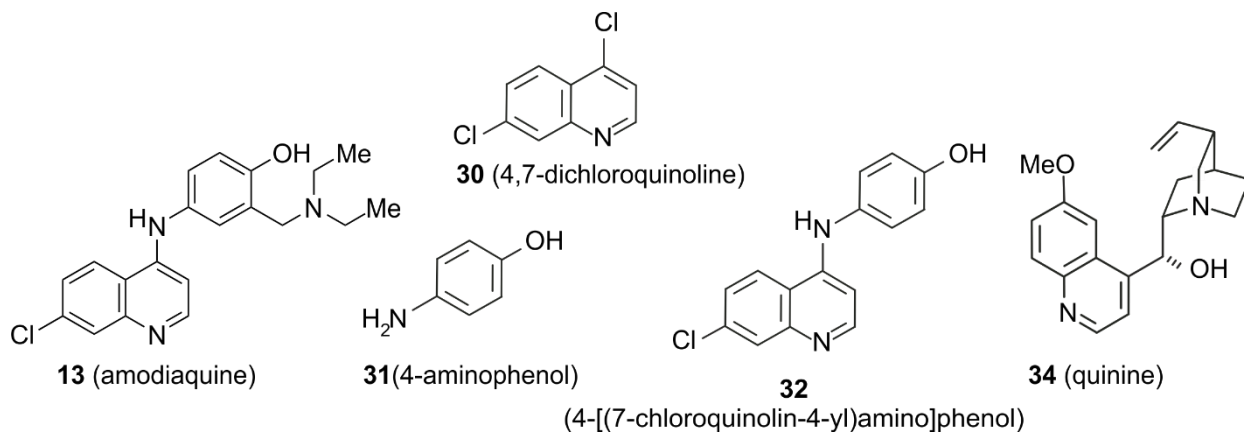
Table 7. Regression data for linearity as well as LOD and LOQ values

Compound	Range [µg mL^{-1}]	Equation of the calibration line	R$^{2[a]}$	LOD [µg mL^{-1}]	LOQ [µg mL^{-1}]
30	25–75	y = 1.0619 x - 0.0136	0.9997	1.5	5.0
31	25–75	y = 0.3127 x + 0.0048	0.9989	3.5	10.0
32	25–75	y = 0.661 x - 0.0485	0.9995	2.5	7.0
13	200–600	y = 0.036 x + 0.0068	0.9990	na$^{[b]}$	na

[a] coefficient of determination. [b] not applicable.

The results of the recovery studies for impurity profiling are given in Table 5. The recovery rates ranged from 96.4 to 108.8% for the related compound 4-[(7-chloroquinolin-4-yl)amino]phenol) (**32**), from 92.7 to 99.2% for 4,7-dichloroquinoline (**30**), and from 77.6 to 83.8% for 4-aminophenol (**31**). The method can therefore be regarded as accurate (acceptance limit of ±15%) except for 4-aminophenol (**31**). This is probably due to the matrix effect of the used drug sample and/or its known[240] chemical instability.

The intra-day and inter-day precision data for the three amodiaquine-related compounds **30**−**32** are presented in Table 6. The % RSD values ranged from 1.0 to 4.5% and from 5.4 to 5.8% for 4-[(7-chloroquinolin-4-yl)amino]phenol (**32**) in intra- and inter-day repeatability, respectively. For 4-aminophenol (**31**), they were from 2.2 to 16.7% and from 9.0 to 15.1% for intra- and inter-day repeatability, respectively. For 4,7-dichloroquinoline (**30**), they ranged from 1.1 to 3.9% and from 4.7 to 8.5% for intra- and inter-day repeatability, respectively. The method can therefore be considered as precise.

The LOD (limit of detection) values ranged from 1.5 to 3.5 µg mL^{-1} (0.03–0.07%), while the LOQ (limit of quantification) values were 5–10 µg mL^{-1} (0.1–0.2%), with 4,7-dichloroquinoline (**30**) having the lowest LOD and LOQ values and 4-aminophenol (**31**) the highest ones. These LOD and LOQ values were found to be suitable for the present study. The individual LOD and LOQ values are presented in Table 7.

During the stability studies on the real-drug samples and standard solutions, significant deviations in content were observed, *i.e.*, more than 2% change as compared to the initial observations. Therefore, all solutions of the related compounds **30**−**32** needed to be freshly prepared before use.

As expected, changing the pH value from 6.0 to 6.4 gave the highest standard deviation mean value (SD = 1.5) of the resolution during the evaluation of the method robustness, while by modifying the remaining parameters (buffer concentration, voltage, and capillary temperature), SD mean values between 0.3 and 0.5 were observed. Therefore, the method can be considered as robust.

II.2.4 Analysis of Antimalarial Drug Samples

The newly developed and validated method was successfully applied to analyze four batches of ASAQ drug samples (Winthrop®, Arteplus®, Sunat-A forte®, Sunat-A®) that had been collected in Kinshasa, DRC. The results of the evaluation shown in Table 8 demonstrate a good conformity of the quantitative measurements of the main component with those obtained by the HPLC method described in *The International Pharmacopoeia*.[215] All drug samples were found to comply with the specification concerning the content of the active pharmaceutical ingredient (API), *i.e.*, 90−110% of the label claim. In contrast to the compendial HPLC method mentioned above, the present protocol is even applicable to ASAQ double-layered formulations, in which artesunate (**11**) and amodiaquine (**13**) are co-formulated in one tablet unit.

Table 8. Comparison of analysis results [%] for amodiaquine (**13**) using a compendial method and the newly developed one

Brand name, manufacturer, batch number, and formulation	Declared composition [mg]		API content (mean ± SD) in [%]		Impurity profiling (CZE) [% content]			
	Artesunate	Amo-diaquine	CZE assay	HPLC assay (Ph. Int.)	Cpd. **29**	Cpd. **30**	Cpd. **31**	Unknown
Winthrop (Maphar, Morocco) 5MA315 Double-layer	100	270	102.7 ± 4.0	na	nd	nd	nd	nd
Arte-Plus (Guilin Pharm, India) SH150501 Double-layer	100	270	97.4 ± 0.7	na	nd	nd	nd	nd
Sunat-A Forte (Shalina, India) J6001 Co-blister	200	612.4	103.8 ± 1.8	96.4 ± 1.8	nd	nd	0.030 ± 0.004[a]	nq
Sunat-A (Shalina, India) J5001 Co-blister	100	306.2	99.2 ± 0.7	95.5 ± 1.2	nd	nd	0.048 ± 0.002 [a]	0.076 ± 0.004 [b]

na: not applicable. nd: not detectable. nq: not quantifiable. [a] estimation based on the reference compound **32**. [b] estimation based on comparison of the peak area with that of amodiaquine (**13**)

When applying the newly developed method to the analysis of the related compounds in real-drug samples (Table 8), impurities were found in all samples at levels below the acceptance limit of 0.5%: Two batches from a distinct manufacturer contained two detectable impurities, one was 4-[(7-chloroquinolin-4-yl)amino]phenol (**32**), the other one was unknown ("?" in Figure 18B). Although the HPLC method described in *The International Pharmacopoeia*[215] is not intended to focus on the impurity profiling of amodiaquine (**13**), the analysis of the two-drug samples (in higher concentration) and that of an artificial mixture of amodiaquine and the impurities **30**−**32** showed that the amodiaquine peak was well resolved from all the three related compounds, and the presence of compound **32** and other unknown impurities was confirmed.

II.2.5 Conclusion

The present chapter describes the development and validation of a CZE method for the content determination of amodiaquine (**13**) and for the impurity profiling with respect to three of its related compounds, 4,7-dichloroquinoline (**30**), 4-aminophenol (**31**), and 4-[(7-chloroquinolin-4-yl)amino]-phenol (**32**) using a fused-silica capillary, a background electrolyte of 100 mM sodium phosphate buffer (pH = 6.2), a voltage of +20 kV, and a detection wavelength of 220 nm. Determination of the analytes is possible within 20 min and, thus, the newly developed method can be used for determining the quality of amodiaquine (**13**) as a bulk drug as well as for pharmaceutical finished products like tablets. Thus, it can be used as a reliable alternative to chromatographic methods like HPLC, as described, *e.g.*, in *The International Pharmacopoeia*.[215]

II.3 Phytochemical Investigations on a Congolese *Ancistrocladus* Liana

II.3.1 Introduction

With four out of 18 taxonomically accepted *Ancistrocladus* species,[50,241,49] the Democratic Republic of the Congo (DRC) is a great source of plants belonging to the monogenic family Ancistrocladaceae, comprising a small group of palaeotropical lianas. A recent molecular field study[242] suggested the presence of a yet unrecognized taxon in DRC, where several expeditions have been conducted during the past two decades. In July 2006, Prof. V. Mudogo collected plant material of a botanically yet unidentified *Ancistrocladus* species in the vicinity of the village Leeke, near the town Ikela, in the Central region of DRC. A voucher specimen has been deposited at the Herbarium Bringmann, Institute of Organic Chemistry, University of Würzburg.

This thesis describes, the isolation, structural elucidation, and biological activities of six new naphthylisoquinoline alkaloids from this as yet uninvestigated Congolese species,[243] including four 5,8'-coupled monomeric compounds, ikelacongolines A−D (**35a**, **35b**, **36**, and **37**), and two dimeric representatives, mbandakamines B$_3$ (**38**) and B$_4$ (**39**) (Figure 19).
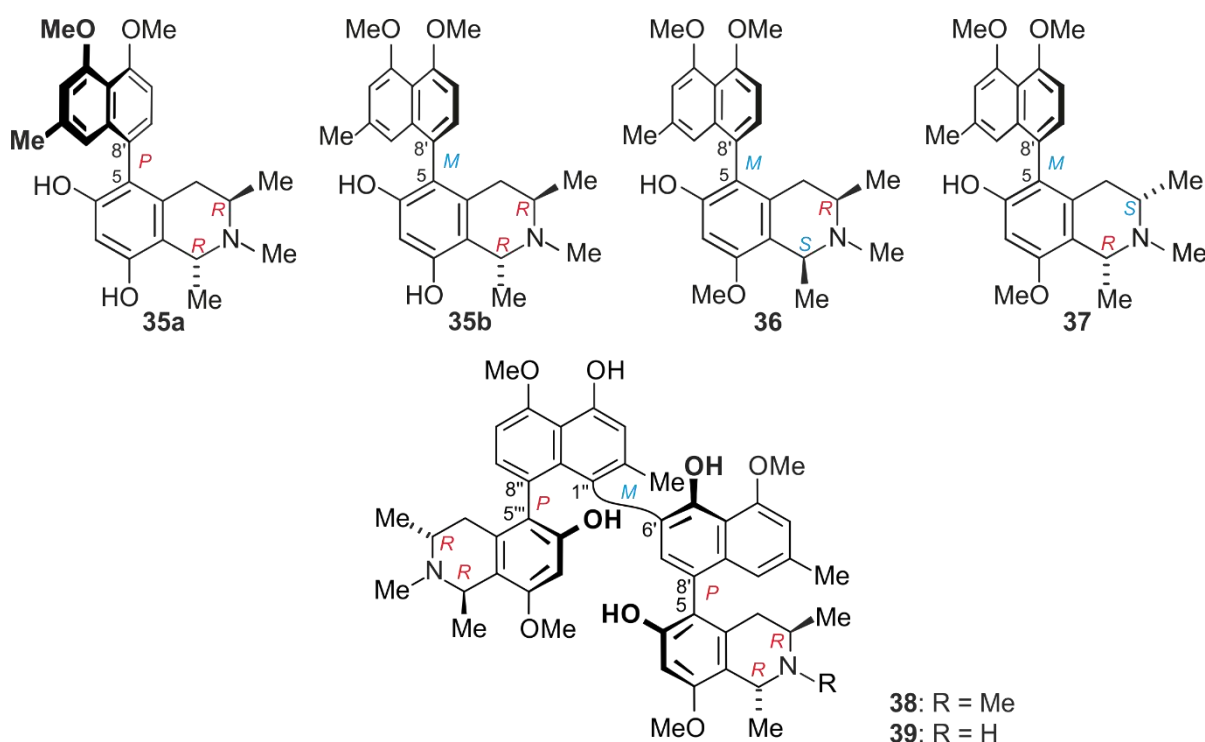
Figure 19. Structures of the four here discovered new monomeric NIQs, ikelacongolines A−D, **35a**, **35b**, **36**, and **37**, and of the two new dimers, mbandakamines B$_3$ (**38**) and B$_4$ (**39**).

Besides the above-mentioned six new alkaloids, seven previously known[244–248,164] compounds were isolated, including five monomers, 5,8'-coupled ancistrocongoline C (**40**), ancistrolikokines C (**41**) and F$_2$ (**42**), two 7,8'-linked ealamines A (**43**) and G (**44**); and two dimers, mbandakamines A (**45**) and B$_2$ (**46**) (Figure 20).
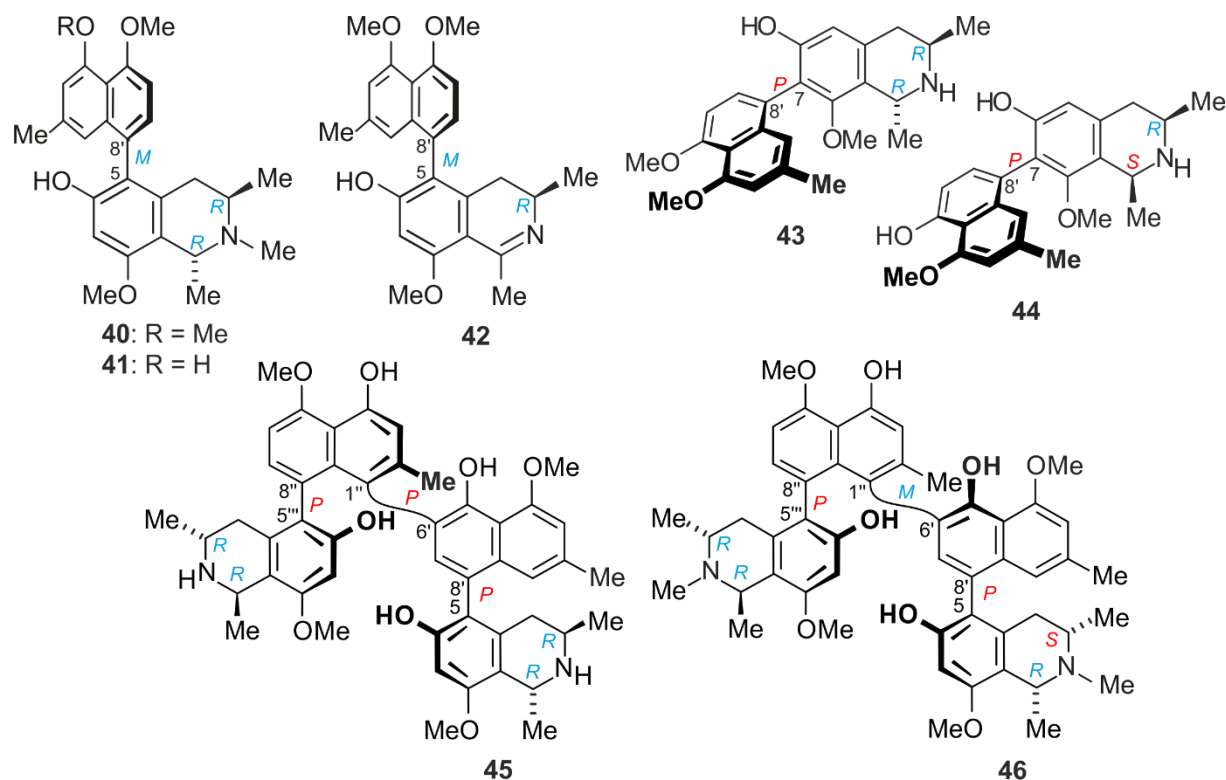
Figure 20. Five known monomeric naphthylisoquinoline alkaloids, **40**–**44**, and two known dimers, mbandakamines A (**45**) and B$_2$ (**46**).

II.3.2 Results and Discussion

Conducted on crude extracts from leaves, root, and stem bark of plant material collected in Leeke village, initial LC-MS measurements had shown that only the leaf extracts hinted at the presence of both, monomeric and dimeric naphthylisoquinoline alkaloids. Therefore, in-depth investigations for the isolation and structural characterization of these compounds were undertaken.

Air-dried leaves were ground and extracted with CH$_2$Cl$_2$/MeOH (1:1). After maceration in water and subsequent dissolution in methanol, the obtained extract was submitted to preparative reverse-phase HPLC allowing the purification of four new monomers (**35a**, **35b**, **36**, and **37**) and two new dimers (**38**, **39**).

As deduced from HRESIMS, the new compounds **35a** and **35b** were found to possess each a molecular formula of $C_{25}H_{29}NO_4$. Both displayed NMR signals typical of an *N*-methylated naphthyl-1,3-dimethyltetrahydroisoquinoline as evinced by the two three-proton doublets (δ_H 1.72/1.74 and 1.24/1.24), further correlated by the presence of a quartet (δ_H 4.72/4.71, H-1), and a methyl singlet with a typical *N*-CH$_3$ chemical shift (δ_H 2.72/2.77). The ^{1}H NMR spectrum revealed the signals of two methoxy groups (δ_H 3.93/3.93 and 3.95/3.95) and five aromatic protons, including three singlets, and two doublets, corresponding each to one proton. Two of these (δ_H 6.65/6.77 and 6.78/6.79) were coupled *meta* to each other. With only two protons in *ortho* position (δ_H 6.95/6.93 and 7.18/7.15), this substitution pattern suggested either a 6'- or an 8'-position of the biaryl axis in the naphthalene moiety. This assumption was supported by the chemical shift of the methyl group at C-2' (δ_H 2.30/2.32). HMBC interactions from H-1' (δ_H 6.65/6.77) and H-6' (δ_H 6.95/9.93) to the quaternary carbon atom C-8' (δ_C 126.6/126.7) in combination with NOESY correlations in the series {H-1' ↔ Me-2' ↔ OMe-4'} evidenced the naphthalene moiety to be linked via C-8' (Figure 21). In the tetrahydroisoquinoline portion, the axis was found to be located at C-5, as supported by HMBC correlations from H-7' and H-7 to C-5 (δ_C 119.7/119.6) and from both of the methylene protons at C-4 to C-5 (Figure 21). In summary, the two new compounds were 5,8'-coupled *N*-methylated naphthyltetrahydroisoquinolines with two methoxy functions at C-4' and C-5'.
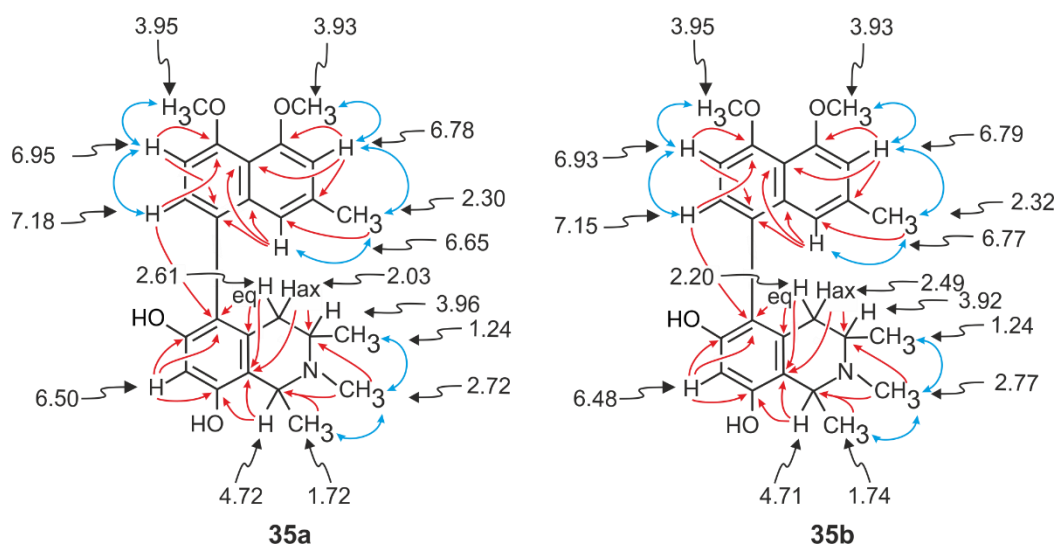
Figure 21. Selected 1D and 2D NMR data of the new compounds **35a** and **35b** indicative of the constitutions: ^{1}H (δ in ppm), HMBC (single red arrows) and NOESY (double blue arrows).

From a NOESY interaction between H-3 (δ_H 3.96/3.92) and Me-1 (δ_H 1.72/1.74) (Figure 22), a relative *trans*-configuration of the two stereocenters at C-1 and C-3 was evidenced. The absolute configurations were deduced from a ruthenium-mediated oxidative degradation developed by our group;[173] they were found to be *R*, both for C-1 and C-3. Based on the hence known absolute configuration at the stereocenters, the relative and thus also the absolute configuration at the biaryl axis was attributed from NOESY interactions between H-4$_{ax}$ and H-1', and H-4$_{eq}$ and H-7', showing the axis to be *P*-configured for compound **35a**, while NOE correlations between H-4$_{ax}$ and H-7', and H-4$_{eq}$ and H-1', revealed the axis to be *M*-configured for compound **35b** (Figure 22).
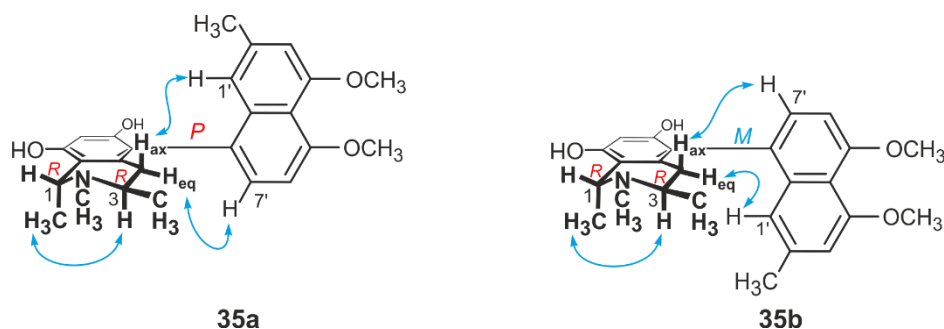
Figure 22. Selected NOESY correlations indicative of the relative configurations at the stereogenic centers and the biaryl axes in **35a** and **35b**.

These assignments were further confirmed by the ECD spectrum of compound **35a**, which was virtually opposite to the one of the *M*-configured. Likewise, 5,8′-linked ancistrocongoline C (**40**) occurs in the plant and has the same profile as compound **35b** (Figure 23). The two new alkaloids were named ikelacongolines A (**35a**) and B (**35b**), after the town of Ikela, where the plant material had been collected. Due to the structural similarities found in previous isolated alkaloids, the new compound **35a** might be assigned as the *N*-methylated analog of korupensamine C (not shown) from the Cameroonian liana *A. korupensis*,[47] or as the 5'-*O*-methyl derivative of ancistrocongoline A (not shown),[249,245] a main metabolite of the two Congolese species *A. congolensis and A. likoko*. And the new alkaloid **35b** was the atropo-diastereomer of **35a**.
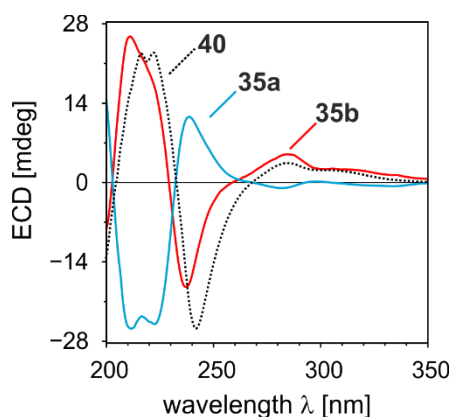
Figure 23. Comparison of the ECD spectra of **40**, **35a** and **35b**.

The two further new monomeric alkaloids, **36** and **37**, displayed each a molecular formula of $C_{26}H_{31}NO_4$ according to HRESIMS. The ^{1}H NMR data indicated signals similar to an *N*-methylated naphthyl-1,3-tetrahydroisoquinoline, thus, very close to compounds **35a** and **35b**. However, an additional upfield-shifted signal was attributed to the presence of a methoxy function at C-8 (δ_H 3.92) in the isoquinoline portion as deduced from the NOESY correlation sequence {Me-1↔ OMe-8↔ H-7}, together with their joint HMBC interaction with C-8 (δ_C 157.2/157.5) (Figure 24).
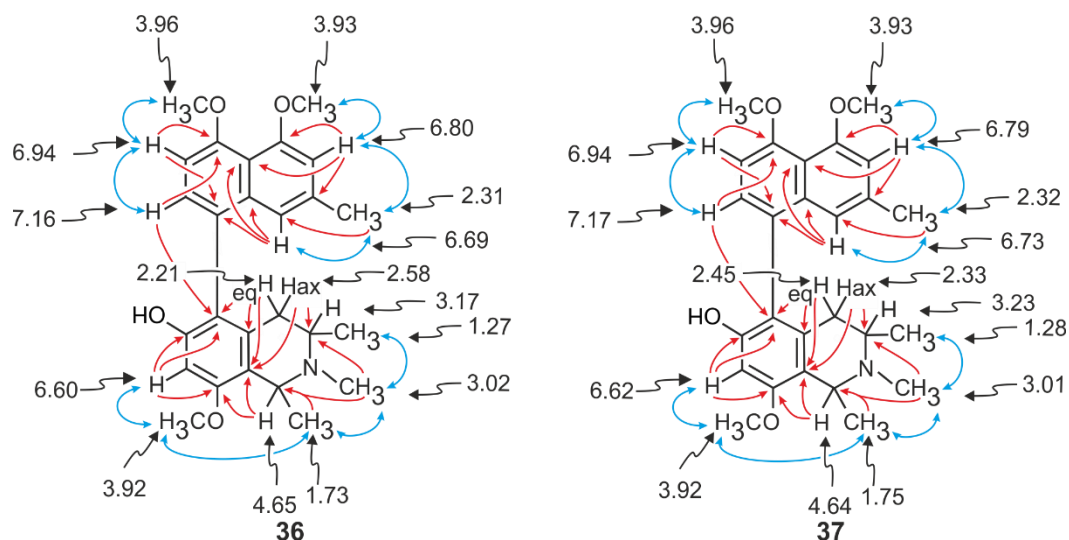
Figure 24. Evidences of the joint constitution of compounds **36** and **37**: ^{1}H (δ in ppm), HMBC (single red arrows) and NOESY (double blue arrows).

Unlike in compounds **35a** and **35b**, the relative configuration at C-1 *versus* C-3 was found to be *cis* as suggested by the NOE correlation between H-1 (δ_H 4.65/4.64) and H-3 (δ_H 3.15/3.23) (Figure 25), while the absolute configurations were assigned to be 1*S*,3*R* for **36** and 1*R*,3*S* for **37** by ruthenium-mediated oxidative degradation.
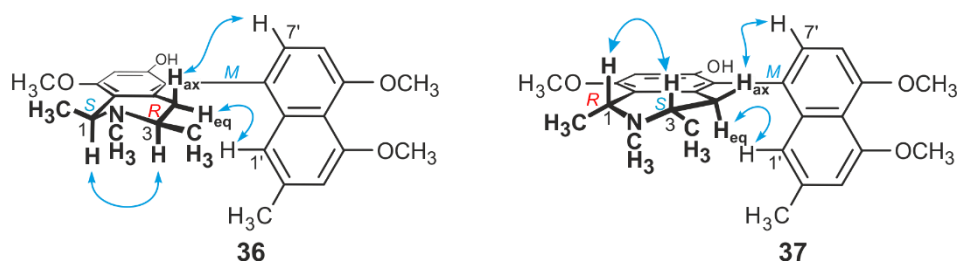
Figure 25. Selected NOESY interactions indicating the configurations at the stereogenic centers relative to each other and to the biaryl axes in compounds **36** and **37**.

ECD spectroscopy and specific NOESY interactions permitted to establish that both compounds were *M*-configured at the biaryl axis (Figure 26). The stereostructures of **36** and **37** were as presented in Figure 18. They were named ikelacongoline C and D, respectively. The constitution of compound **36** was similar to that of ancistroyafungine A (not shown),[250] an alkaloid isolated earlier from a botanically likewise as yet unidentified *Ancistrocladus* liana from the North-Central part of the Congo Basin. Also, the configurations at C-1 and C-3 were the same, but with *M*-configuration at the biaryl axis. The alkaloid might also be addressed as 5-*epi*-ancistroyafungine A.

The pair of alkaloids **36**/**37** was most remarkable because their tetrahydroisoquinoline parts were enantiomeric to each other (1*S*,3*R* *versus* 1*R*,3*S*), while the axes were identically configured. The occurrence of such a pair of naphthylisoquinolines within one plant is unprecedented.
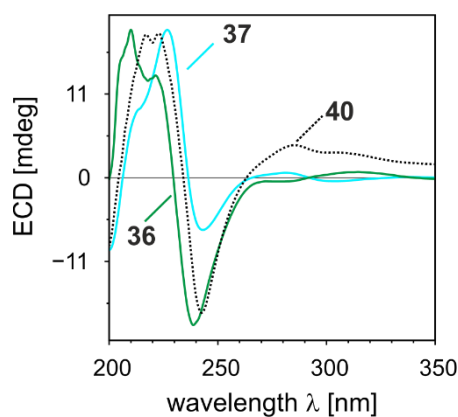
Figure 26. Comparison of the ECD spectra of **40**, **36**, and **37**.

As evident from the HRESIMS data, the new compound **38** was found to possess a molecular formula of $C_{50}H_{56}N_2O_8$, which was identical to that of the previously-reported mbandakamines B_2 (**46**),[247] also present in the plant extracts. Its ^{1}H NMR spectrum exhibited a full set of

signals, indicating the occurrence of a likewise unsymmetric dimeric naphthylisoquinoline alkaloid. The ^{1}H NMR data also revealed the presence of: eight aromatic protons, two methylene groups with diastereotopic protons, six methyl groups, two *N*-methyl functions, and four aromatic *O*-methyl groups.

The 'southeastern' half displayed typical chemical shifts for an *N*-methylated naphthyl-1,3-dimethylitetrahydroisoquinoline with a 5,8'-coupling. It was linked via C-6' (δ_C 136.2) in the naphthalene subunit to a second, 'northwestern' molecular part, which likewise consisted of a naphthyl-1,3-dimethyl-*N*-methyltetra-hydroisoquinoline of the 5,8'-linkage type.

The first, 'southeastern', molecular portion (Figure 27B) was found to possess four aromatic protons, with two singlets (δ_H 6.65 and 6.83) and a two-proton spin system in the naphthalene part exhibiting a *meta*-coupling pattern (δ_H 6.56 and 6.81). The aliphatic region displayed the following signals: a quartet {H-1, (δ_H 4.68)}, a multiplet {H-3, (δ_H 3.95)}, two diastereotopic protons, H-4$_{ax}$ (δ_H 1.74) and H-4$_{eq}$ (δ_H 2.77), and two *O*-methyl groups (δ_H 3.93 and 4.06). In that part of the spectrum, the two three-proton doublets were also monitored, typical of Me-1 (δ_H 1.49) and Me-3 (δ_H 1.08). The two three-proton singlets corresponded to an aryl-methyl group {Me-2', (δ_H 2.30)} in the naphthalene part and to the *N*-methyl group (δ_H 2.54) in the isoquinoline subunit. The latter finding was confirmed by HMBC interactions of the methyl protons with C-1 and with C-3 (Figure 27B). The location of the biaryl linkage at C-8' was established from an HMBC cross peak between H-1' (δ_H 6.56) and the quaternary carbon atom C-8' (δ_C 126.5). The attribution of H-1' in turn was corroborated by its ROESY interaction with H-4$_{ax}$ and by the ROESY correlation sequence {H-1' $\leftrightarrow$ Me-2' $\leftrightarrow$ H-3' $\leftrightarrow$ OMe-4'}. In the tetrahydroisoquinoline portion, the coupling position was deduced to be C-5 (δ_C 119.5), as obviously found from HMBC interactions of H-7 (δ_H 6.65), H-7' (δ_H 6.83), and H-4$_{eq}$ with C-5. The two methoxy groups at δ_H 3.93 and 4.06 showed NOESY interactions with H-7 and H-3' (δ_H 6.81), respectively. Thus, they were located at C-8 in the isoquinoline subunit and at C-4' in the naphthalene part. Consequently, the remaining two oxygen functions could only be free hydroxy groups at C-6 and C-5' (Figure 27B).

The ^{1}H NMR spectrum of the northwestern molecular portion additionally displayed chemical shifts typical of a 5,8'-coupled *N*-methylated naphthyltetrahydroisoquinoline with a methoxy group (δ_H 3.42) at C-8''' (Figure 27A). This was confirmed by ROESY correlations in the series {H-7''' ↔ OMe-8''' ↔ Me-1''' ↔ H-3'''}, and by HMBC interactions from H-7'' (δ_H 6.97), H_{eq}-4''' (δ_H 1.84), and H-7''' (δ_H 5.64) to C-5''' (δ_C 123.0). It evidenced the coupling position of the biaryl axis in the isoquinoline subunit to be located at C-5'''. In contrast to the naphthalene part of the southeastern half, the signal pattern in the ^{1}H NMR spectrum showed an *ortho*-coupling of the two aromatic protons H-7'' (δ_H 6.97) and H-6'' (δ_H 7.01). They were no *meta*-coupled doublets next to the shielded methyl group (δ_H 2.06) at C-2'' but, a singlet only at H-3'' (δ_H 6.87). This suggested C-1'' and C-8'' to be axis-bearing carbon atoms. ROESY correlations between H-6'' and MeO-5'' (δ_H 4.16) revealed the naphthalene unit of the northwestern naphthylisoquinoline to possess a methoxy function at C-5'. HMBC interactions from H-7'' to C-5'' (δ_C 158.2) and C-9'' (δ_C 137.9) as well as H-6'' to C-8'', established C-8'' to be quaternary. This suggested that the isoquinoline and the naphthalene portions of the northwestern molecular half were coupled through C-5''' and C-8'' (Figure 26A). The proximity of a second aryl substituent to the methyl group (δ_H 2.06) of the naphthalene subunit in the northwestern part of the dimer became evident from the strongly upfield-shifted signal of Me-2'', which revealed the central biaryl axis to connect the two molecular halves of the isolated alkaloid by a 6',1''-coupling of the two naphthalene subunits. This assignment was further proven by ^3J HMBC interactions from H-3'', Me-2'', and H-7' to C-1'' (Figure 27A), and by ROESY data between H-1', Me-2', H-3', and MeO-4' in the naphthalene unit of the northwestern naphthylisoquinoline and OMe-8''' in the isoquinoline portion of the southeastern half of the dimer (Figure 27A). Therefore, the central axis had to be in one of the *peri*-positions neighboring one of the outer axes, which leads to an extremely high steric hindrance at that 6',1''-linked central biaryl axis. In conclusion, the new compound **38** had the same constitution as **46**.[247]
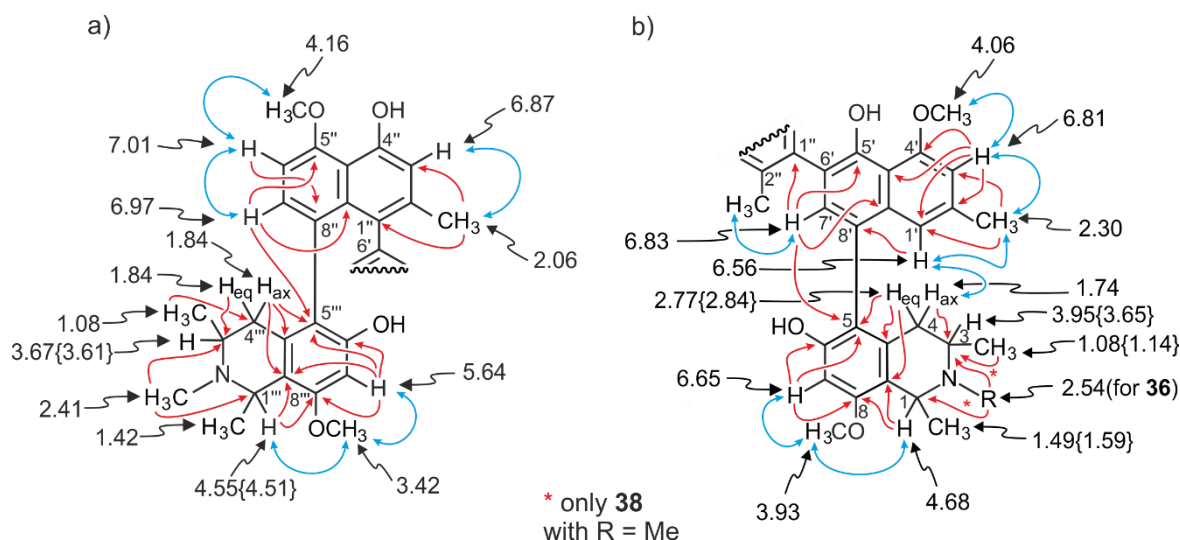
Figure 27. Selected ^{1}H NMR data, HMBC (single orange arrows) and NOE (double blue arrows) interactions indicative of the constitutions of the a) 'northwestern' and the b) 'southeastern' naphthylisoquinoline portions of mbandakamines B$_3$ (**38**) and B$_4$ (**39**): The values of **39** that are different from those of **38** are given in { }. All other NMR data of **38** and **39** are nearly identical ($\pm$ 0.02 ppm).

In contrast to **46**, the relative configurations at the stereogenic centers in the two molecular halves were both *trans* as suggested by the ROESY interactions between Me-1 (δ_H 1.49) and H-3 (δ_H 3.95), and between Me-1''' (δ_H 1.48) and H-3''' (δ_H 3.67) (Figure 28). The absolute configurations at C-3 and C-3''' were found to be *R* as established by oxidative degradation,[173] which indicated the alkaloid to be 1*R*, 3*R*, 1'''*R*, 3'''*R*-configured. The absolute configurations at the two 'outer' axes were established by long-range NOE correlations, taking into consideration H-7' (δ_H 6.83) and H-4$_{eq}$ (δ_H 2.77) as well as H-1' (δ_H 6.56) and H-4$_{ax}$ (δ_H 1.74) in the first molecular half including H-7'' (δ_H 6.97) and H-4'''$_{eq}$ (δ_H 1.84) in the second molecular portion in view of the character of the stereogenic centers, the absolute configuration was *P* in both moieties (Figure 28).

As deduced by ROESY interactions between H-7' and H-4'''$_{ax}$ and between MeO-4' (δ_H 4.06) and H-7''' (δ_H 5.64), the central biaryl axis was assigned to be *M*. The confirmation of this stereochemical feature was performed by the superposition of the ECD spectrum of **38** with the one of mbandakamine B$_2$ (**46**), showing virtually identical spectra. But they were nearly mirror-imaged to the spectrum of mbandakamine A (**45**) (Figure 29), which is *P*-configured at the central biaryl axis. Thus, the new alkaloid was named mbandakamine B$_3$. Due to its structural similarity with **46**,[247] it could also be named 3-*epi*-mbandakamine B$_2$.
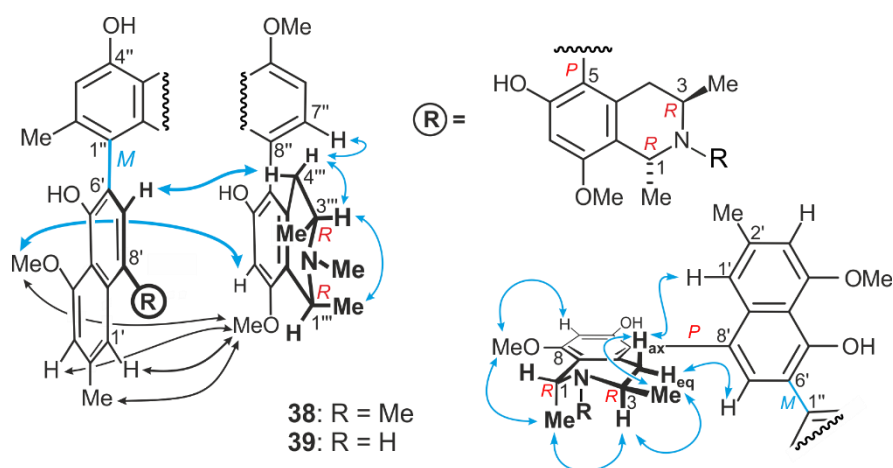
Figure 28. Selected ROESY correlations between the naphthalene subunit of the 'northwestern' half and the isoquinoline part of the 'southeastern' moiety establishing the 6',1"-coupling sites in the central binaphthalene core (black arrows) and the relative configuration at the centers and the two outer axes (blue arrows) and at the central biaryl axis (bold blue arrows) of **38** and **39**.

The molecular formula of the alkaloid **39** was found to be $C_{49}H_{54}N_2O_8$ as suggested from HRESIMS experiments. Its NMR data hinted at another unsymmetric 6',1"-linked dimer comprising two 5,8'-coupled monomeric moieties, with structural features analogous to those of mbandakamines B_2 (**46**) and B_3 (**38**), but one methyl group fewer than **38** and **46**. This was attributed to the lack of *N*-Me in the first molecular half, while the presence of *N'''*-Me (δ_H 2.42) was evidenced by its typical chemical shift, by the ROESY interactions with Me-1''' (δ_H 1.42) and Me-3''' (δ_H 1.08), and by the HMBC correlations with C-1''' (δ_C 59.0) and C-3''' (δ_C 50.1) in the second molecular portion (Figure 27).

Based on NOE corrections, the relative configurations in the stereogenic centers were likewise found to be *trans* in both molecular moieties, while an oxidative degradation allowed to determine the absolute configurations at both C-3 and C-3''' to be *R* as well. In combination with the above *trans* relative configurations, the stereocenters at C-1 and C-1''' were assigned to be *R*-configured. Long-range ROESY interactions between H-7' (δ_H 6.83) and H-4$_{eq}$ (δ_H 2.84) as well as between H-1' (δ_H 6.54) and H-4$_{ax}$ (δ_H 1.75) in the first molecular half including between H-7" (δ_H 6.97) and H-4'''$_{eq}$ (δ_H 1.86) in the second molecular portion (Figure 27), allowed the assignment of the two 'outer' biaryl axes to be likewise *P*. Further ROESY correlations between H-7' and H-4'''$_{ax}$ as well as between MeO-4' (δ_H 4.06) and H-7''' (δ_H 5.64) established the central biaryl axis to also be *M*.

The ECD spectrum of the new alkaloid **39** confirmed the findings. The assignments were identical to those of the likewise *M*-configured mbandakamines B$_2$ and B$_3$ (Figure 29). Consequently, the new dimer was found to possess the full stereostructure as described in Figure 19. It was named mbandakamine B$_4$. In view of its structural similarity with mbandakamine B$_3$ (**38**), it could be addressed as *N*-demethyl mbandakamine B$_3$.
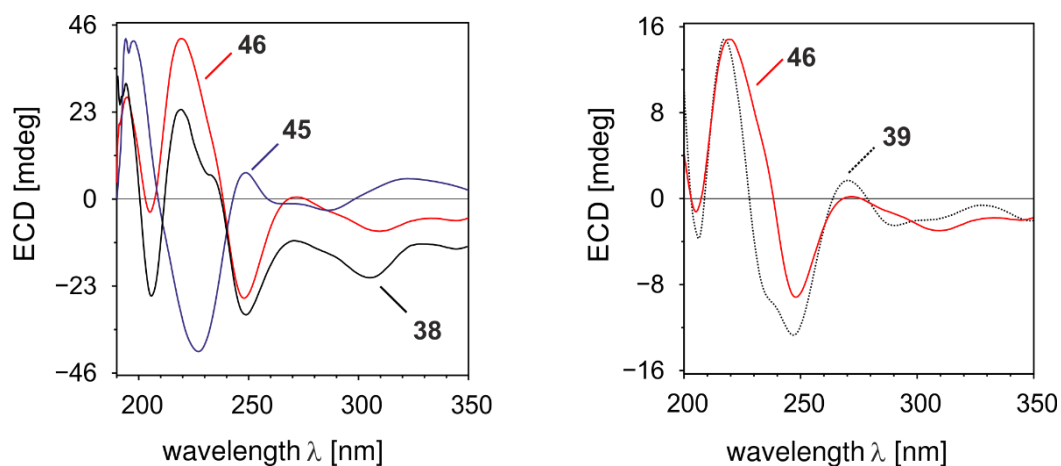
Figure 29. Confirmation of the absolute configuration of **38** and **39** at the central biaryl axis by comparison of their ECD spectra with those of the known related mbandakamines A (**45**, central axis: *P*) and B$_2$ (**46**, central axis: *M*).

45 (mbandakamine A)

46 (mbandakamine B$_2$)

38: R = Me (mbandakamine B$_3$)
39: R = H (mbandakamine B$_4$)
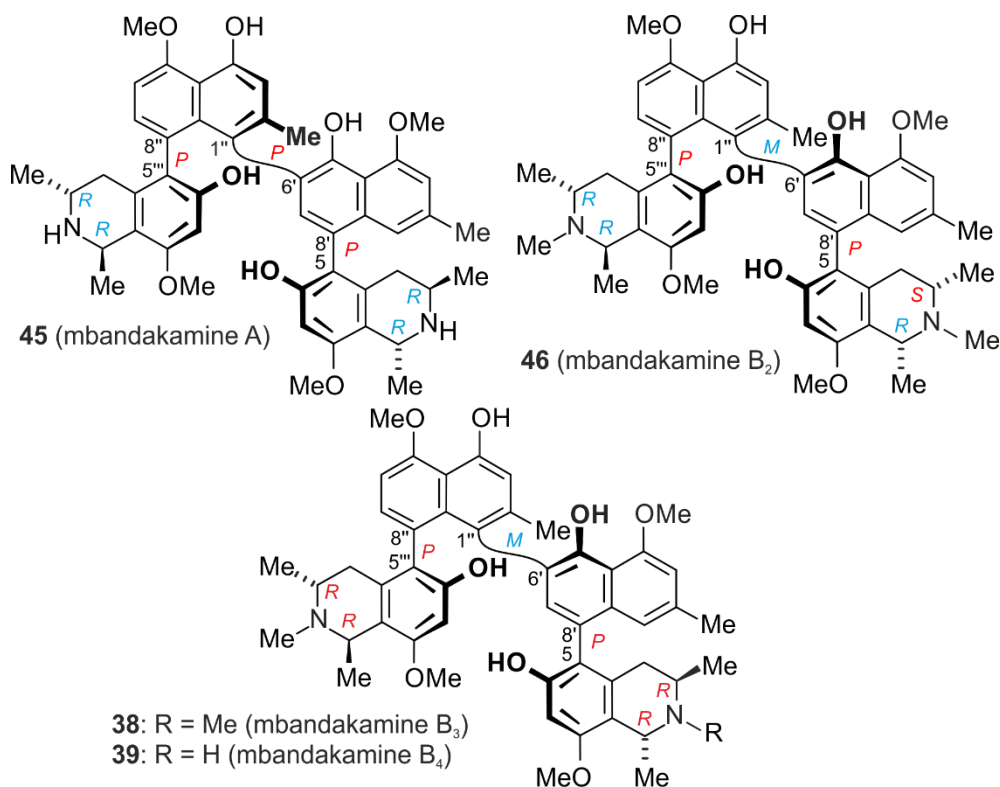
II.3.3 Biological Evaluation

The two newly discovered mbandakamine-type naphthylisoquinoline dimers **38** and **39** exhibited excellent *in vitro* biological activities against both the chloroquine-sensitive (NF54) and the chloroquine-resistant (K1) strains of the malaria parasite *Plasmodium falciparum*, with half-maximum inhibition concentration values (IC$_{50}$) of 39 (NF54) and 6 nM (K1) for mbandakamine B$_3$ (**38**), and 66 (NF54) and 26 nM (K1) for mbandakamine B$_4$ (**39**) (Table 9). Thus, their antiplasmodial activities were comparable to those of the structurally closely related and likewise strongly active mbandakamine B$_2$ (**46**).[247] They were in the same order of magnitude as those of the two standard agents, chloroquine (**1**) and artemisinin (**4**) (Table 9).

1 (chloroquine)   **4** (artemisinin)
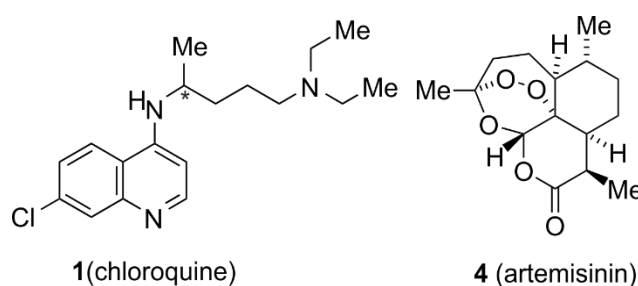
Table 9. Antiparasitic activities of mbandakamines B$_3$ (**38**) and B$_4$ (**39**), and ikelacongolines A (**35a**), B (**35b**), and C (**36**) against *Plasmodium falciparum* (K1 and NF54 strains), *Trypanosoma cruzi*, *Trypanosoma brucei rhodesiense*, *Leishmania donovani*, and cytotoxicity against rat skeletal myoblast (L6) cells

Compound	IC$_{50}$ [μM][a]						
	P. falciparum (K1 strain)	*P. falciparum* (NF54 strain)	*T. cruzi*	*T. brucei rhodesiense*	*L. donovani*	L6 cell (cytotoxicity)	Selectivity index[b] (K1/NF54)
standard	0.293[c] 0.010[d]	0.009[c] 0.021[d]	6.109[e]	0.030[f]	1.077[g]	0.0096[h]	– / –[b]
46[i]	0.004[i]	0.017[i]	2.98[i]	0.005[i]	94.2[i]	1.37[i]	342 / 80.6
38	0.006	0.039	15.1	0.476	65.5	6.64	1107 / 170
39	0.026	0.066	19.7	0.211	59.5	6.68	257 / 101
35a	2.87	6.38	130	47.2	> 100	182	63.4 / 28.5
35b	2.75	8.10	72.2	15.3	> 100	60.5	22.0 / 7.47
36	1.41	4.51	92.9	15.1	> 100	49.9	35.4 / 11.1

[a] The IC$_{50}$ values are the means of two independent assays; the individual values vary by a factor of less than 2. [b] The selectivity index is calculated as the ratio of the IC$_{50}$ values concerning L6 cells to the IC$_{50}$ data relative to *P. falciparum*. [c] Chloroquine. [d] Artemisinin. [e] Benznidazole. [f] Melarsoprol. [g] Miltefosine. [h] Podophyllotoxin. [i] Values reported earlier.

Noteworthy were the pronounced antiplasmodial activities of **38**, **39**, and **46** against the K1 strain, with inhibitory potentials significantly better than that of the standard chloroquine by a factor of 73 (for **46**), 49 (for **38**), and 11 (for **39**). The new mbandakamine B$_3$ (**38**) was found

the most active among the naphthylisoquinolines against the resistant strain K1. In addition, given the comparatively low cytotoxicity of **38** (6.64 μM), this dimer possessed a high selectivity index of *ca*. 1,110. These findings made the mbandakamines B$_3$ (**38**) and B$_4$ (**39**) promising candidates for further biological evaluations, considering the fact that they also displayed good to strong activities against the pathogen of the African sleeping sickness, *Trypanosoma brucei rhodesiense*, with IC$_{50}$ values of 0.476 μM for **38** and 0.211 μM for **39** (Table 9). Their inhibitory potentials, however, were less efficient than that of mbandakamine B$_2$ (**46**), which showed a pronounced effect *in vitro* in the nanomolar range (IC$_{50}$ = 5.0 nM),[247] stronger than that of any other of the numerous alkaloids tested so far.[164,251,247,252,163,157,187,253,189,254,46,255,256]

The inhibitory effects of the new monomeric alkaloids ikelacongolines A (**35a**), B (**35b**), and C (**36**) against the strains NF54 and K1 of *P. falciparum* were drastically lower compared to those of the dimers, mbandakamines B$_2$ (**46**), B$_3$ (**38**), and B$_4$ (**39**). Due to a low amount of material available, ikelacongoline D (**37**) was not tested. Indeed, compounds **35a**, **35b**, and **36** displayed only moderate antiplasmodial activities, with micromolar IC$_{50}$ values ranging from 1.41 to 8.10 (Table 9), and thus being 115 to 480 times less effective than mbandakamines **38**, **39**, and **46**.

These biological test results clearly demonstrated that the dimeric architecture of the mbandakamines had a significant impact on the bioactivity of 5,8'-linked naphthylisoquinoline alkaloids. A similar effect had likewise been observed for jozimine-type naphthylisoquinoline dimers of natural[163,254] and synthetic[257–259] origin consisting of two 7,1'-coupled monomeric halves (structures not shown).

Against *Leishmania donovani*, the causative agent of visceral leishmaniasis, only very weak or virtually no activities were recorded for any of the investigated naphthylisoquinolines, while for the pathogen of Chagas' disease, *Trypanosoma cruzi*, at least some low inhibitory effects were displayed by the mbandakamines **38**, **39**, and **46** were observed (Table 9).

Furthermore, the 13 isolated compounds (**35a**, **35b**, **36**–**46**) were investigated for their cytotoxic activities against the PANC-1 human pancreatic cancer cell line in nutrient-deprived medium (NDM) and in normal nutrient-rich Dulbecco's modified Eagle's medium (DMEM). The anti-austerity approach,[260,261] which aims at the identification and development of new therapeutic agents with preferential cytotoxicity to pancreatic tumor cells under nutrient-deficient circumstances was considered.

II.3 Phytochemical Investigations

The preferential cytotoxicities are characterized by PC_{50} values, *i.e.*, the concentration at which 50% of the pancreatic cancer cell line are killed in NDM without exhibiting toxicity in DMEM. All the 13 tested alkaloids showed moderate preferential cytotoxicities against PANC-1 cells, with PC_{50} values ranging from 7.10 to 87.00 μM (Table 10). Among the four new monomers **35a**, **35b**, **36**, and **37**, ikelacongoline D (**37**) displayed the most potent effects in NDM, with a PC_{50} values of 11.5 μM, far above the highly potent agent ancistrolikokine E_3 (PC_{50} = 2.5 μM),[262] while the two new dimers **38** and **39** showed nearly the same PC_{50} values (Table 10).

Table 10. Preferential cytotoxicity of the 13 isolated compounds on human pancreatic cancer PANC-1 cells in NDM

Compound	PC_{50}[a] [in μM]	Compound	PC_{50}[a] [in μM]
35a	80.04	**41**	7.10
35b	31.01	**42**	87.00
36	51.36	**43**	12.52
37	11.51	**44**	33.69
38	8.68	**45**	8.80
39	8.03	**46**	15.29
40	46.04	arctigenin[b]	0.475

[a] Concentration at which 50% of the cells were killed preferentially in NDM. [b] Used as a reference compound.

II.3.4 Conclusion

Prior to this work, mbandakamine-type naphthylisoquinoline dimers had been known only from two *Ancistrocladus* species indigenous to the north-western region of the Democratic Republic of the Congo. The as yet unidentified liana reported in this chapter is so far the only *Ancistrocladus* plant discovered in the rainforests of the Central Congo Basin. It was found to produce such mbandakamine-type compounds, too.

From the leaves of this botanically unknown liana, four representatives were isolated, among them two new dimers, the mbandakamines B_3 (**38**) and B_4 (**39**). They were identified together with a series of four new 5,8'-coupled monomeric naphthylisoquinoline alkaloids, named ikelacongolines A−D (**35a**, **35b**, **36**, and **37**), along with five alkaloids (**40**−**44**) known from previous phytochemical studies on related Congolese *Ancistrocladus* species; three of them likewise belonging to the subclass of 5,8'-linked alkaloids, whereas two compounds were representatives of the quite rare 7,8'-coupling type. Particularly striking was the considerable number of *N*-methylated naphthylisoquinolines found in this botanically and phytochemically so far unexplored plant, among them the two new mbandakamines **38** and **39** and the four new monomeric ikelacongolines A−D (**35a**, **35b**, **36**, and **37**). More than half of the metabolites isolated from the leaf extract showed the presence of such an *N*-methyl group.

35a (ikelacongoline A)   **35b** (ikelacongoline B)   **36** (ikelacongoline C)   **37** (ikelacongoline D)

38: R = Me (mbandakamine B$_3$)
39: R = H (mbandakamine B$_4$)
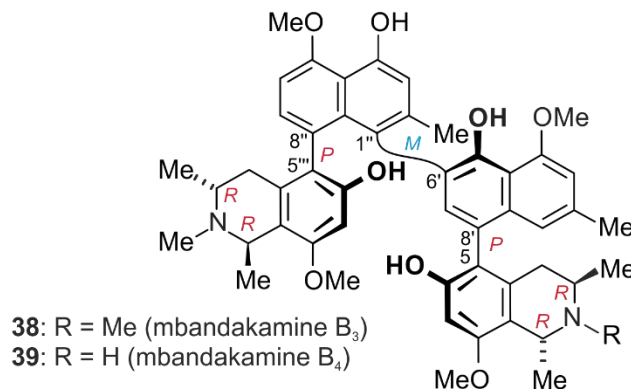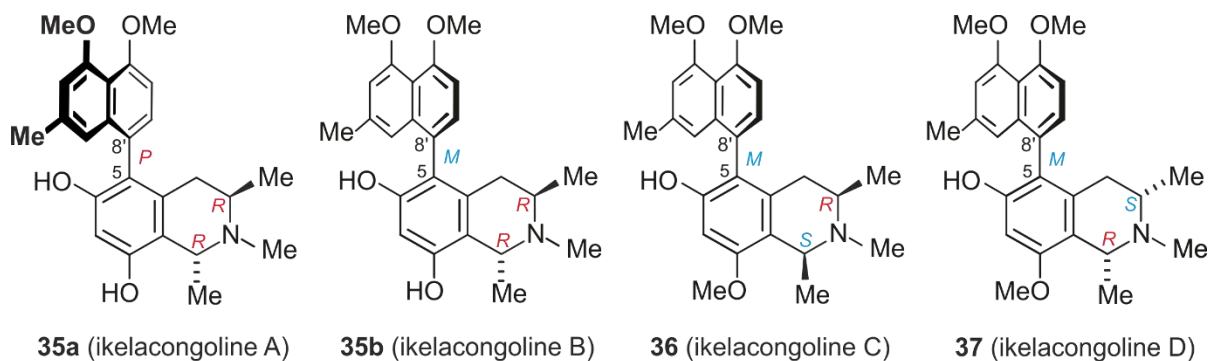
II.3 Phytochemical Investigations

The structures of these mono- and dimeric naphthylisoquinolines were chemotaxonomically quite significant, indicating a close phylogenetic relationship of this botanically unknown *Ancistrocladus* plant to other species from the Congo Basin, particularly in *A. ealaensis* and another, as yet unidentified taxon from the north-western part of the Democratic Republic of the Congo. These two species are likewise known to produce a high number of 5,8'-linked monomeric alkaloids along with mbandakamine-type dimers, and – like the unknown Central *Ancistrocladus* species presented here – their metabolite profiles were also dominated by mixed Ancistrocladaceae/Dioncophyllaceae, *i.e.*, hybrid-type alkaloids with *R*-configuration at C-3 and an oxygen function at C-6.

Furthermore, the new mbandakamines B$_3$ (**38**) and B$_4$ (**39**) have proven to be potent bioactive compounds. They displayed good to strong inhibitory effects against the pathogen of the African sleeping sickness, *Trypanosoma brucei rhodesiense*. They also exerted excellent activities against chloroquine-sensitive (NF54) and chloroquine-resistant (K1) strains of the malaria parasite *Plasmodium falciparum*. As many recommended therapeutic agents routinely used for the treatment of infectious diseases are threatened in their effectiveness by increasing resistance, the discovery of new agents is urgently needed. The promising activities of mbandakamine-type dimers warrant further investigations towards their antiparasitic potential, and with a focus on mono- and dimeric naphthylisoquinoline alkaloids in general.

II.4 (*R*)-Tonkafuranone and Related Compounds: Improved Synthesis, Stereochemical Purity in Nature, and Bioactivities of the Pure Enantiomers

II.4.1 Introduction

Due to their attractive and characteristic odor, terpenoids are frequently used natural flavor additives in the food and cosmetic industry. Most of them are constituents of essential oils in plants like *Mentha piperati* or *Bursera graveolens*.[263,264] Both species contain enantiomers of dehydromenthofurolactone (**7**), classified as an alicyclic lactone with $\alpha,\beta,\gamma,\delta$-unsaturation.[57] The compound has the chemical name of 5,6-dihydro-3,6-dimethyl-benzo-[*b*]-furan-2(4*H*)-one. Because of its occurrence in tonka beans (*Dipteryx odorata*), the *R*-enantiomer of **7**, compound **7a**, has also been named (*R*)-tonkafuranone. This stereoisomer was first described[265,57] as the dehydrogenated autoxidation product of menthofurane (**56**) and was later found in peppermint oils, contributing to their sweet and persistent coumarinic odor.[266,267] Moreover, it has been listed by the *Flavor and Extract Manufacturers' Association* (FEMA) and the U.S. *Food and Drug Administration* (FDA) *Center for Food Safety and Applied Nutrition* (CFSAN) as a *Generally Recognized As* Safe (GRAS) product.[57] Furthermore, the *S*-enantiomer of **7**, compound **7b**, was described to occur in the woody material of *Bursera graveolens*.[268]

However, recent toxicological studies on the chemically related mycotoxin patulin (**8**), generally found in rotten apples and several other foods, suggested that $\alpha,\beta,\gamma,\delta$-unsaturated lactones might form adducts with DNA bases by a Michael-addition mechanism,[269,270] raising new questions regarding the mutagenic properties of (*R*)-tonkafuranone (**7a**) and, thus, its safe usage in general.[269–271] In addition, patulin (**8**) was reported to be neurotoxic both *in vitro* and *in vivo*,[271–274] making more in-depth investigations of other, structurally related, lactones an urgent task.[271–273]

The current chapter represents a cooperation work between the research groups of Prof. M. Decker (synthetic and biological part), Prof. L. Lehmann (biological part), and our group (analytical part).[275] It describes a new, efficient access to both enantiomers **7a** and **7b** of tonkafuranone and derived analogs (Figure 30), all bearing the $\alpha,\beta,\gamma,\delta$-unsaturated lactone structure, starting from cheap and easily accessible chemicals. Using a newly developed separation protocol, the possible regioisomers and, where applicable, the enantiomers were successfully resolved and made available for biotesting.

II.4 (*R*)-Tonkafuranone and Related Compounds

Investigations in L. Lehmann's group showed low cytotoxicity in V79 cells, indicating that the molecular mechanisms that contribute to the high reactivity of patulin (**8**) towards cellular nucleophiles were not applicable for (*R*)-tonkafuranone (**7a**).
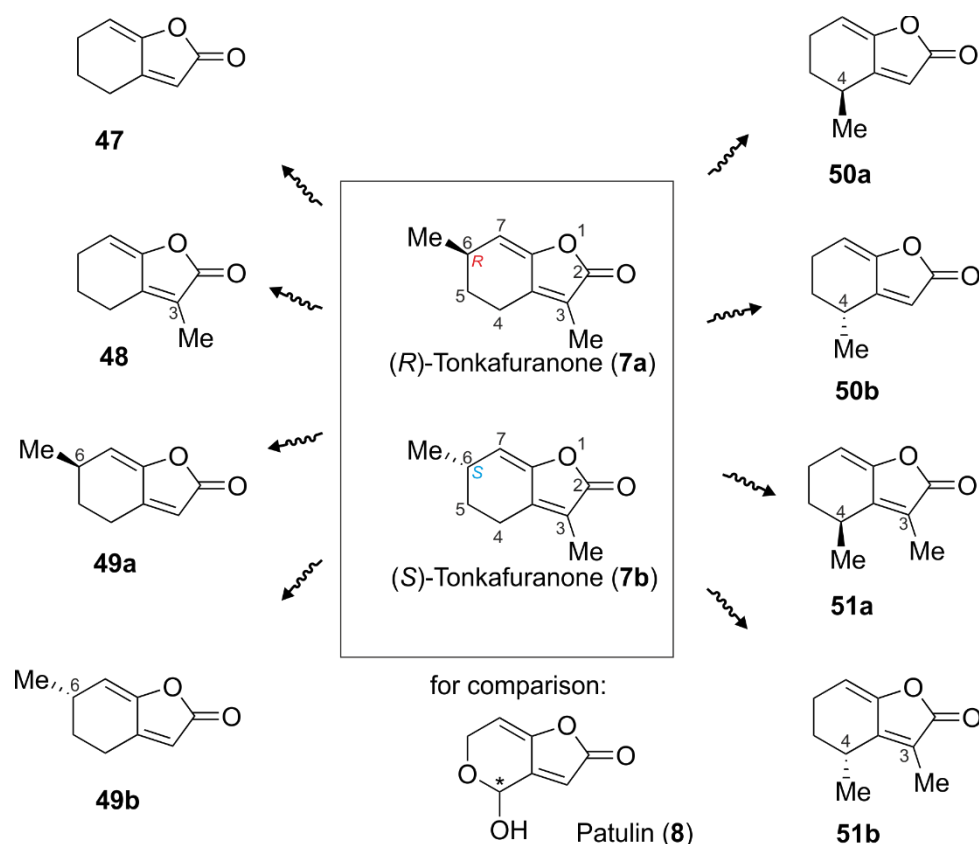
Figure 30. A series of 6- and/or 3-methylated and non-methylated *α,β,γ,δ*-unsaturated lactones inspired by the structure of the natural (*R*)- and (*S*)-tonkafuranones (**7a** and **7b**). Compound **7a** is a component of tonka beans and *Mentha piperita*,[266,276] while **7b** occurs in *Bursera graveolens*.[268] In the case of **49**, the pure enantiomers, **49a** and **49b**, were new, while the respective racemate was known.[277] For **50a/50b** and **51a/51b**, which are minor side products, even the racemates are new; but they were not considered for the biological evaluations due to the small quantities available. All other compounds, namely **47**, **48**, and racemates **49a/49b** and **7a/7b**, had already been described in the literature.[268,265,278,279] For comparison, see the related structure of patulin (**8**).

II.4.2 Results and Discussion

A general strategy described earlier, applying an aldol condensation and a lactone-formation in a one-pot procedure,[279,280] was used in Prof. Decker's group for the synthesis of all tonkafuranone-related compounds described in this chapter.

For the synthesis of the 6- and 3-unsubstituted analog **47** (Scheme 1), cyclohexanone (**52**) and glyoxylic acid (**53**) were used as starting materials.

The aldol condensation and lactonization took place in concentrated phosphoric acid, as described in the literature.[280] The methyl-free achiral product **47** was obtained after elimination of the acid, followed by flash column chromatography on silica gel. Likewise, the reaction of **52** with pyruvic acid (**54**) gave the 3-methylated analog **48**.

52   **53**: R = H   **47**: R = H
          54: R = Me   **48**: R = Me
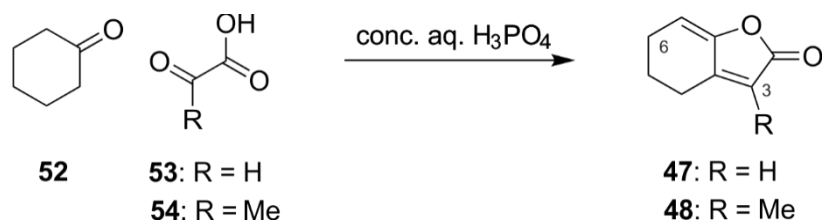
Scheme 1. Synthesis of 6-demethylated analogs of **7**.

In the case of 6-methyl derivatives (Scheme 2), the synthesis was conducted in the same manner, but starting with 3-methylcyclohexanone (**55**) as the educt, leading to the two regioisomers **49** and **50** in a ratio of 7:1 when using **53** as the α-keto acid, while **54** gave **7** and **51** in a regioisomeric ratio of 3:1.

55   **53**: R = H   **49**: R = H   **50**: R = H
          54: R = Me   **7**: R = Me   **51**: R = Me
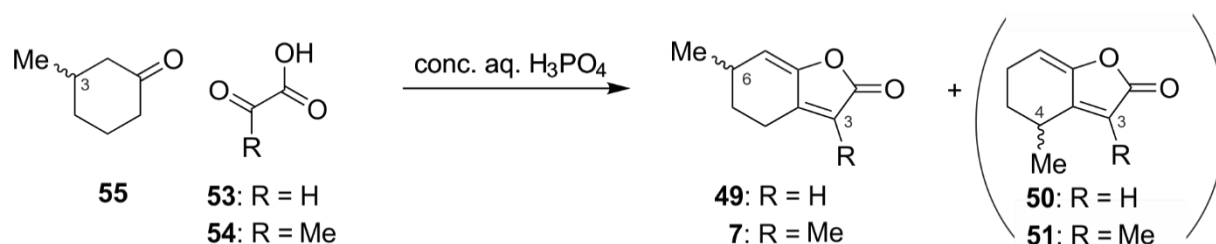
Scheme 2. Synthesis of the 6-methylated furanone derivatives **7** and **49**–**51**.

An achiral reverse-phase HPLC method using an (achiral) C18 Symmetry column was developed by the author of this series to resolve the regioisomeric mixture of **49/50**. A slightly modified method was used for the separation of the regioisomers **7/51** (Figure 31).
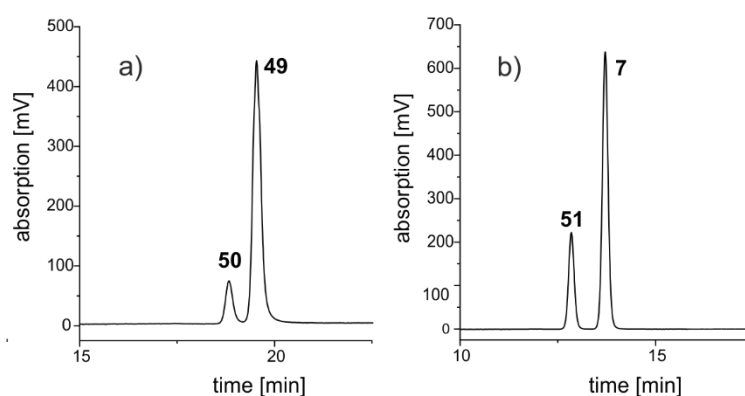
Figure 31. HPLC chromatograms, showing the successful resolution of a) the regioisomers **49** and **50**, and of b) **7** and **51** on an achiral C18 column.

The baseline enantio-separation of the resulting pure racemates **7** and **49–51** was achieved analytically and, in the case of **7** and **49**, on a preparative scale, using a chiral Lux cellulose-1 column. After resolution of **7** into pure **7a** and **7b** and that of **49** into pure **49a** and **49b**, their respective specific rotations were measured. Since the $[\alpha]_D^{25}$ values of **7a** and **7b** were known from the literature,[268,263] an unambiguous assignment of the peaks to the respective enantiomer was possible. However, for **49a** and **49b**, which were both new compounds, their absolute configurations were deduced online, by LC-ECD using a chiral stationary phase.

For the measurement of reference ECD spectra, the *R*-enantiomer **7a** was additionally provided by an independent semi-synthesis from a stereochemically well-known[281] chiral natural product, (+)-menthofuran (**56**), which is *R*-configured, by a previously described[282] oxidation with 2,3-dichloro-5,6-dicyano-1,4-benzoquinone (DDQ) (Scheme 3), performed by M. Hoffmann. In addition to its synthesis, the *S*-enantiomer **7b** was isolated by the author of this thesis from the woody part of *Bursera graveolens*, as described in the literature.[268,263]
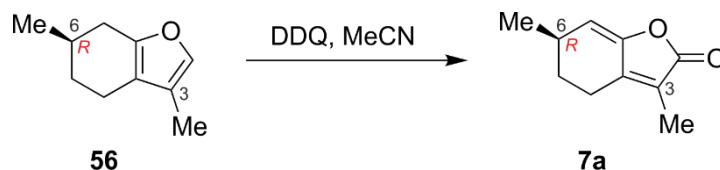
Scheme 3. Stereochemically unequivocal synthesis of **7a** as a reference compound for HPLC and ECD comparison.

Co-elution experiments confirmed that peaks **A** (t_R = 9.7 min) and **B** (t_R = 10.7 min) corresponded to the *S*- and *R*-enantiomers, respectively (Figure 32). These assignments were further corroborated by the measurement of an ECD spectrum of peak **A**, which was nearly identical to that of **7b**, and of an ECD curve of peak **B**, which, in turn, was most like that of **7a** (not shown).

Since **49** and **7** had the same chromophore, the absolute configuration of the new compounds **49a** and **49b** were assigned by comparison of their online ECD spectra with those of **7a** and **7b**. Accordingly, **49a** was *S*-configured and corresponded to peak **A'** (t_R = 18.4 min), while **49b** was *R*-configured and was contained in peak **B'** (t_R = 19.2 min) (not shown).
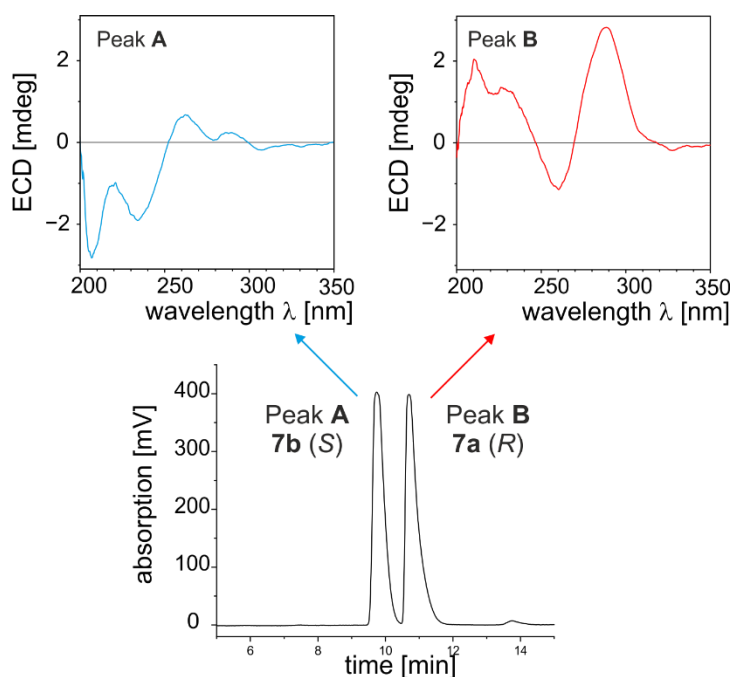
Figure 32. Resolution of the racemate **7b**/**7a** on a chiral phase (bottom) and the online ECD spectra of the resolved enantiomers **7b** and **7a** (top). Accordingly, peaks **A** and **B** correspond to **7b** (*S*) and **7a** (*R*), respectively.

In addition, due to the possibly occurring scalemic nature of chiral products,[283] the newly developed stereo-analytical method was also used by the author of this series to evaluate the enantiomeric purity of (*S*)-**7** isolated from the woody part of the incense tree *Bursera graveolens*. It was found that the used plant material contained this compound in an enantiomerically pure form (*S*:*R* = '100:0').

The compounds resulted from either synthesis or isolation by M. Hoffmann and the author of this thesis were assessed for their toxicity on V79 cells, previously used for the study of the cytotoxic and mutagenic patulin (**8**) in the group of Prof. L. Lehmann.[284] All tested compounds showed much less cytotoxic potential in V79 than the positive control patulin (**8**) (Table 11, Figure 33).

II.4 (*R*)-Tonkafuranone and Related Compounds

Table 11. Decrease in the number of V79 cells after treatment with various concentrations of patulin (**8**) (0.04–10 μM) and synthesized compounds (4–1,000 μM) over 24 h. Lowest concentrations inducing a significant decrease in the number of viable cells (Benchmark concentration) were identified by one-way ANOVA followed by Dunnett's test ($p < 0.05$) using the data from independent experiments

Compound	Benchmark concentration [μM]
Patulin (**8**)	0.26
7a	1,000
7b	1,000
47	160
48	> 1,000
49a	64
49b	64
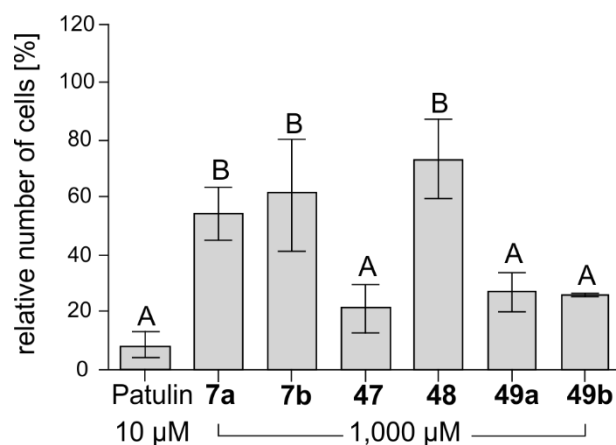
Figure 33. Relative numbers of living cells observed after treatment with the highest concentrations tested in relation to the number of living cells observed after incubation with solvent only (1% final methanol concentration, number of cells set at 100%). Depicted are means and standard deviations of independent experiments. Differences between relative numbers of living cells observed after treatment with different compounds were identified by one-way analysis of variance (ANOVA) with means comparison by Tukey's test ($p < 0.05$)[285] and are indicated by different alphabetic characters.

The furanone derivatives without substitution at C-3 (**47** and both enantiomers of **49**) exhibited both an important reduction in cell numbers at lower concentrations and a more pronounced

71

decrease of relative cell numbers at the highest tested concentration, when compared to the 3-methylated compounds (**48** and both enantiomers of **7**). Methylation at C-6 seemed not to affect the magnitude of the cytotoxic effect (Figure 33) nor did it strongly influence the benchmark concentration (Table 11). Furthermore, no substantial differences in cytotoxicity were observed between the enantiomers (**7a** *versus* **7b** and **49a** *versus* **49b**).

In murine hippocampal HT-22 cells, no toxicity was observed in the research group of Prof. M. Decker at the tested concentration (50 µM, Figure 34), which was below the lowest benchmark concentration in V79 cells (64 µM, Table 11). This finding suggested that hippocampal cells did not respond more sensitively to the synthesized compounds than V79 fibroblasts.
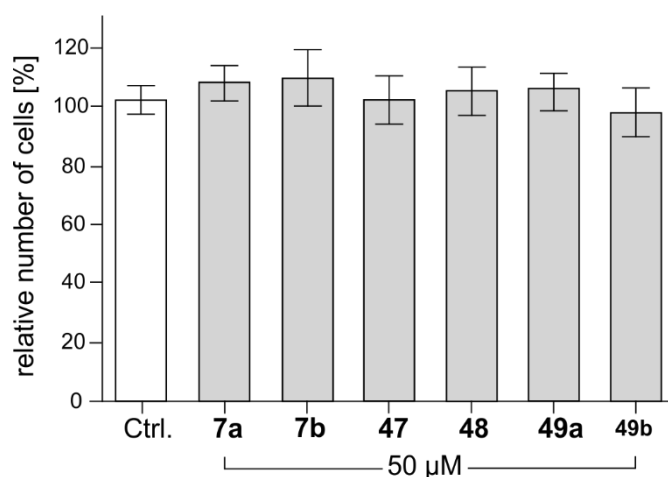
Figure 34. Relative number of HT-22 cells incubated for 24 h with compounds **7a**, **7b**, **47**, **48**, **49a**, and **49b** at a concentration of 50 µM. Results are presented as percentage to control cells (Ctrl.) treated with 0.05% DMSO (number of cells set at 100%). Data are expressed as means ± SD of three independent experiments. One-way ANOVA showed no significant difference between the different treatment groups.

II.4.3 Conclusion

This chapter describes a convenient one-step synthesis of the natural food flavor (*R*)-tonkafuranone (**7a**, also known as dehydromenthofurolactone) and of its likewise natural (*S*)-enantiomer **7b** together with of a series of related mono- and dimethyl compounds (**47**, **48**, and **49**). This synthetic strategy developed by the Decker's group was combined with a simple and efficient resolution of the regioisomers and, where chiral compounds were concerned, the enantio-separation as elaborated in this thesis, jointly making this approach an attractive option for obtaining material to be submitted to structure-biological activity studies within this class of compounds. It could easily be enlarged using various other acids or ketones as raw materials.

With this series of compounds in hands, it was possible to assess the structure-activity relationship towards the cytotoxicity of *α,β,γ,δ*-unsaturated bicyclic lactones in Prof. L. Lehmann's group, which revealed that methylation at C-3 could decrease their toxicity. However, methylation at C-6 and the absolute configuration of the stereogenic center in position 6, seemed not to influence their toxicity in a pronounced manner.

Moreover, all studied compounds were at least 250 times less toxic than patulin (**8**), which shares with them a similar *α,β,γ,δ*-unsaturated lactone structure. Patulin (**8**) had recently been reported to undergo Michael-like 1,6-addition reactions with nucleophiles, but also to be subjected a simultaneous shift of the double bond giving a *β,γ*-unsaturated enol-lactone, susceptible to a further nucleophilic attack to the carbonyl group.[269,286] The same reactions could also be possible with the synthesized compounds lacking a methyl group in position 3. Yet, in the case of patulin (**8**), further reactions involving its hemiacetal ring (not present in the synthesized compounds) are known to be possible.[286,270] Thus, the molecular mechanisms contributing to the high reactivity of patulin (**8**) towards cellular nucleophiles seem not to apply for (*R*)-tonkafuranone (**7a**). Nevertheless, a cytotoxic potential does not necessarily imply a mutagenic one. Therefore, tests evaluating the mutagenicity of the synthesized compounds with respect to their mechanism of reaction towards cellular nucleophiles are currently being done in Prof. L. Lehmann's group.

III. Summary/Zusammenfassung

III.1 Summary

Nowadays, the management of infectious diseases is especially threatened by the rapid emergence of drug resistance. It has been suggested that the medicine quality assurance combined with a good medication adherence may help reducing this impendence. Moreover, the search of new antimicrobial agents from medicinal plants is strongly encouraged for the exploration of alternatives to existing therapies. In this context, the present work focused on both the quality evaluation of commercialized antimalarial medicines from the Democratic Republic of the Congo (DRC) and on the phytochemical investigations of a Congolese *Ancistrocladus* species.

The results obtained in this dissertation are detailed in the following lines:

1) Quality of the antimalarial medicine artemether - lumefantrine in eight cities of the Democratic Republic of the Congo

The visual inspection showed that nearly half of the 150 collected samples had been manufactured in India and more than a quarter had been produced locally (DRC). Most samples had shelf-lives of two or three years except for three Coartem® samples, which were labeled as originating from the USA or from China, with the batch numbers F2929, F2153, and X1341. Their unusually long shelf-lives (four or five years) made these three samples suspicious, being the first ones to be chemically investigated.

During TLC analysis, the three suspicious Coartem® samples were the only ones without any of the declared active ingredients. Together with the results from the visual inspection, they were considered as falsified. These samples had been collected in Mbandaka and Mbuji-Mayi. A sample collected in Matadi showed only one spot corresponding to lumefantrine (**12**). This sample was considered as a falsified product as well.

HPLC analysis confirmed the qualitative results obtained by TLC, showing the absence of both APIs in the falsified Coartem® samples and the lack of artemether in the sample from Matadi. Quantitative outcomes showed that the artemether (**10a**) content ranged between 0 and 147.3% and the lumefantrine (**12**) content varied from 0 to 142.7%.

10a   **12**

Summary of the HPLC-UV assays; contents in %.

Country of origin	Formulation	Artemether (**10a**)			Lumefantrine (**12**)		
		x < 90	x > 110	90 ≥x ≤ 110	x < 90	x > 110	90 ≥x ≤ 110
China	T	1	-	2	1	-	2
	P	-	-	-	-	-	-
DRC	T	-	1	11	-	1	11
	P	12	3	16	16	1	14
India	T	7	1	36	-	-	44
	P	18	8	9	12	6	17
Netherlands	T	-	-	-	-	-	-
	P	6	-	2	1	-	7
USA	T	2	4	11	2	-	15
	P	-	-	-	-	-	-
Totals		46	17	87	32	8	110
Frequency [%]		30.7	11.3	58	21.3	5.3	73.3

T: tablet; P: powder for oral suspension; x: the amount of the API determined relative to the amount stated on the packaging.

HPLC analysis also permitted to classify the samples following their chromatographic impurity profiles. Apart from the peaks corresponding to the active ingredients (artemether (**10a**) and lumefantrine (**12**)), 15 samples were found to have two additional peaks and 28 samples even shared three additional compounds, eluting near the artemether peak.

LC-MS measurements carried out on selected samples showed that the molecular weights of the additional peaks found during HPLC analysis were related to that of lumefantrine (*viz.*, *m/z* = 406, 420, 436), corresponding to compounds previously described in the literature.

2) Capillary zone electrophoresis for the determination of amodiaquine and three of its synthetic impurities in pharmaceutical formulations

III.1 Summary

During method development, the following conditions were found to be optimal for the simultaneous determination of amodiaquine (**13**), of the three related compounds **30–32**, and of the internal standard **34**: The buffer contained sodium phosphate (100 mM) adjusted at pH 6.2 with phosphoric acid. The applied voltage was +20 kV and the temperature was 25 °C, using a fused-silica capillary and a detection wavelength of 220 nm. The total analysis time was as short as 20 min, although the longest migration time was 13.2 min. Under these conditions the generated current was around 46.8 μA. The lowest resolution value between the related compound **32** and the internal standard **34** was used for the system suitability test.
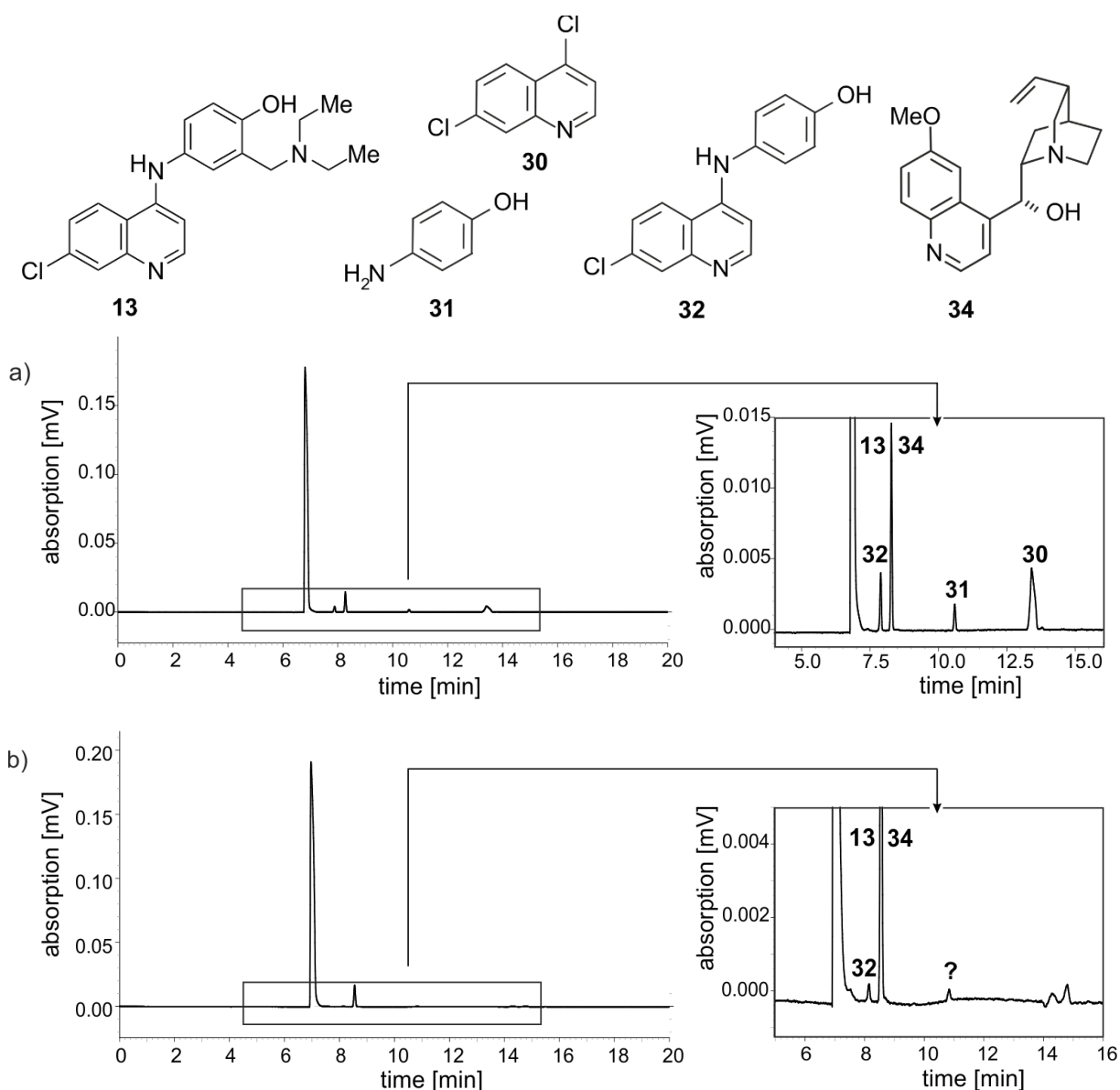
The developed method was validated for both the content determination of the main component (amodiaquine, **13**) as well as for the impurity profiling according to the *International Conference for Harmonization* (ICH) guidelines. During method validation, the following

criteria were evaluated: specificity, linearity, accuracy, stability of the solutions, limits of detection (LOD), and quantification (LOQ), robustness. The method was found to be appropriate for the intended purposes.

The developed and validated method was successfully applied to assess the quality of four batches of ASAQ drug samples (Winthrop®, Arteplus®, Sunat-A forte®, Sunat-A®) that had been collected in Kinshasa, DRC. This assessment demonstrated a good conformity of the results of the quantitative measurements of the main component (amodiaquine, **13**) with those obtained by the HPLC method described in *The International Pharmacopoeia*. All analyzed drug samples were found to comply with the specification concerning the content of the API, *i.e.*, 90−110% of the label claim. Two batches from the same manufacturer contained two detectable impurities, one was 4-[(7-chloroquinolin-4-yl)amino]phenol (**32**). The other one was unknown. The presence of **32** and other unknown impurities was likewise confirmed by HPLC.

3) Phytochemical investigations on a Congolese *Ancistrocladus* liana

From an as yet undescribed *Ancistrocladus* species, four mbandakamine-type naphthylisoquinoline dimers, among them two new ones, the mbandakamines B_3 (**38**) and B_4 (**39**), were isolated and structurally characterized using spectroscopic, chemical, and chiroptical methods. They were all unsymmetric 6',1''-linked dimeric representatives consisting of two 5,8'-coupled monomeric moieties. Pharmacologically, compounds **38** and **39** showed excellent antiplasmodial activities against both NF54 and K1 strains *of P. falciparum*, with IC_{50} values of 39 (NF54) and 6 nM (K1) for **38**, and 66 (NF54) and 26 nM (K1) for **39**.

III.1 Summary
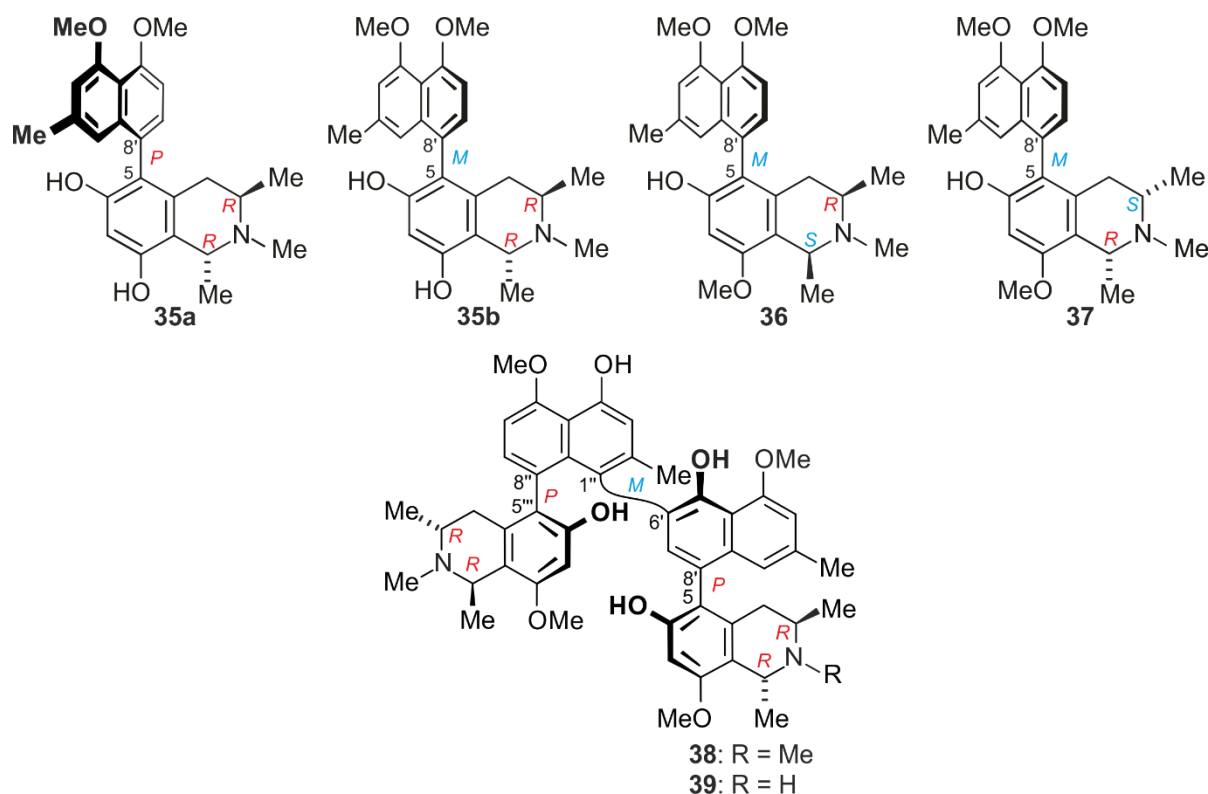
Besides the mbandakamines, four new 5,8'-coupled monomeric naphthylisoquinoline alkaloids, named ikelacongolines A–D (**35a**, **35b**, **36**, and **37**), were also identified, together with five alkaloids, compounds **40–44**, known from previous phytochemical studies on related Congolese *Ancistrocladus* species; three of them likewise belonged to the subclass of 5,8'-linked alkaloids, whereas two compounds were representatives of the quite rare 7,8'-coupling type.

4) (*R*)-Tonkafuranone and related compounds: improved synthesis, stereochemical purity in nature, and bioactivities of the pure enantiomers

A convenient one-pot synthesis (developed by M. Hoffmann from the research group of Prof. M. Decker) of the natural food flavor (*R*)-tonkafuranone (**7a**), of its likewise natural *S*-enantiomer **7b**, and of a series of dimethyl and monomethyl compounds, **47**, **48**, and **49**, was achieved. This one-pot synthesis was combined with a simple and efficient separation of the resulting regioisomers and, where chiral compounds were involved, their enantio-resolution, making this joint strategy an attractive option for structure-activity studies within this class of compounds.
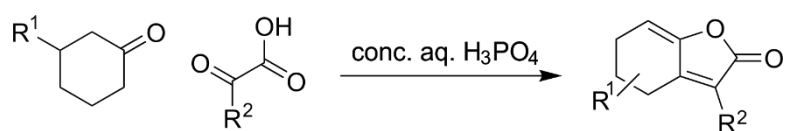
The availability of this series of compounds in hands made it possible to assess the structure-activity relationship to characterize the cytotoxicity of these $\alpha,\beta,\gamma,\delta$-unsaturated bicyclic lactones (done by Dr. C. Kleider from the research group of Prof. L. Lehmann), showing that methylation at C-3 apparently decreased their cytotoxicity. However, the presence of a methyl group at C-6 and the absolute configuration of the stereogenic center in position 6 seemed to not strongly affect the general toxicity.

In conclusion, this dissertation contributes to tackle the problems related to the fight against malaria, the antimicrobial drug resistance by the evaluation of the quality of antimalarial medicines sold in the Congo, and the discovery of novel antiplasmodial naphthylisoquinoline alkaloids.

III.2 Zusammenfassung

Heute ist die Behandlung von Infektionskrankheiten besonders durch das schnelle Auftreten von Arzneimittelresistenzen bedroht. Es wurde vorgeschlagen, dass eine gute Arzneimittelqualitätssicherung in Verbindung mit einer sicheren Medikamentenhaftung dazu beitragen kann, dieser Gefahr entgegenzuwirken. Darüber hinaus wird unter anderem die Suche nach neuen antimikrobiellen Wirkstoffen aus Heilpflanzen dringend empfohlen, um nach Alternativen zu bestehenden Therapien Ausschau zu halten. In diesem Zusammenhang konzentrierte sich die vorliegende Arbeit sowohl auf die Qualitätsbewertung der in der Demokratischen Republik Kongo (DR Kongo) vermarkteten Malariamittel, als auch auf die phytochemische Untersuchung einer kongolesischen *Ancistrocladus*-Art.

Die Ergebnisse dieser Dissertation sind in den folgenden Zeilen detailliert dargestellt:

1) Die Qualität des Malaria-Medikaments Artemether - Lumefantrin wurde in acht Städten der Demokratischen Republik Kongo untersucht.

Die visuelle Inspektion ergab, dass fast die Hälfte der 150 gesammelten Proben in Indien hergestellt worden war und mehr als ein Viertel lokal produziert worden war (DR Kongo). Die meisten Proben hatten eine Haltbarkeit von zwei oder drei Jahren, mit Ausnahme von drei Coartem®-Proben, deren Herkunftsländer als USA oder China bezeichnet wurden, mit den Chargennummern F2929, F2153 und X1341. Ihre ungewöhnlich langen Haltbarkeitszeiten (vier oder fünf Jahre) machten diese drei Proben verdächtig, sie wurden daher als erste chemisch untersucht.

Bei der DC-Analyse waren die drei verdächtigen Coartem®-Proben die einzigen ohne die genannten Wirkstoffe. Zusammen mit den Ergebnissen der visuellen Inspektion wurden diese Proben als Fälschung betrachtet. Diese Proben waren in Mbandaka und Mbuji-Mayi gesammelt worden. Eine in Matadi gesammelte Probe zeigte in der Dünnschicht-Chromatographie nur einen Spot, der Lumefantrin (**12**) entsprach. Diese Probe wurde ebenfalls als gefälschtes Produkt betrachtet.

Die HPLC-Analyse bestätigte die per DC erhaltenen qualitativen Ergebnisse: das Fehlen beider APIs in den gefälschten Coartem®-Proben und das Fehlen von Artemether (**10a**) in der Probe von Matadi. Quantitative Ergebnisse zeigten, dass der Gehalt an Artemether (**10a**) zwischen 0 und 147.3% lag und der Lumefantringehalt zwischen 0 und 142.7% variierte.

10a   **12**
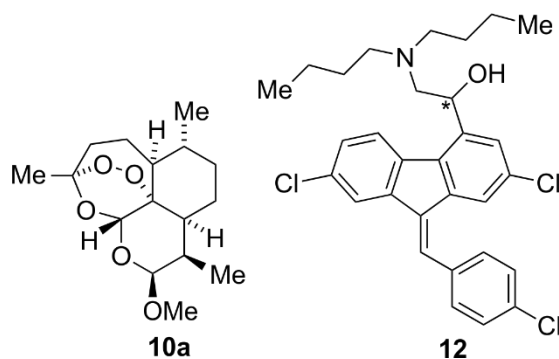
Zusammenfassung der HPLC-UV-Assays; Gehalt in %

Herkunftsland	Arzneiform	Artemether (**10a**)			Lumefantrin (**12**)		
		x < 90	x > 110	90 ≥ x ≤ 110	x < 90	x > 110	90 ≥ x ≤ 110
China	T	1	-	2	1	-	2
	P	-	-	-	-	-	-
DR Kongo	T	-	1	11	-	1	11
	P	12	3	16	16	1	14
Indien	T	7	1	36	-	-	44
	P	18	8	9	12	6	17
Niederlande	T	-	-	-	-	-	-
	P	6	-	2	1	-	7
USA	T	2	4	11	2	-	15
	P	-	-	-	-	-	-
Summen		46	17	87	32	8	110
Häufigkeit [%]		30.7	11.3	58	21.3	5.3	73.3

T: Tablette; P: Pulver zur oralen Suspension; x: Der Wirkstoffgehalt wird in Bezug auf die auf der Verpackung angegebene Masse bestimmt.

Die HPLC-Analyse ermöglichte auch die Klassifizierung der Proben nach ihren chromatographischen Verunreinigungsprofilen: Abgesehen von den Peaks, die den aktiven Bestandteilen (Artemether (**10a**) und Lumefantrin (**12**)) entsprachen, wurden bei 15 Proben zwei zusätzliche Peaks gefunden, in 28 Proben sogar drei Peaks, die in der Nähe des Artemether-Peaks eluierten.

III.2 Zusammenfassung

An ausgewählten Proben durchgeführte LC-MS-Messungen zeigten, dass die Molekulargewichte der zusätzlichen Peaks, die während der HPLC-Analyse gefunden wurden, mit denen von Lumefantrin (**12**) in Beziehung standen (d.h. *m/z* = 406, 420, 436), entsprechend den zuvor in der Literatur beschriebenen Verbindungen.

2) Kapillarzonenelektrophorese wurde zur Bestimmung von Amodiaquin und drei seiner synthetischen Verunreinigungen in pharmazeutischen Formulierungen durchgeführt.

Während der Verfahrensentwicklung erwiesen sich die folgenden Bedingungen als optimal für die gleichzeitige Bestimmung von Amodiaquin (**13**), den drei verwandten Verbindungen **30–32** und dem internen Standard **34**: Der verwendete Puffer wurde mit 100 mM Natriumphosphat, das mit Phosphorsäure auf pH 6.2 eingestellt wurde, angesetzt. Unter Verwendung einer Quarzglas-Kapillare wurde eine Spannung von +20 kV bei einer Temperatur von 25 °C angelegt. Als Detektionswellenlänge wurde 220 nm ausgewählt. Die Gesamtanalysezeit betrug nur 20 Minuten, obwohl die längste Migrationszeit 13.2 Minuten betrug. Unter diesen Bedingungen lag die erzeugte Stromstärke bei etwa 46.8 A. Der niedrigste Auflösungswert zwischen der verwandten Verbindung **32** und dem internen Standard **34** wurde für den Systemeignungstest verwendet.
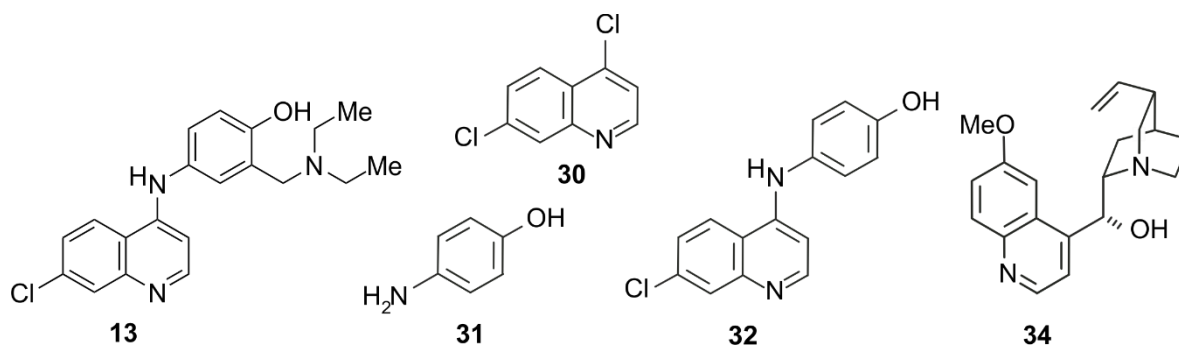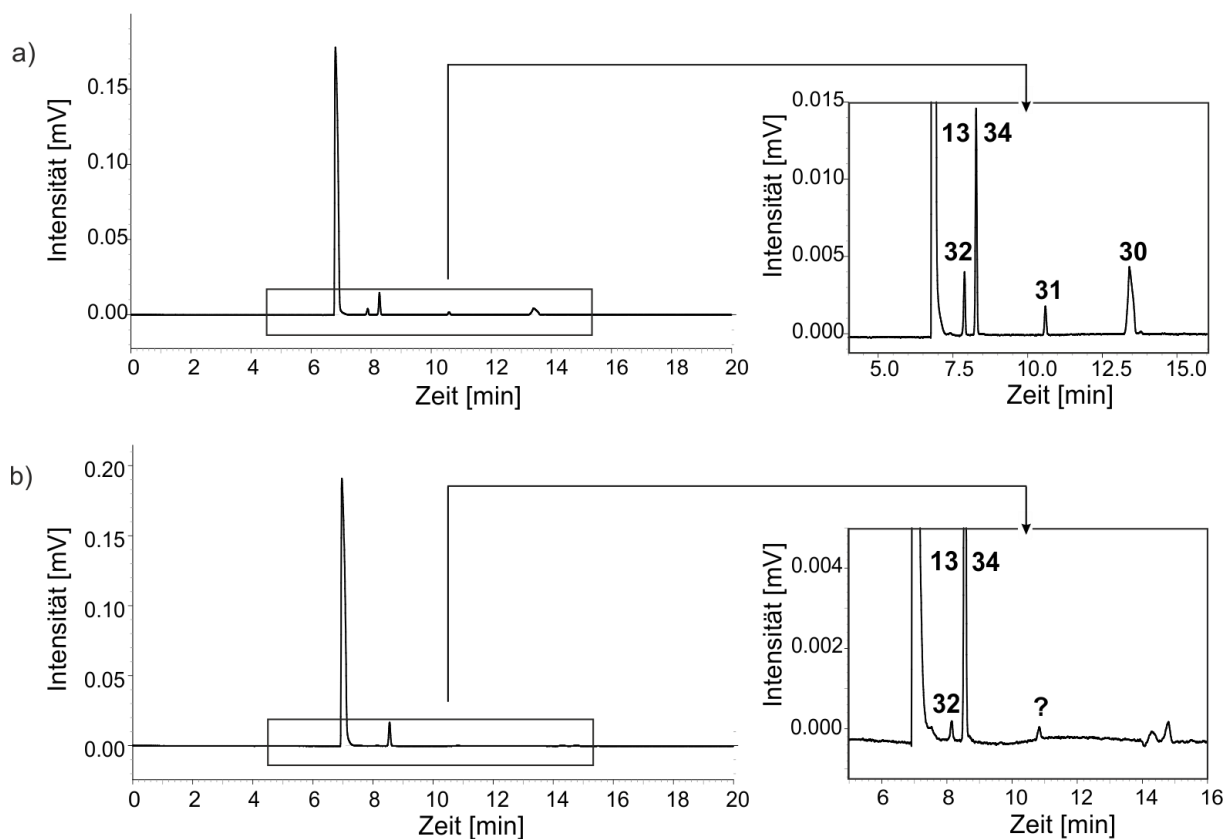
Die entwickelte Methode wurde sowohl für die Inhaltsbestimmung der Hauptkomponente Amodiaquin (**13**) als auch für die Verunreinigungsprofilierung gemäß den Richtlinien des *International Council for Harmonization* (ICH) validiert. Bei der Methodenvalidierung wurden die folgenden Kriterien bewertet: Spezifität, Linearität, Genauigkeit, Stabilität der Lösungen, Nachweisgrenzen (LOD) und Quantifizierung (LOQ) sowie Robustheit. Die Methode wurde für die beabsichtigten Zwecke als geeignet befunden.

Die entwickelte und validierte Methode wurde erfolgreich auf die Bewertung der Qualität von vier Chargen von ASAQ-Arzneimittelproben (Winthrop®, Arteplus®, Sunat-A forte®, Sunat-A®) angewendet, die in Kinshasa, DR Kongo, gesammelt worden waren. Die Ergebnisse dieser Bewertung zeigten eine gute Übereinstimmung der quantitativen Messungen der Hauptkomponente Amodiaquin (**13**) mit denen, die durch die in *The International Pharmacopoeia* beschriebene HPLC-Methode erhalten worden waren. Es wurde festgestellt, dass alle analysierten Arzneimittelproben in Bezug auf den Inhalt der API der Spezifikation entsprachen, d. h. 90−110% des Kennzeichnungsanspruchs.

86

III.2 Zusammenfassung

Zwei Chargen desselben Herstellers enthielten zwei nachweisbare Verunreinigungen, von denen eine 4-[(7-Chlorchinolin-4-yl)amino]phenol (**32**) und die andere unbekannt war. Das Vorhandensein der verwandten Verbindung **32** und anderer unbekannter Verunreinigungen wurde ebenfalls durch die HPLC-Analyse bestätigt.

3) Phytochemische Untersuchung an einer kongolesischen *Ancistrocladus*-Pflanze

Von einer noch nicht beschriebenen *Ancistrocladus*-Art wurden vier Naphthylisochinolin-Dimere vom Mbandakamin-Typ, darunter zwei neue, die Mbandakamine B₃ (**38**) und B₄ (**39**), isoliert und mit spektroskopischen, chemischen und chiroptischen Methoden strukturell charakterisiert. Bei beiden Verbindungen handelte es sich um unsymmetrische, 6',1''-verknüpfte dimere NIQs, die aus zwei 5,8'-gekuppelten Monomereinheiten bestehen. Pharmakologisch zeigten die Verbindungen **38** und **39** ausgezeichnete antiplasmodiale Aktivitäten sowohl gegen den NF54- als auch gegen den K1-Stamm von *P. falciparum*, mit IC$_{50}$-Werten von 39 (NF54) und 6 nM (K1) für **38** und 66 (NF54) und 26 nM (K1) für **39**.

38: R = Me
39: R = H
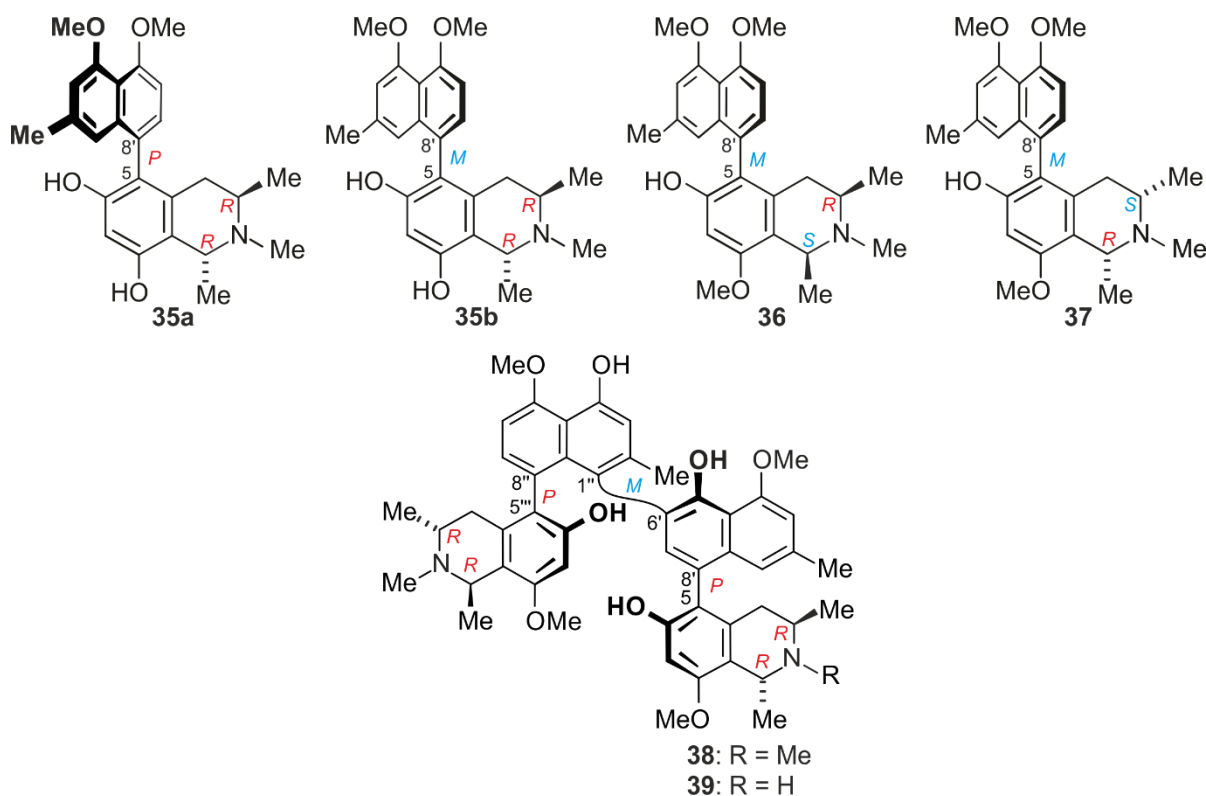
Neben den Mbandakaminen wurden vier neue 5,8'-gekuppelte monomere Naphthylisochinolin-Alkaloide, genannt Ikelacongoline A–D (**35a**, **35b**, **36** und **37**) zusammen mit fünf Alkaloiden, **40–44**, identifiziert, die aus früheren phytochemischen Studien mit verwandten kongolesischen *Ancistrocladus*-Arten bekannt waren; drei von ihnen gehörten ebenfalls zur Unterklasse der 5,8'-verknüpften Alkaloide, während zwei Verbindungen Vertreter des recht seltenen 7,8'-Kupplungstyps waren.

4) (*R*)-Tonkafuranon und verwandte Verbindungen: verbesserte Synthese, stereochemische Reinheit in der Natur und Bioaktivität der reinen Enantiomere

Mit einer praktikablen Eintopfsynthese (entwickelt von M. Hoffmann aus der Forschungsgruppe von Prof. M. Decker) des natürlichen Aromastoffs (*R*)-Tonkafuranon (**7a**), seines ebenfalls natürlichen *S*-Enantiomers **7b** und einer Reihe von Dimethyl und Monomethyl wurden die Verbindungen **47**, **48** und **49** gewonnen. Diese Eintopfsynthese wurde kombiniert mit einer einfachen und effizienten Trennung der resultierenden Regioisomere und ihrer Racemattrennung, was diese Strategie zu einer attraktiven Option für Struktur-Aktivitätsstudien innerhalb dieser Verbindungsklasse machte.
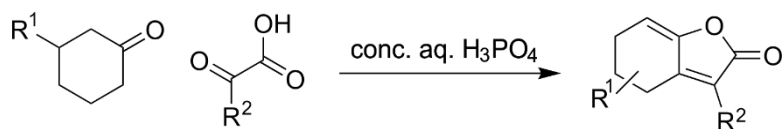
Mit dieser Reihe von Verbindungen wurde eine Struktur-Aktivitäts-Beziehung aufgestellt, die die Zytotoxizität solcher α, β, γ, δ-ungesättigten bicyclischen Lactone charakterisiert (durchgeführt von C. Kleider aus der Forschungsgruppe von Prof. L. Lehmann). Diese zeigte, dass eine Methylierung an C-3 die Zytotoxizität verringert. Eine Methylierung an C-6 und die absolute Konfiguration des stereogenen Zentrums in Position 6 schienen jedoch die allgemeine Toxizität nicht stark zu beeinflussen.

Zusammenfassend trägt diese Dissertation dazu bei, die Entwicklung der Resistenz gegen antimikrobielle Wirkstoffe zu reduzieren, indem die Qualität der im Kongo verkauften Malaria-Medikamente bewertet und neue antiplasmodische Naphthylisochinolin-Alkaloide entdeckt wurden.

IV. Experimental Section

IV.1 General Aspects

IV.1.1 Analytical Instruments

Ultraviolet spectroscopy (*UV*): UV spectra were measured at room temperature with a Shimadzu UV-1800 spectrophotometer.

Infrared spectroscopy (*IR*)**:** IR spectra were recorded with a Jasco FT-IR-4600 type A spectrometer.

Electronic circular dichroism spectroscopy (*ECD*): ECD spectra were measured at room temperature with a J-715 spectropolarimeter with quartz crystal cells. The differential absorption coefficient $\varepsilon\Delta$ [$cm^2\, mol^{-1}$] at different wavelengths λ [nm] was measured in the given solvent. For baseline correction, a blank sample of eluent was measured. They were processed using SpecDis.[287]

Optical rotation**:** Optical rotation values were recorded on a Jasco P-1020 polarimeter at the sodium-D line ($\lambda = 589$ nm).

Gas chromatography coupled to mass spectrometry (*GC-MSD*): GC-MSD analyses were carried out on a Shimadzu GCMS-QP 2010SE.

Nuclear magnetic resonance spectroscopy (*NMR*): 1D and 2D NMR spectra were recorded on Bruker AVANCE III HD 400 (400 MHz) and 600 (600 MHz) instruments in deuterated methanol or chloroform ($CDCl_3$, CD_3OD). Chemical shifts (δ) are reported in parts per million (ppm) with the ^1H and ^{13}C signals of the solvent (^1H, $\delta = 3.31/7.26$ ppm; ^{13}C, $\delta = 49.15/77.01$ ppm) as the internal reference. Signal multiplicity is given using the following abbreviations: singlet = s, doublet = d, doublet of doublets = dd, triplet = t, doublet of triplets = dt, quartet = q, and multiplet = m. Coupling constants are described in Hertz (Hz), where ^nJ gives the number of bonds. Spectra were acquired and processed using the Topspin 3.5 software (Bruker Daltonics).

High-resolution electrospray ionization mass spectrometry (*HRESIMS*): HRESIMS spectra were measured on a Bruker microTOF-focus and a micrOTOF-Q III mass spectrometers.

Liquid chromatography coupled to electrospray ionization mass spectrometry (*HPLC-ESI-MS*): HPLC-ESI-MS analysis were performed on an Agilent 1100 Series System equipped with an HPLC pump, MSD Ion Trap mass spectrometer (nebulizer pressure: 50 psi, drying gas flow: 10 L/min, drying gas temperature: 230 °C, capillary voltage: 3500 V; N_2 as the heating gas).

Thin-layer chromatography (*TLC*): All TLC analyses were carried out using silica gel 60 F_{254} plates (Merck, Darmstadt, Germany) and appropriate solvent systems. Spots were revealed using visible light, UV light (254 or 366 nm), or a staining reagent like I_2, $KMnO_4$, or H_2SO_4.

Column chromatography (*CC*): CC experiments were conducted using silica gel with a particle size of 40−63 μM (VWR chemicals, Leuven, Belgium) as the stationary phase and appropriate eluent system like petroleum ether (PE) and ethyl acetate (EA).

High-performance liquid chromatography (HPLC): Analytical HPLC experiments were performed using several instruments, including an Agilent 1100 Series System (see description above), a Shimadzu System equipped with a DGU-20A3R controller, an LC20AB liquid chromatograph, and SPD-20A UV/Vis detector, a Merck/Hitachi HPLC system with a DAD detector. Preparative HPLC separation was carried out on a Jasco HPLC system (PU-2087, UV-2077, LC-NetII/ADC) or on a Jasco System (PU-1580 Plus) in combination with UV/Vis detection at 200−680 nm (Jasco MD-2010 Plus diode array detector) at room temperature. Likewise, several columns were used, namely a SymmetryPrep C18 column (Waters, 19 × 300 mm, 7 μm) or an Agilent Eclipse XDB C18 column (150 × 4.6 mm, 5 μm particle size)

Capillary electrophoresis (*CE*): CE analyses were performed on a Beckman P/ACE MDQ capillary electrophoresis instrument (Beckman Coulter GmbH, Krefeld, Germany), equipped with a capillary cartridge cooling system and a photodiode array detector (PDA). The data were acquired and processed using the Beckman 32 Karat software (version 4.01). The capillary tubes (length 60.2 cm, effective length 50 cm, internal diameter 50 μm) were obtained from BGB Analytik (Schloßboeckelheim, Germany). The applied voltage was 20 kV using normal polarity. The temperature of the capillary was maintained at 25 °C and all samples were injected applying a pressure of 0.5 psi for 10 s. The detector was set to 220 nm using a data sampling rate of 4 Hz, a bandwidth of 10 nm, and the normal filtering. New capillaries were preconditioned at 40 °C by rinsing them with 100 mM aqueous NaOH (10 min), purified water (5 min), 100 mM aqueous H_3PO_4 (10 min), and for a second time, with purified water (5 min) at a pressure of 40 psi.

Between two runs, the capillary was flushed using the following reagents at 40 psi and 25 °C: 0.1 M NaOH for 5 min, 0.1 M H_3PO_4 for 3 min, purified water for 3 min, and the running buffer for 5 min. The pH values were determined using a calibrated glass electrode from Radiometer Analytical (Villeurbanne, France). All solutions were passed through 0.2 μm syringe filters prior to use.

Other apparatuses: 24-well plates (Nunc™, 8.6 x 10^3 cells per cm^2) were purchased from Thermo Fisher Scientific (Schwerte, Germany), CASY Model DT was obtained from Schaerfe System GmbH (Reutlingen, Germany), sterile 96-well plates (TC-Plate 96 Well, Standard, F) were supplied by Sarstedt (Nümbrecht, Germany), and a multi-well plate photometer (SpectraMax 250) was fromTecan (Männedorf, Switzerland).

IV.1.2 Chemicals and Cell Lines

Solvents: All used organic solvents were of analytical-grade quality and obtained from different sources, including VWR International GmbH (Ismaning, Germany). Ultrapure water was provided by the Purelab Classic System (Elga, VWS, UK) or by a Milli-Q® laboratory water system from Merck Millipore (Darmstadt, Germany).

Other chemicals: Artemether (**10a**, purity 98%) was purchased from abcr (Karlsruhe, Germany). Lumefantrine (**12**, purity 99.98%), sodium hexane sulfonate monohydrate (purity ≥ 98%), 1-propanol (purity 99.9%), amodiaquine (**13**) dihydrochloride dihydrate, *N*-deethylamodiaquine (**33**), 4-[(7-chloroquinolin-4-yl)amino]-phenol, 4,7-dichloroquinoline (**30**), 4-aminophenol (**31**), chloroquine (**1**) diphosphate, quinine (**34**), sodium dodecyl sulfate, tris(hydroxymethyl)aminomethane (Tris), (*S*)-MTPA, and sodium tetraborate decahydrate were obtained from Sigma-Aldrich (Steinheim, Germany). Disodium hydrogen phosphate dihydrate and sodium dihydrogen phosphate monohydrate were obtained from Merck (Darmstadt, Germany). Orthophosphoric acid, sodium hydroxide, potassium hydroxide, potassium dihydrogen phosphate, hydrochloric acid, acetic acid, sodium acetate, triethanolamine, and triethylamine were purchased from Gruessing (Filsum, Germany). Fetal calf serum (Invitrogen™) was obtained from Thermo Fisher Scientific (Karlsruhe, Germany). Patulin (**8**) was kindly provided by M. Metzler and R. Fliege (Karlsruhe Institute of Technology, Germany) to Prof. L. Lehmann's research group, it was biosynthesized, purified, and characterized as described previously.[288]

Cell lines: Used in the research group of Prof. L. Lehmann, V79 cells, exhibiting defined glutathione-*S*-transferase activity, were kindly provided by H. Glatt (German Institute of Human Nutrition, Potsdam, Germany),[289] while HT-22 cells were generously donated by Prof. D. Schubert (Salk Institute for Biological Studies, San Diego, US) and utilized in Prof. M. Decker's group.

IV.2 Quality of the Antimalarial Medicine Artemether - Lumefantrine in Eight Cities of the Democratic Republic of the Congo

IV.2.1 Sample Collection

The samples were collected in eight provincial capital cities: in the east (Goma), in the west (Kikwit, Matadi, and Kinshasa), in the north-east (Kisangani), in the south-east (Lubumbashi), in the north-west (Mbandaka), and in the center (Mbuji-Mayi) (Figure 2). In each city, AL-containing pharmaceuticals – oral suspensions and tablets – were collected in pharmaceutical outlets most accessible to the public, including pharmacies and drug stores.

From each outlet, the sample amounts ranged from a minimum of 30 to a maximum of 48 dosage units for tablets, and from three to five bottles for oral suspensions. Medicines purchased from the same outlet with the same brand name, strength, size, batch number, and manufacturing and expiry dates were considered as 1 sample. The sample collection took place between December 2013 and March 2014.

Figure 35. Map of DRC showing the sampling sites.

IV.2.2 Visual Inspection

All collected samples were transported to Germany in their original packaging. Each drug product was macroscopically checked to classify the samples by the trade name, the dosage form (oral suspension or tablet), the drug strength (mg per unit), the batch or lot number, the dates of manufacture and expiry, and the manufacturer's name and full address.[290] Inconsistencies in labeling and in manufacturing, as well as expiry dates were also checked during this visual inspection.

IV.2.3 Testing by Thin-Layer Chromatography

Thin-layer chromatography (TLC) experiments were conducted as described in the respective monographs on artemether and lumefantrine tablet and on powder for oral suspension of *The International Pharmacopoeia*.[215] Briefly, an aliquot of 10 µL of the sample solution, corresponding to 1 mg of artemether and 6 mg of lumefantrine per mL, was spotted on silica gel 60 F_{254} plates. For comparison, solutions containing the reference compounds were tested in parallel. As the mobile phase, a mixture of light petroleum, ethyl acetate, and glacial acetic acid (40:10:5, v/v) was used. Lumefantrine was detected at 254 nm, whereas artemether was identified by spraying the plates with a mixture of sulfuric acid and methanol (10:90, v/v) and warming with a heat gun to provide a grey spot visible in daylight. A drug sample passed the TLC test if the result was positive with artemether and lumefantrine and it failed if the result was negative for artemether and/or lumefantrine.

IV.2.4 Analysis by High-Performance Liquid Chromatography

High-performance liquid chromatography (HPLC) experiments were pursued according to *The International Pharmacopoeia*,[215] with slight modifications: For separation, an Eclipse XDB‐C18 column (Agilent, 4.6 × 150 mm, 5 µm particle size) was used, possessing column dimensions different from the ones described (3.9 × 150 mm, 5 µm particle size), and the flow rate was adjusted to 1.9 mL min^{-1} instead of 1.3 mL min^{-1}. Samples were prepared in duplicate by dissolving an appropriate portion of the powder from crushed tablets (sonication time: 120 min) or of oral suspensions (homogenized by pulverizing prior to use) in a mixture of acetonitrile, the ion-pair reagent, 1-propanol, and water (5:1:1:0.3, v/v) to obtain a final solution containing 0.2 mg mL^{-1} of artemether (**10a**) and 1.2 mg mL^{-1} of lumefantrine (**12**). Reference solutions were prepared in duplicate as well, in the same solvent and in the same concentration as the samples. For the quantification of **10a** and **12**, the detection was set at 210 nm and 380 nm, respectively.

The ion-pair reagent solution was prepared by dissolving 5.65 g of sodium hexane sulfonate and 2.75 g of sodium dihydrogen phosphate in 900 mL of water. The pH value of the mixture was adjusted to 2.3 using phosphoric acid, and the volume was filled up to 1000.0 mL using the same solvent. Mobile phases A and B were prepared by mixing the ion-pair reagent solution with acetonitrile in a ratio of 7:3 (A) and 3:7 (B). The following gradient elution program was applied: 0–28 min (A: 60%; B: 40%), 28–29 min (A: 60 to 0%; B: 40 to 100%), 29–45 min (A: 0%; B: 100%), 45–46 min (A: 0 to 60%; B: 100 to 40%), and 46–55 min (A: 60%; B: 40%).

A sample was considered of good quality if the contents of the two APIs were between 90 and 110% of the amounts indicated on the label.[215]

IV.2.5 Analysis by Liquid Chromatography - Mass Spectrometry

For separation, a Symmetry-C18 column (Waters, 2.1 × 150 mm, 5 μm particle size) was used. Mobile phase A consisted of an aqueous 10 mM ammonium formate solution adjusted to pH 2.7 with formic acid, whereas mobile phase B was methanol. The following gradient elution was applied: 0–20 min: 30% to 100% B; 20–25 min: 100% B; 25–26 min: 100% to 30% B; 26–30 min: 30% B, with a flow rate set at 0.4 mL min^{-1}. A quantity of the tablet powder corresponding to 50 mg of artemether (**10a**) and 400 mg of lumefantrine (**12**) was dispersed in 5 mL of methanol, sonicated for 30 min, centrifuged for 5 min (6000 rpm), and the supernatant was passed through a 0.45 μm syringe filter and diluted down to a fourth. The final mixture thus obtained was used for measurements. A solution of reference compounds containing the APIs in concentration identical to those of the samples was prepared in the same manner.

10a   **12**
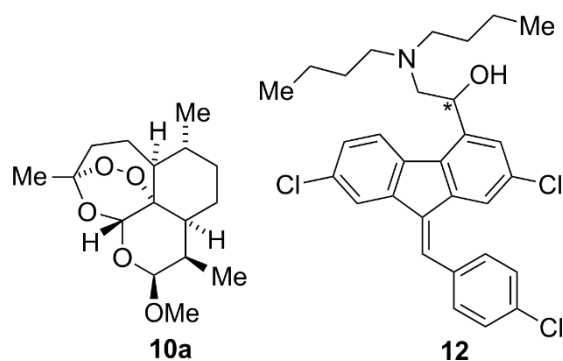
Table 12. Description of the collected drug samples, measured API content (% of declared content), and number of additional peaks (HPLC-UV)

Indicated country of origin	Brand name	Batch number	Type of formulation	Manufacturer name	Artemether [% of the declared content]	Lumefantrine [% of the declared content]	Number of additional peaks
China	Coartem	F2807	Tablet	Novartis	100.6	97.2	1
China	Coartem	F2807	Tablet	Novartis	98.3	98.5	1
China	Coartem	X1341	Tablet	Novartis	0.0	0.0	0
DRC	Cether- L adulte	821513	Tablet	New Cesamex	110.3	101.7	1
DRC	Cether- L adulte	821813	Tablet	New Cesamex	104.1	99.5	2
DRC	Cether- L adulte	822813	Tablet	New Cesamex	90.7	94.0	2
DRC	Cether- L adulte	822813	Tablet	New Cesamex	97.4	101.1	2
DRC	Cether- L adulte	8211013	Tablet	New Cesamex	96.2	91.0	2
DRC	Cether- L adulte	8211013	Tablet	New Cesamex	102.2	94.4	2
DRC	Cether- L adulte	8211113	Tablet	New Cesamex	102.2	94.4	2
DRC	Cether- L adulte	8221113	Tablet	New Cesamex	98.7	96.3	0
DRC	Cether- L adulte	8221113	Tablet	New Cesamex	95.1	94.8	2
DRC	Cether- L adulte	8231013	Tablet	New Cesamex	95.5	93.4	2
DRC	Cether- L adulte	8231113	Tablet	New Cesamex	106.9	104.0	2
DRC	Cether-L	371113	Suspension	New Cesamex	74.4	79.1	1
DRC	Cether-L	371213	Suspension	New Cesamex	97.4	91.5	1
DRC	Cether-L	371313	Suspension	New Cesamex	88.6	82.3	1
DRC	Cether-L	372313	Suspension	New Cesamex	89.3	86.1	1
DRC	Cether-L	373113	Suspension	New Cesamex	94.2	86.3	1
DRC	Cether-L	373413	Suspension	New Cesamex	97.1	89.3	1
DRC	Cether-L	373813	Suspension	New Cesamex	99.3	93.9	0
DRC	Cether-L	374813	Suspension	New Cesamex	95.3	89.6	2
DRC	Cether-L	374813	Suspension	New Cesamex	97.4	87.7	2

IV.2 Quality of the Antimalarial Medicine Artemether - Lumefantrine

Table 12. Continued

Indicated country of origin	Brand name	Batch number	Type of formulation	Manufacturer name	Artemether [% of the declared content]	Lumefantrine [% of the declared content]	Number of additional peaks
DRC	Cether-L	374813	Suspension	New Cesamex	101.3	98.6	2
DRC	Cether-L	376413	Suspension	New Cesamex	95.7	89.6	1
DRC	Cether-L	376813	Suspension	New Cesamex	109.6	104.9	2
DRC	Cether-L	376813	Suspension	New Cesamex	99.3	100.2	2
DRC	Cether-L	3711113	Suspension	New Cesamex	92.6	90.3	2
DRC	Cether-L	3741013	Suspension	New Cesamex	93.8	91.8	2
DRC	Cether-L	3761013	Suspension	New Cesamex	94.3	90.6	2
DRC	Co-Artluf	12P-18	Suspension	Zenufa	85.3	86.4	1
DRC	Co-Artluf	12P-31	Suspension	Zenufa	80.2	68.4	1
DRC	Co-Artluf	12P-31	Suspension	Zenufa	87.4	69.0	1
DRC	Co-Artluf	13P-09	Suspension	Zenufa	77.0	82.7	1
DRC	Co-Artluf	13P-118	Suspension	Zenufa	74.4	65.3	2
DRC	Co-Artluf	13P-118	Suspension	Zenufa	83.5	72.1	2
DRC	Co-Artluf	13P-131	Suspension	Zenufa	102.2	96.1	2
DRC	Co-Artluf	13P-47	Suspension	Zenufa	111.2	108.9	3
DRC	Co-Artluf	13P-74	Suspension	Zenufa	115.8	116.1	1
DRC	Co-Artluf	13P-74	Suspension	Zenufa	54.3	48.9	1
DRC	Lufamet	DGOC 113	Suspension	Ave Pharma	101.3	104.6	1
DRC	Lufamet DS	TG 02113	Tablet	Ave Pharma	107.4	111.4	1
DRC	M-2	2013	Suspension	Ets Kim Pharma	73.1	89.7	1
DRC	M-2	2013	Suspension	Ets Kim Pharma	80.8	94.1	1
DRC	M-2	2014	Suspension	Ets Kim Pharma	98.5	92.6	1
DRC	M-2	2014	Suspension	Ets Kim Pharma	114.7	95.0	1

Table 12. Continued

Indicated country of origin	Brand name	Batch number	Type of formulation	Manufacturer name	Artemether [% of the declared content]	Lumefantrine [% of the declared content]	Number of additional peaks
India	Aludoc	207204	Suspension	Norris Medicines	73.9	87.9	3
India	Aludoc Forte	218201	Tablet	Norris Medicines	0.0	92.3	1
India	Aludoc Forte	218203	Tablet	Norris Medicines	87.6	96.0	3
India	Aludoc Forte	218203	Tablet	Norris Medicines	87.2	99.8	3
India	Artefan	P03021	Tablet	Ajanta	97.9	100.7	1
India	Arte-ped	10	Suspension	Vardhman Exports	117.6	87.0	1
India	Co-arther	O5	Suspension	Axelia	77.7	88.5	1
India	Co-Artluf	12T-123	Tablet	Mamta Pharma	82.0	92.5	2
India	Co-Artluf Forte	ZT-07	Tablet	Mamta Pharma	91.2	96.5	1
India	Co-Artluf Forte	ZT-07	Tablet	Mamta Pharma	108.6	107.1	1
India	Co-Artluf Forte	ZT-07	Tablet	Mamta Pharma	106.1	104.2	1
India	Co-Artluf Forte	ZT-08	Tablet	Mamta Pharma	103.9	95.8	1
India	Co-Artluf Forte	ZT-08	Tablet	Mamta Pharma	99.6	93.9	1
India	Co-Artluf Forte	ZT-08	Tablet	Mamta pPharma	99.7	92.7	1
India	Colart	CWY 023006	Tablet	Ipca	101.7	100.4	0
India	Co-Nometa	CS 12001	Suspension	Lika Labs Ltd	65.1	88.3	0
India	Co-rimétar	2013	Tablet	Mepro Pharm	98.7	102.8	1
India	Co-rimétar	2013	Tablet	Mepro Pharm	99.0	104.9	1
India	Co-rimétar	2023	Tablet	Mepro Pharm	94.6	95.2	0
India	Co-rimétar	2023	Tablet	Mepro Pharm	92.0	95.6	0
India	Co-rimétar	2032	Suspension	Mepro Pharm	147.3	142.7	1

IV.2 Quality of the Antimalarial Medicine Artemether - Lumefantrine

Table 12. Continued

Indicated country of origin	Brand name	Batch number	Type of formulation	Manufacturer name	Artemether [% of the declared content]	Lumefantrine [% of the declared content]	Number of additional peaks
India	Co-rimétar	2032	Suspension	Mepro Pharm	143.8	136.4	1
India	Co-rimétar	2032	Tablet	Mepro Pharm	104.1	108.5	1
India	Co-rimétar	2032	Tablet	Mepro Pharm	89.7	92.1	1
India	Co-rimétar	2052	Suspension	Mepro Pharm	144.2	136.2	1
India	Co-rimétar	2062	Suspension	Mepro Pharm	144.2	137.9	1
India	Co-rimétar	2072	Suspension	Mepro Pharm	147.0	140.0	1
India	Co-rimétar	2112	Suspension	Mepro Pharm	143.5	140.0	1
India	Curamart	CSC 302	Suspension	Therachem	98.6	89.0	1
India	Gvither Plus	GX-13	Suspension	Bliss Gvs Pharma	81.3	85.8	1
India	Gvither Plus	GX-15	Suspension	Bliss Gvs Pharma	90.4	102.0	1
India	Ipca	DYI1403136	Tablet	Ipca	97.4	102.1	1
India	L-Artem	1002	Tablet	Shalina	91.8	97.0	2
India	L-Artem	2001	Tablet	Shalina	88.2	92.9	2
India	L-Artem	2004	Suspension	Shalina	82.1	91.7	1
India	L-Artem	2004	Suspension	Shalina	100.5	99.4	1
India	L-Artem	2004	Suspension	Shalina	83.1	94.7	1
India	L-Artem	2008	Suspension	Shalina	95.1	100.1	1
India	L-Artem	G3004	Suspension	Shalina	101.7	97.3	1
India	L-Artem	G3006	Suspension	Shalina	101.7	94.1	0
India	L-Artem	J 3011	Tablet	Shalina	96.6	97.7	1
India	L-Artem	J3002	Tablet	Shalina	94.9	98.1	1
India	L-Artem	J3002	Tablet	Shalina	92.7	97.7	2
India	L-Artem Forte	2001	Tablet	Shalina	92.5	93.1	1

Table 12. Continued

Indicated country of origin	Brand name	Batch number	Type of formulation	Manufacturer name	Artemether [% of the declared content]	Lumefantrine [% of the declared content]	Number of additional peaks
India	L-Artem Forte	2001	Tablet	Shalina	101.1	102.8	1
India	L-Artem Forte	2001	Tablet	Shalina	97.9	98.9	1
India	L-Artem Forte	J3001	Tablet	Shalina	98.6	99.7	1
India	L-Artem Forte	J3001	Tablet	Shalina	97.6	99.0	1
India	Lonart	LD-224	Suspension	Bliss Gvs Pharma	78.5	92.1	1
India	Lonart DS	LD-550	Tablet	Bliss Gvs Pharma	95.6	95.2	1
India	Lonart DS	LD-551	Tablet	Bliss Gvs Pharma	104.6	106.9	0
India	Lufamet	NL 42	Suspension	Intermed	62.5	49.7	3
India	Lumether	O10	Tablet	Astra Lifecare	88.1	96.2	3
India	Luther	DE 2158	Suspension	Zest Pharma	96.2	98.3	1
India	Luther	DE 3001	Suspension	Zest Pharma	82.7	88.4	3
India	Luther	DE 3005	Suspension	Zest Pharma	87.1	93.8	3
India	Luther	DE 3005	Suspension	Zest Pharma	100.6	97.7	3
India	Luther	DE 3013	Suspension	Zest Pharma	111.6	106.8	3
India	Luther	DE3016	Suspension	Zest Pharma	103.4	101.4	1
India	Luther DP	E12090	Tablet	Zest Pharma	90.0	95.3	2
India	Luther DP	E13013	Tablet	Zest Pharma	101.4	96.5	3
India	Luther DP	E13013	Tablet	Zest Pharma	96.2	102.0	3
India	Luther DP	E13022	Tablet	Zest Pharma	96.2	99.7	1
India	Luther DP	E13180	Tablet	Zest Pharma	118.0	99.0	3
India	Luther Forte	E12449	Tablet	Zest Pharma	93.7	97.6	0
India	Luther Forte	E13012	Tablet	Zest Pharma	93.0	90.2	3

IV.2 Quality of the Antimalarial Medicine Artemether - Lumefantrine

Table 12. Continued

Indicated country of origin	Brand name	Batch number	Type of formulation	Manufacturer name	Artemether [% of the declared content]	Lumefantrine [% of the declared content]	Number of additional peaks
India	Luther Forte	E13012	Tablet	Zest Pharma	91.9	92.4	3
India	Luther Forte	E13021	Tablet	Zest Pharma	92.4	99.8	1
India	Mefanther	AQ 2002	Suspension	S Kant	71.4	84.5	2
India	Mefanther	AQ 2003	Suspension	S Kant	78.9	88.1	2
India	Mefanther	AQ 3001	Suspension	S Kant	82.1	87.8	2
India	Mefanther	MN 005	Suspension	Ally Pharma	86.5	81.5	0
India	Mefanther	MN-003	Suspension	Ally Pharma	68.2	97.7	1
India	Mefanther	MN-005	Suspension	Ally Pharm	79.4	97.4	1
India	Mefanther	MN-006	Suspension	Ally Pharma	73.2	97.6	1
India	Mefanther	MN-008	Suspension	Ally Pharma	82.5	90.6	1
India	Mefanther DS	LU 3001	Tablet	S Kant	100.7	102.3	1
India	Mefanther DS	LU 3001	Tablet	S Kant	102.6	104.9	0
India	Mefanthet DS	LU 3008	Tablet	S Kant	105.7	101.3	0
Netherlands	Co-Artésiane	29307	Suspension	MPF bv	83.5	94.2	0
Netherlands	Co-Artésiane	29308	Suspension	MPF bv	84.2	95.5	0
Netherlands	Co-Artésiane	29572	Suspension	MPF bv	87.8	95.0	0
Netherlands	Co-Artésiane	29573	Suspension	MPF bv	84.8	96.0	0
Netherlands	Co-Artésiane	30157	Suspension	MPF bv	92.8	97.3	0
Netherlands	Co-Artésiane	30159	Suspension	MPF bv	96.2	95.3	0
Netherlands	Co-Artésiane	30502	Suspension	MPF bv	86.9	98.4	0
Netherlands	Co-Artésiane	31651	Suspension	MPF bv	79.9	86.7	0
USA	Coartem	F0720	Tablet	Novartis	99.6	96.1	1
USA	Coartem	F0788	Tablet	Novartis	100.3	94.4	0

Table 12. Continued

| Indicated country of origin	Brand name	Batch number	Type of formulation	Manufacturer name	Artemether [% of the declared content]	Lumefantrine [% of the declared content]	Number of additional peaks
USA	Coartem	F0867	Tablet	Novartis	107.9	96.6	1
USA	Coartem	F0934	Tablet	Novartis	103.8	94.2	1
USA	Coartem	F2153	Tablet	Novartis	0.0	0.0	0
USA	Coartem	F2801	Tablet	Novartis	109.0	97.2	1
USA	Coartem	F2929	Tablet	Novartis	0.0	0.0	0
USA	Coartem	F3001	Tablet	Novartis	106.4	97.4	1
USA	Coartem	F3013	Tablet	Novartis	101.0	95.4	1
USA	Coartem	F3013	Tablet	Novartis	110.8	100.1	1
USA	Coartem	F3018	Tablet	Novartis	116.5	104.3	1
USA	Coartem	F3021	Tablet	Novartis	111.2	97.1	0
USA	Coartem	F3031	Tablet	Novartis	100.2	100.7	0
USA	Coartem	F3076	Tablet	Novartis	102.8	96.3	0
USA	Coartem	F3079	Tablet	Novartis	103.2	99.9	1
USA	Coartem	F3092	Tablet	Novartis	106.1	96.0	0
USA	Coartem	F3093	Tablet	Novartis	122.4	106.9	1
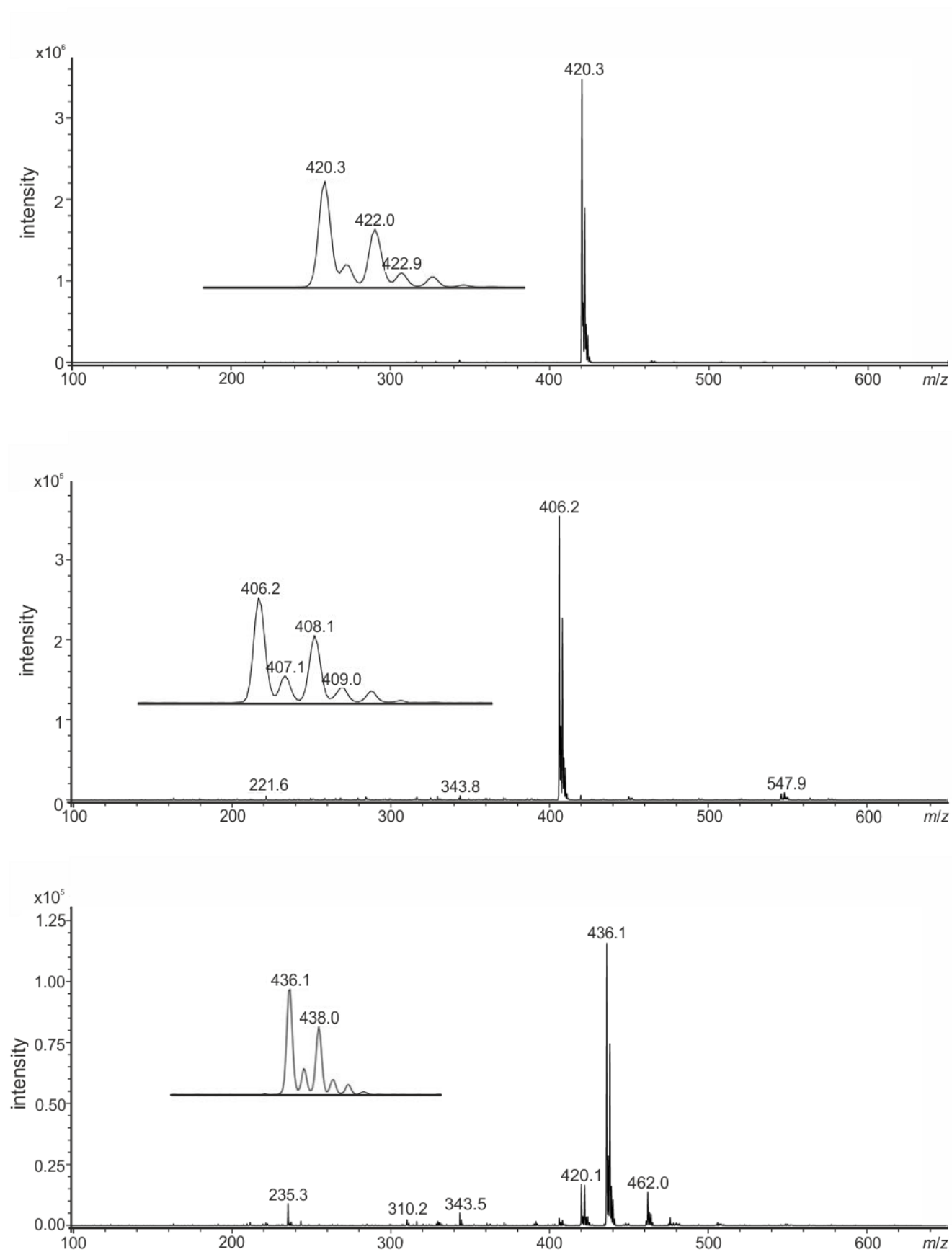
Figure 36. Mass spectra of the three unidentified degradation products from LC-MS measurements.

IV.3 Capillary Zone Electrophoresis (CZE) for the Determination of Amodiaquine (13) and Three of its Synthetic Impurities in Pharmaceutical Formulations

IV.3.1 Buffers and Background Electrolyte (BGE)

Sodium dihydrogen phosphate monohydrate (13.8 g, 0.1 mol) and disodium hydrogen phosphate dihydrate (17.8 g, 0.1 mol) were separately dissolved in 500.0 mL of water to obtain solutions A and B, respectively. Solutions A and B were mixed in a 81.5:18.5 (v/v) ratio and 50.0 mL of this mixture were diluted with water to a volume of 90 mL; the pH value was adjusted to 6.2 with sodium hydroxide solution (1 M) and the volume was made up to 100.0 mL using the same solvent to achieve a final concentration of 100 mM.

IV.3.2 Sample Solution Preparation

Unless stated otherwise, all solutions were prepared using two different diluents made as follows:

- Diluent A: 50.0 mg of quinine (internal standard) was dissolved in 500.0 mL of aqueous hydrochloric acid (100 mM).
- Diluent B: 10.0 mg of quinine was dissolved in 50.0 mL of aqueous hydrochloric acid (100 mM).

The resulting solution was sonicated for 10 min to facilitate dissolution and filtered before use.

IV.3.2.1 Content Determination

Standard stock solutions were prepared by dissolving 10.0 mg of amodiaquine (13) in 10.0 mL of Diluent A, whereas for the drug product sample stock solutions, portions equivalent to 10.0 mg of 4 were weighed from crushed tablets and dissolved in 10.0 mL of Diluent A. Standard and drug sample working solutions were prepared by diluting 0.8 mL aliquots of the respective stock solution to give a final volume of 2.0 mL using the same diluent (0.4 mg mL^{-1}).

IV.3.2.2 Impurity Profiling

Stock solutions were prepared by dissolving an equivalent of 100 mg of amodiaquine (13) in 10.0 mL of diluent A, while working solutions were obtained by diluting 1.0 mL aliquots of the respective stock solution to a final volume of 2.0 mL using the same diluent (5 mg mL^{-1}).

IV.3.3 Method Validation

IV.3.3.1 Content Determination

Specificity of the method was evaluated by preparing the following solutions: 10.0 mg of a reference standard (Solution 1) of amodiaquine (**13**) as well as quantities of crushed tablets with artesunate (Solution 2) and without artesunate (solution 3) corresponding to 10 mg of **13** were accurately weighed and individually dissolved in diluent A to obtain final solutions at a concentration level of 0.4 mg mL^{-1}. The three solutions were subjected to CZE to check any interference that might arise from the excipients.

For determining the linearity of the calibration curve, a stock solution was prepared by dissolving an amount of 10.0 mg of amodiaquine (**13**) in 10.0 mL of diluent A. Serial dilutions using the same diluent were prepared to obtain five levels (50, 80, 100, 120, and 150% of the nominal concentration of 0.4 mg mL^{-1}). The calibration curve was constructed by plotting the peak responses versus the respective concentration.

Accuracy was determined by evaluating the mean recovery of the analyte at the concentration levels of 80, 100, and 120% (of the nominal concentration of 0.4 mg mL^{-1}) from a spiked sample, i.e. an aqueous solution of amodiaquine (**13**) obtained from tablets.

Intra- and inter-day precision was determined by independently preparing six replicates of working solutions at a concentration corresponding to a level of 100% (0.4 mg mL^{-1}). This was performed on three consecutive days, while on each day all sample solutions were freshly prepared. The relative standard deviations (% RSD) for **13** were calculated with respect to recovery and migration times.

Stability of the standard and real-drug sample solutions was investigated by preparing a solution having a concentration level of 0.4 mg mL^{-1} of **13**. Recovery was subsequently determined at three different time points (0, 24, and 48 h).

Method robustness was determined by deliberately varying the following four electrophoretic conditions: (i) the buffer concentration (90–110 mM), (ii) the pH value of the buffer solution (6.0–6.4); (iii) the voltage (19–21 kV); (iv) the capillary temperature (24–26 °C).

IV.3.3.2 Impurity Profiling

The specificity of the method was studied by preparing amodiaquine (**13**) standard solutions, each containing one of the related substances 4,7-dichloroquinoline (**30**), 4-aminophenol (**31**), or 4-[(7-chloroquinolin-4-yl)amino]phenol (**32**). Individual solutions as well as a spiked real-drug solution were analyzed.
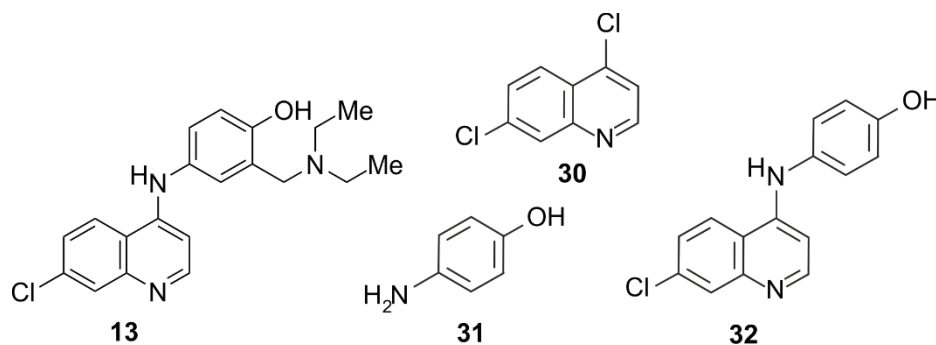
For determining the linearity of the calibration curve, 5.0 mg of each of the anticipated impurities **30**−**32** were accurately weighed, individually dissolved in 3.0 mL of methanol, and sonicated for 10 min. The solutions were diluted to a final volume of 5.0 mL using the same solvent (1 mg mL^{-1}) and then diluted two times with Diluent B to obtain the respective stock solutions. Five calibration solutions were prepared by diluting appropriate aliquots of each stock solution to obtain the desired concentration levels (i.e., 0.5, 0.8, 1.0, 1.2, and 1.5% of the amodiaquine nominal sample solution concentration of 5.0 mg mL^{-1}).

Accuracy of the method was investigated by recovery studies carried out by addition of a standard in which a known amount of each of the impurities **30**−**32** was added to the tablet sample solutions at levels of 0.5, 1.0, or 1.5%.

The tablet sample solutions were prepared by weighing powder amounts equivalent to 100 mg of amodiaquine (**13**), suspending them in 7.0 mL of Diluent A, and sonicating the solutions for 15 min. The suspensions were diluted to a final volume of 10.0 mL using the same diluent and filtered, discarding the first 2.0 mL. The unspiked matrix was injected and used to correct the peak areas in the spiked matrix as well as to avoid interference during the investigation.

For evaluating the precision, six spiked sample solutions (three for each of the two levels, i.e. 0.5 and 1.0%) were prepared for each of the related substances **30**−**32**. This was investigated on three different days using individually weighed amounts of the compounds as described for the determination of the linearity of the calibration curve.

The limits of detection (LOD) and limits of quantification (LOQ) were determined based on the standard deviation of the response and the slope using five concentration levels as described above ("linearity"). The values for LOD and LOQ were calculated as provided within the ICH guideline Q2(R1)[234] and confirmed by using the signal-to-noise ratio (S/N) approach.

The stability of the standard and spiked sample solutions was investigated by preparing all solutions at a level of 1.0% of each of the studied impurities **30−32**. Determination of the recovery rate was carried out at three different time points (0, 24, and 48 h). The robustness was assessed as described for the content determination.

IV.3.4 Content Determination Using the HPLC Method Described in *The International Pharmacopoeia*

As the mobile phase, a mixture of methanol and the following buffer solution (62:38, v/v) was utilized: 100.0 mL of a potassium dihydrogen phosphate solution (13.6 g/L) and 1.4 mL of triethylamine were mixed, diluted to 900.0 mL with water, the pH adjusted to 9.0 by addition of a concentrated potassium hydroxide solution (55 g/L), and the solution diluted to 1000.0 mL. The sample solutions were prepared as follows: To a quantity of tablet powder containing the equivalent amount of 115 mg of amodiaquine (**13**), 70.0 mL of water was added, followed by sonication for 15 min and diluting the suspension to 100.0 mL. A portion of this suspension was filtered through a nylon syringe filter (0.2 μm), discarding the first few mL of the filtrate. A portion of 5.0 mL of the filtrate was diluted to 50.0 mL. A reference solution was prepared using 0.15 mg mL^{-1} of the dihydrochloride of amodiaquine (**13**). For system suitability test, a mixture of 0.15 mg mL^{-1} of amodiaquine (**13**) and 0.15 mg mL^{-1} of the diphosphate of chloroquine (**1**) was used. The operating flow rate was 1.5 mL min^{-1}. UV detection was carried out at a wavelength of 254 nm. The acceptance limit of 90−110% of the amount of **13** stated on the label was used.[215]
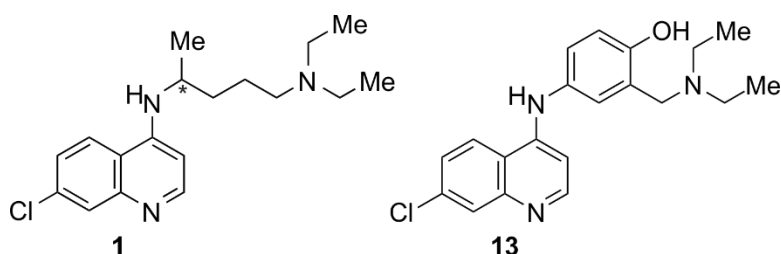
IV.4 Phytochemical Investigation on a Congolese *Ancistrocladus* Liana

IV.4.1 Plant Material

Leaves of the botanically as yet unidentified *Ancistrocladus* plant were collected by Prof. Mudogo in July 2006, in the vicinity of the village Leeke near the town of Ikela, Province Tshuapa, Democratic Republic of the Congo. A voucher specimen (No. 114) has been deposited at the Herbarium Bringmann, Institute of Organic Chemistry, University of Würzburg.

IV.4.2 Extraction and Isolation

For the isolation and purification of the constituents of the plant extracts, unless otherwise stated, SymmetryPrep^{TM} C18 column (19 x 300 mm, 7 μm, Waters) was used, flow rate 10 mL min^{-1}; mobile phases: (A) 90% H_2O with 10% MeCN (0.05% trifluoroacetic acid) and (B) 90% MeCN with 10% H_2O (0.05% trifluoroacetic acid), using linear gradients (details given below).

Air-dried leaves (ca. 300 g) were ground and exhaustively extracted with CH_2Cl_2/MeOH (1:1, v/v) at room temperature. The combined extracts were concentrated under reduced pressure to give 22.1 g of a crude residue. The solid extract was macerated in H_2O, with mechanical shaking (160 RPM), then filtered and dissolved in MeOH. After filtration, the raw methanolic extract was directly subjected to preparative HPLC on a SymmetryPrep^{TM} C18 column, applying a linear gradient (0 min 20% B, 28 min 45% B), finally providing 11 fractions (F1−F11).

Fractions F1 (3.1 mg) and F2 (4.2 mg) were resolved by preparative HPLC, using an isocratic solvent system consisting of the Mobile Phases A and B (16:84, v/v) to give pure ikelacongoline B (**35b**) (2.7 mg) (retention time 25.4 min) and ikelacongoline A (**35a**) (3.5 mg) (retention time 28.9 min). From Fraction F3 (2.6 mg), ealamine A (**43**) (1.7 mg) (retention time 18.9 min) was obtained, by isocratic HPLC using the Solvents A and B (80:20, v/v). Fraction F5 (8.5 mg) was subjected to preparative HPLC on a Chromolith SemiPrep RP-18e column (Merck, 10 x100 mm) applying a linear gradient (0 min 5% B, 6 min 15% B, 9 min 25% B, 12 min 35% B, 15 min 45% B) at a flow rate of 5 mL min-1, affording pure mbandakamine A (**1**) (2.1 mg) (retention time 10.4 min) and an alkaloid-containing subfraction, which was further purified by preparative HPLC on a SymmetryPrep^{TM} C18 column. Using an isocratic solvent system similar to the one described above, but with MeOH instead of MeCN, consisting of the Solvents A' and B' (4.5:5.5, v/v), resolution of this subfraction at a flow rate of 10 mL min^{-1} furnished pure ikelacongoline C (**36**) (4.9 mg) (retention time 11.9 min) and ikelacongoline D (**37**) (1.3 mg) (retention time 14.0 min).

IV.4 Phytochemical Investigations

Purification of Fraction F6 (9.1 mg) by preparative HPLC on a Chromolith SemiPrep RP-18e column under the conditions described above again yielded mbandakamine A (**45**) (3.6 mg) (retention time 10.4 min) and, additionally, ancistrocongoline C (**40**) (5.1 mg) (retention time 7.9 min). From Fractions F7 (8.7 mg) and F8 (8.3 mg), ealamine G (**44**) and ancistrolikokine F2 (**42**) were isolated by preparative HPLC on a Chromolith SemiPrep RP-18e column under the conditions given above; the two compounds were further purified by semi-preparative HPLC on a Waters XSelect HSS PFP column (10 x 250 mm, 5 μm) using a mobile phase system consisting of the Solvents A' and B' under linear-gradient conditions (0 min 50% B, 20 min 100% B) at a flow rate of 5 mL min^{-1}, thus finally giving rise to pure **44** (1.5 mg) (retention time 7.9 min) and pure **42** (1.3 mg) (retention time 10.2 min).

Fraction F9 (8.1 mg) was resolved on a Chromolith SemiPrep RP-18e column under the conditions described above, furnishing pure ancistrolikokine C (**41**) (5.1 mg) (retention time 9.5 min) and mbandakamine B$_4$ (**4**) (3.0 mg) (retention time 11.2 min). Resolution of fraction F10 (9.3 mg) by preparative HPLC on a Chromolith SemiPrep RP-18e column, followed by chromatography on a SymmetryPrep C18 column, using the solvent systems A and B, with a linear gradient (0 min 20% B, 20 min 45% B), at a flow rate of 10 mL min^{-1} gave pure mbandakamine B$_3$ (**38**) (3.8 mg) (retention time 18.9 min) and mbandakamine B$_2$ (**46**) (5.1 mg) (retention time 19.4 min).

IV.4.3 Newly Isolated Alkaloids

IV.4.3.1 Mbandakamine B₃ (38)

Pale-yellow amorphous solid;

$[\alpha]_D^{25} = -19.1$ (*c* 0.08, MeOH);

UV (MeOH) (log ε): λ$_{max}$ 226 (3.9) nm;

ECD (*c* 0.1, MeOH) λ$_{max}$ (Δε): 205 (−3.0), 218 (+6.1), 233 (+2.9), 249 (−3.9), 270 (−0.3), 289 (−1.0), 305 (−2.1), 329 (−0.4), 345 (−0.7), and 376 (+0.1) nm;

IR (ATR) ν$_{max}$: 3357, 2923, 2851, 1976, 1672, 1598, 1418, 1313, 1256, 1200, 1132, 1076, 1039, 833, 800, and 720 cm^{-1};

^{1}H and ^{13}C NMR data, see Table 13; HRESIMS: *m/z* 813.4108 [M+H]$^+$ (calculated for C$_{50}$H$_{57}$N$_2$O$_8$, 813.4114).

IV.4.3.2 Mbandakamine B₄ (39)
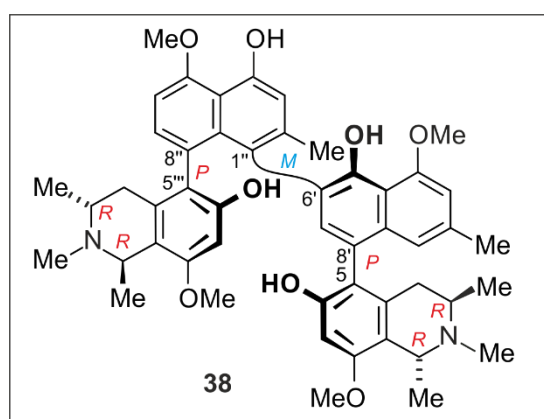
IV.4.3.2 Mbandakamine B₄ (39)

Pale-yellow amorphous solid;

$[\alpha]_D^{25} = -22.5$ (c 0.09, MeOH);

UV (MeOH) (log ε): λ_{max} 229 (3.9) nm;

ECD (c 0.1, MeOH) λ_{max} (Δε): 207 (–6.7), 218 (+9.9), 235 (–9.1), 240 (–9.6), 246 (–11.3), 271 (+1.6), 288 (–2.1), 302 (–1.8), 329 (–0.7), 350 (–1.8), 368 (+0.2), and 400 (+0.5) nm;

IR (ATR) ν_{max}: 33534, 2940, 2848, 2013, 1983, 1674, 1446, 1334, 1201, 1134, 838, 800, and 723 cm^{-1};

^{1}H and ^{13}C NMR data, see Table 13; HRESIMS: *m/z* 799.3957 [M+H]$^+$ (calculated for $C_{49}H_{55}N_2O_8$, 799.3958).
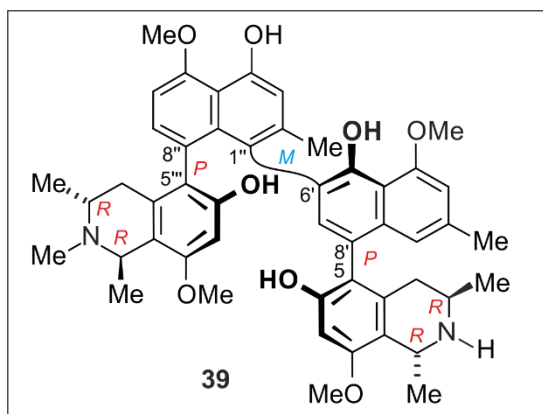
Table 13. ^{1}H and ^{13}C NMR data of mbandakamines B$_3$ (**38**) and B$_4$ (**39**) in methanol-d_4 (150 MHz, δ in ppm)

No.	**38**		**39**	
	δ_H (J in Hz)	δ_C	δ_H (J in Hz)	δ_C
1/1'''	4.68, q (6.6) / 4.55, q (6.8)	58.9 / 58.1	4.70, q (6.7) / 4.51, q (6.7)	49.0 / 59.0
3/3'''	3.95, m / 3.67, m	50.1 / 50.0	3.65, m / 3.61, m	44.7 / 50.1
4$_{ax}$/4$_{ax}$'''	1.74, dd (18.2, 11.2) / 1.84, dd (18.2, 11.8)	32.2 /29.3	1.75, dd (17.9, 11.4) / 1.86, dd (17.9, 5.1)	33.4 / 29.3
4$_{eq}$/4$_{eq}$'''	2.77, dd (18.3, 4.5) / 1.84, dd (18.2, 5.1)		2.84, dd (17.8, 4.7) / 1.86, dd (17.9, 11.5)	
5/5'''		119.5 / 123.0		119.7 / 122.9
6/6'''		156.3 / 155.7		156.7/ 155.7
7/7'''	6.65, s / 5.64, s	97.9 / 98.3	6.66, s / 5.63, s	98.0 / 98.3
8/8'''		158.0 / 157.0		157.8 / 157.1
9/9'''		115.6 / 112.4		114.8 / 112.3
10/10'''		134.0 / 130.8		134.0 / 130.6
1'/1''	6.56, s / −	118.7/ 126.5	6.54, s / −	118.8 / 126.5
2'/2''		137.0 / 139.5		136.9 / 139.4
3'/3''	6.81, s / 6.87, s	108.1 / 114.8	6.81, s / 6.88, s	108.1 / 114.8
4'/4''		158.0 / 155.6		158.2 / 155.6
5'/5''		152.6 / 158.2		152.6 / 158.2
6'/6''	− / 7.01, d (8.1)	136.2 / 104.8	− / 7.02, d (8.0)	136.2 / 104.9
7'/7''	6.83, s / 6.97, d (8.0)	132.8 / 132.8	6.83, s / 6.97, d (8.0)	132.7 / 132.8
8'/8''		126.5 / 126.5		126.5 / 127.3
9'/9''		137.0 / 137.9		136.9 / 137.9
10'/10''		115.6 / 115.9		115.6 / 115.9
1-CH$_3$/1'''-CH$_3$	1.49, d (6.5) / 1.42, d (6.7)	17.3 / 18.9	1.56, d (6.7) / 1.42 (6.6)	18.7 / 18.9
3-CH$_3$/3'''-CH$_3$	1.08, d (6.4) / 1.08, d (6.4)	17.5 / 16.9	1.14, d (6.4) / 1.08 (6.5)	19.2 / 16.9
N-CH$_3$/N'''-CH$_3$	2.54, s / 2.41, s	35.7 / 34.7	− / 2.42, s	− / 34.6
8-OCH$_3$/8'''-OCH$_3$	3.93, s / 3.42, s	56.1 / 55.7	3.94, s / 3.41, s	56.2 / 55.7
2'-CH$_3$/2''-CH$_3$	2.30, s / 2.06, s	22.1 / 22.7	2.29, s / 2.07, s	22.1 / 22.7
4'-OCH$_3$	4.06, s	57.0	4.06, s	57.0
5''-OCH$_3$	4.16, s	56.9	4.16, s	56.9

IV.4.3.3 Ikelacongoline A (35a)

Yellow amorphous solid;

$[\alpha]_D^{25} = -11.5$ (c 0.05, MeOH);

UV (MeOH) (log ε): λ$_{max}$ 229 (3.5) nm;

ECD (c 0.1, MeOH) λ$_{max}$ (Δε): 196 (+15.1), 211 (−15.9), 217 (−14.6), 223 (−15.5), 238 (+7.2), 266 (+0.1), 280 (−0.6), 300 (+0.1), 334 (−0.4), and 350 (−0.1) nm;

IR (ATR) ν$_{max}$: 3373, 2943, 2015, 1673, 1604, 1585, 1524, 1490, 1456, 1434, 1392, 1298, 1264, 1201, 1137, 1091, 1041, and 722 cm^{-1};
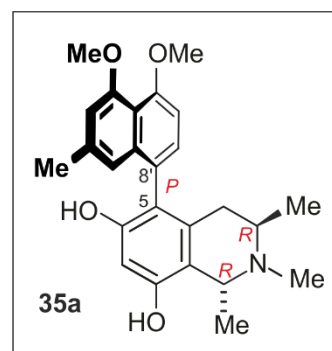
^{1}H and ^{13}C NMR data, see Table 14;

HRESIMS: m/z 408.21699 [M+H]$^+$ (calculated for $C_{25}H_{30}NO_4$, 408.21748)

IV.4.3.4 Ikelacongoline B (35b)

Yellow amorphous solid;

$[\alpha]_D^{25} = -18.3$ (c 0.05, MeOH);

UV (MeOH) (log ε): λ_{max} 230 (3.6) nm;

ECD (c 0.1, MeOH) λ_{max} (Δε): 198 (–6.7), 211 (+11.1), 215 (+9.8), 224 (+6.5), 237 (–8.8), 261 (+0.1), 284 (+1.7), 300 (+0.3), and 350 (–0.2) nm;

IR (ATR) ν_{max}: 3220, 2941, 2839, 1672, 1584, 1456, 1200, 1137, 837, 800, and 722 cm^{-1};

^{1}H and ^{13}C NMR data, see Table 14;

HRESIMS: m/z 408.21747 [M+H]$^+$ (calculated for $C_{25}H_{30}NO_4$, 408.21748).

IV.4.3.5 Ikelacongoline C (36)

Brown amorphous solid;

$[\alpha]_D^{25} = [\alpha]^{25}{}_D -24.4$ (c 0.05, MeOH);

UV (MeOH) (log ε): λ_{max} 231 (3.6) nm;

ECD (c 0.1, MeOH) λ_{max} (Δε): 196 (–4.1), 210 (+12.4), 218 (+8.2), 222 (+8.6), 239 (–12.4), 277 (–0.3), 300 (+0.3), 318 (+0.5), and 351 (–0.1) nm;

IR (ATR) ν_{max}: 3379, 2941, 2839, 1671, 1583, 1542, 1449, 1363, 1198, 1021, 832, 800, and 720 cm^{-1};

^{1}H and ^{13}C NMR data, see Table 14;

HRESIMS: m/z 422.23133 [M+H]$^+$ (calculated for $C_{26}H_{32}NO_4$, 422.23313).
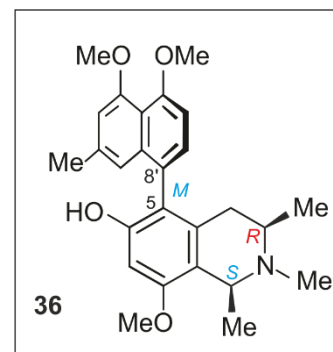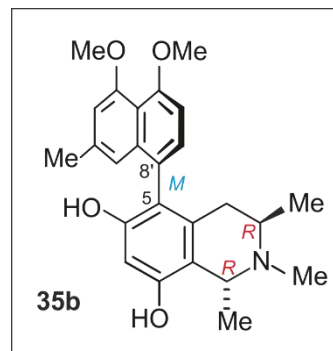
IV.4.3.6 Ikelacongoline D (37)

Brown amorphous solid;

$[\alpha]_D^{25}$ = +44.3 (c 0.05, MeOH);

UV (MeOH) (log ε): λ$_{max}$ 231 (3.6) nm;

ECD (c 0.1, MeOH) λ$_{max}$ (Δε): 200 (–15.5), 214 (+14.7), 227 (+31.8), 243 (–11.2), 268 (+0.3), 285 (+0.9), 301 (–0.7), and 310 (–0.6) nm;

IR (ATR) ν$_{max}$: 3415, 2927, 2851, 2273, 1674, 1585, 1437, 1204, 1137, 841, 802, and 724 cm^{-1};

^{1}H and ^{13}C NMR data, see Tables 14;

HRESIMS: m/z 422.23227 [M+H]$^+$ (calculated for C$_{26}$H$_{32}$NO$_4$, 422.23313).

Table 14. ^{1}H (600 MHz) and ^{13}C (150 MHz) NMR data of ikelacongolines A (**35a**), B (**35b**), C (**36**), and D (**37**) in methanol-d_4 (δ in ppm).

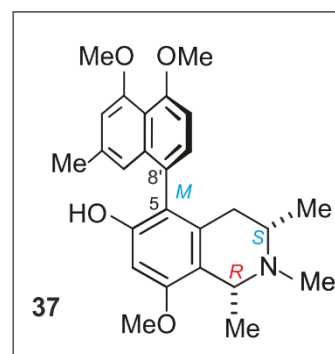| no.	Ikelacongoline A (**35a**) δ_H (*J* in Hz)	δ_C, type	Ikelacongoline B (**35b**) δ_H (*J* in Hz)	δ_C, type	Ikelacongoline C (**36**) δ_H (*J* in Hz)	δ_C, type	Ikelacongoline D (**37**) δ_H (*J* in Hz)	δ_C, type
1	4.72, q (6.7)	60.0, CH	4.71, q (6.7)	60.1, CH	4.65, q (6.6)	62.1, CH	4.64, q (6.7)	61.7, CH
3	3.96, m	50.8, CH	3.92, m	50.8, CH	3.15, m	60.3, CH	3.23, m	59.9, CH
4$_{ax}$	2.03, dd (18.6, 11.9)	29.4, CH^{ax}	2.49, dd (18.6, 12.2)	29.9, CH^{ax}	2.58, dd (17.3, 11.5)	34.0, CH^{ax}	2.23, dd (17.3, 11.0)	33.1, CH^{ax}
4$_{eq}$	2.61, dd (18.5, 4.9)	29.4, CH^{eq}	2.20, dd (18.8, 5.0)	29.9, CH^{eq}	2.21, dd (17.3, 2.9)	34.0, CH^{eq}	2.45, dd (17.3, 3.4)	33.1, CH^{eq}
5		119.7, C		119.6, C		119.9, C		120.0, CH
6		157.2, C		157.2, C		157.5, C		157.2, C
7	6.50, s	102.6, CH	6.48, s	102.6, CH	6.60, s	99.0, CH	6.62, s	99.3, CH
8		156.4, C		156.4, C		157.2, C		157.5, C
9		110.9, C		111.0, C		114.3, C		114.0, C
10		132.2, C		132.1, C		134.7, C		134.7, C
1'	6.65, s	118.0, CH	6.77, s	118.4, CH	6.69, s	118.3, CH	6.73, s	118.3, CH
2'		138.2, C		138.0, C		137.9, C		137.9, C
3'	6.78, s	110.0, CH	6.79, s	110.1, CH	6.80, s	109.9, CH	6.79, s	109.8, CH
4'		159.0, C		158.8, C		158.7, C		158.8, C
5'		158.4, C		158.4, C		158.4, C		158.4, C
6'	6.95, d (8.0)	107.0, CH	6.93, d (8.0)	106.9, CH	6.94, d (8.0)	106.6, CH	6.94, d (8.0)	106.6, CH
7'	7.18, d (7.9)	130.4, CH	7.15, d (7.9)	130.8, CH	7.16, d (7.9)	130.9, CH	7.17, d (8.0)	130.4, CH
8'		126.6, C		126.7, C		126.1, C		126.0, C
9'		138.0, C		137.8, C		137.5, C		138.1, C
10'		117.8, C		117.8, C		117.4, C		117.6, C
1-CH$_3$	1.72, d (6.7)	19.1, Me	1.74, d (6.7)	19.3, Me	1.73, d (6.6)	19.8, Me	1.75, d (6.6)	20.0, Me
3-CH$_3$	1.24, d (6.6)	16.7, Me	1.24, d (6.6)	16.9, Me	1.27, d (6.5)	17.9, Me	1.28, d (6.5)	17.9, Me
N-CH$_3$	2.72, s	34.2, Me	2.77, s	34.2, Me	3.02, s	41.4, Me	3.01, s	41.4, Me
8-OCH$_3$					3.92, s	56.1, Me	3.92, s	56.1, Me
2'-CH$_3$	2.30, s	22.2, Me	2.32, s	22.2, Me	2.31, s	22.0, Me	2.32, s	22.1, Me
4'-OCH$_3$	3.93, s	57.1, Me	3.93, s	57.1, Me	3.93, s	56.9, Me	3.93, s	56.9, Me
5'-OCH$_3$	3.95, s	56.9, Me	3.95, s	56.9, Me	3.96, s	56.7, Me	3.96, s	56.7, Me

IV.4.4 Known Alkaloids Isolated

The likewise isolated known monomeric and dimeric naphthylisoquinoline alkaloids ancistrocongoline C (**40**), ancistrolikokines C (**41**) and F$_2$ (**42**), ealamines A (**43**) and G (**44**), and mbandakamines A (**45**) and B$_2$ (**46**), now isolated for the first time from the leaves of this as yet unidentified Central Congolese *Ancistrocladus* liana, were found to be identical in their spectroscopic, physical, and chromatographic behavior with the data reported previously.[164,247,253,249,245,244,246]

IV.4.5 Oxidative Degradation

Following a procedure described earlier in our research group,[173] ca. 0.8 mg of ikelacongolines A (**35a**), B (**35b**), C (**36**), or D (**37**), or mbandakamines B$_3$ (**38**) or B$_4$ (**39**) were subjected to ruthenium(VIII)-catalyzed periodate oxidation, followed by conversion of the resulting chiral amino with MeOH/HCl to the respective methyl esters and Mosher-type derivatization with (*R*)-α-methoxy-α-trifluoromethylphenylacetyl chloride [(*R*)-MTPA-Cl, prepared from (*S*)-MTPA]. The absolute configurations of **35a**, **35b**, **36**, **37**, **38**, and **39** at C-3 were assigned by gas chromatography coupled to mass-selective detection (GC-MSD) and comparison with the corresponding derivatives of the authentic amino acids of known absolute configuration.

IV.4.6 Antiprotozoal Assay

Conducted in the research groups of Prof. M. Kaiser and Prof. R. Brun, the *in vitro* antiparasitic activities of the ikelacongolines A (**35a**), B (**35b**), and C (**36**), and of the mbandakamines B$_3$ (**38**) and B$_4$ (**39**) (Table 9) against the pathogens *Plasmodium falciparum* (NF54 and K1 strains), *Trypanosoma cruzi* (Tulahuen C4 strain, amastigotes), *Trypanosoma brucei rhodesiense* (STIB 900 strain, trypomastigotes), and *Leishmania donovani* (MHOM-ET-67/L82, amastigotes), and the cytotoxicity against mammalian host cells (rat skeletal myoblast L6 cells) were determined as described previously.[291]

IV.4.6 Antiausterity Assay

The antiausterity assay in both DMEM and NDM of all the isolated alkaloids (**35a**, **35b**, **36**–**46**) was evaluated in collaboration with the research group of Prof. S. Awale as previously described in the literature.[292]

IV.5 (*R*)-Tonkafuranone and Related Compounds: Improved synthesis, Stereochemical Purity in Nature, and Bioactivities of the Pure Enantiomers

### IV.5.1 Syntheses of Bicyclic Lactones (done by M. Hoffmann)

IV.5.1.1 General Synthetic Procedure

For the preparation of the bicyclic lactones, ketone (1 eq.) and α-keto acid (1.3 eq.) were mixed, the mixture was heated to 120 °C for 1−5 h in concentrated H_3PO_4 (15 mL) was added and. The mixture was cooled down to 25 °C and poured onto ice, followed by neutralization with NaOH (10 M). The aqueous layer was extracted with ethyl acetate (three times) and the combined organic layers were washed with water and brine, dried over Na_2SO_4, filtered, and evaporated to dryness under reduced pressure. The residue was pre-purified by flash column chromatography before HPLC analysis.

IV.5.1.2 5,6-dihydrobenzofuran-2(4H)-one (47)

Following the general synthetic procedure (GSP) developed in the research group of Prof. M. Decker, **47** was synthesized by M. Hoffmann from cyclohexanone (**52**) (1.58 mL, 1.5 g, 11 mmol) and glyoxylic acid monohydrate (**53**·H_2O) (1.32 g, 14.3 mmol, 1.3 eq.) after heating for one h at 120 °C. Flash column chromatography (PE / EA = 9/1, R_f = 0.05) yielded **47** as a colorless oil (539 mg, 3.96 mmol, 36%).[293,277,278]

^{1}H NMR (400 MHz, CDCl3): δ = 5.86 (t, *J* = 5.9, 1 H), 5.75 (s, 1 H), 2.70 (t, *J* = 6.4 Hz, 2 H), 2.38 (dd, *J* = 10.8, 5.5 Hz, 2 H), 1.86 (dt, *J* = 12.3, 6.1 Hz, 2 H) ppm;

47
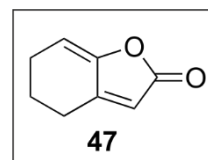
^{13}C NMR (101 MHz, CDCl3): δ = 170.20 (1 C), 155.77 (1 C), 150.48 (1 C), 111.12 (1 C), 111.05 (1 C), 24.35(1 C), 23.83 (1 C), 22.77 (1 C) ppm;

HPLC (analytical method): t_R = 9.52 min, purity = 96.9%;

MSESI: *m/z* 137.00 [M+H]$^+$ (calculated for $C_8H_9O_2$, 137.06).[293,277,278]

IV.5.1.3 3-methyl-5,6-dihydrobenzofuran-2(4H)-one (48)

Following the GSP, **48** was likewise synthesized by M. Hoffmann from cyclohexanone (**52**) (2 mL, 1.896 g, 36.6 mmol) and pyruvic acid (**54**) (3.3 mL, 4.190 g, 47.58 mmol, 1.3 eq.) after heating to 120 °C for 3 h. Flash column chromatography (PE / EA = 9/1, R_f = 0.07) yielded **48** as a colorless oil (2473 mg, 16.47 mmol, 45%).[280]

48 Me
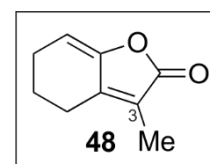
^{1}H NMR (400 MHz, CD₃OD): δ = 5.81 (t, *J* = 6.0, 1 H), 2.69–2.59 (m, 2 H), 2.45–2.35 (m, 2 H), 1.89–1.77 (m, 5 H) ppm;

^{13}C NMR (101 MHz, CD₃OD): δ = 170.25 (1 C), 155.79 (1 C), 150.52 (1 C), 127.31 (1 C), 111.21 (1 C), 24.34 (1 C), 23.89 (1 C), 22.73 (1 C), 8.77 (1 C) ppm;

HPLC (analytical method): t_R = 10.26 min, purity = 97.8%;

MSESI: *m/z* 151.00 [M+H]⁺ (calculated for $C_9H_{10}O_2H$, 151.08).

Spectral data were in accordance with those reported in the literature.[280]

IV.5.1.4 (R/S)-6-methyl-5,6-dihydrobenzofuran-2(4H)-one (49a/49b) and (R/S)-4-methyl-5,6 dihydrobenzofuran-2(4H)-one (50a/50b)

Following the GSP, the mixture of **49a**/**49b** and **50a**/**50b** was also synthesized by M. Hoffmann from 3-methylyclohexanone (**55**) (1.5 mL, 1.371 g, 12.2 mmol) and glyoxylic acid monohydrate (**53**·H2O) (1.46 g, 15.86 mmol, 1.3 eq.) after heating for 3 h at 120 °C. Flash column chromatography (PE / EA = 9/1) yielded a racemic mixture of the regioisomers **49/50** as a colorless oil (531 mg, 3.59 mmol, 29%). The isomers **49/50** were separated by preparative HPLC (done by the author of this thesis). HPLC (method 1): **49a/b**; retention time, t_R = 16.37 min; **50a/b**, t_R = 16.02 min. HPLC (chiral method 1): **49a**, t_R = 19.2 min (purity 91.4%); **49b**, t_R = 18.4 min (purity 99.8%).[277,278]

(*R/S*)-6-methyl-5,6-dihydrobenzofuran-2(4H)-one (**49a/49b**):

^{1}H NMR (400 MHz, CD₃OD): δ = 5.78–5.70 (m, 1 H), 5.81–5.79 (m, 1 H), 2.92-2.85 (m, 1H), 2.69–2.55 (m, 2 H), 2.03–1.96 (m, 1 H), 1.51-1.41 (m, 1H), 1.16 (d, J = 7.11 Hz, 3 H) ppm;
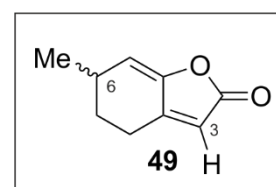
^{13}C NMR (101 MHz, CD₃OD): δ = 172.43 (1 C), 158.00 (1 C), 151.44 (1 C), 118.25 (1 C), 111.50 (1 C), 58.37 (1 C), 32.24 (1 C), 31.14 (1 C), 23.93 (1 C), (1 C) ppm;

HPLC (analytical method): t_R =11.1 min;

MSESI: *m/z* 151.00 [M+H]⁺ (calculated for $C_{10}H_{12}O_2H$, 151.08).

49a: $[\alpha]_D^{25}$ = +133.82±5.34 (MeOH, *c* = 0.11 g 100 mL⁻¹).

49b: $[\alpha]_D^{25}$ = −125.3±0.7 (CH₂Cl₂, *c* = 0.27 g 100 mL⁻¹);

$[\alpha]_D^{25}$= −133.7±4.45 (MeOH, *c* = 0.19 g 100 mL⁻¹).[277,278]
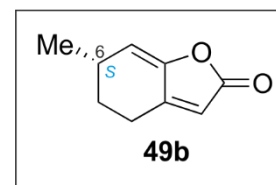
(*R/S*)-4-methyl-5,6-dihydrobenzofuran-2(4H)-one (**50a/50b**): HPLC (analytical method): t_R = 11.1 min; MS (ESI): [M+H]$^+$ calculated for $C_{10}H_{12}O_2H$ (151.08), found 151.00.

IV.5.1.5 (*R/S*)-3,6-dimethyl-5,6-dihydrobenzofuran-2(4H)-one (**7a/7b**) *and* (*R/S*)-3,4-dimethyl-5,6-dihydrobenzofuran-2(4H)-one (**51a/51b**)

Following the GSP, the mixture of **7a/7b** and **51a/51b** was synthesized by M. Hoffmann as well from 3-methylcyclohexanone (**55**) (1.5 mL, 1.371 g, 12.2 mmol) and pyruvic acid (**54**) (1.1 mL, 1.397 g, 15.86 mmol, 1.3 eq.) after heating to 120 °C for 5 h. Flash column chromatography (PE / EA = 9/1) yielded a mixture of the regioisomers **7** and **51** as a colorless oil (540 mg, 3.29 mmol, 27%). The regioisomers **7** and **51** were separated by preparative HPLC (done by the author of this thesis). HPLC (method 2): **7a/b**, t_R = 19.35 min; **51a/b**, t_R = 18.43 min. HPLC (chiral method 1): **7a**, t_R = 10.7 min (purity 96.5%); **7b**, t_R = 9.7 min (purity 99.4%).

For the NMR data of **7**, see (*R*)-3,6-dimethyl-5,6-dihydrobenzofuran-2(4H)-one (**7a**) below.

(*R/S*)-3,4-dimethyl-5,6-dihydrobenzofuran-2(4*H*)-one (**51a/51b**):

^{1}H NMR (400 MHz, CD$_3$OD): δ = 5.79 (dd, *J* = 5.13, 4.00, 1 H), 3.08-3.00 (m, 1H), 2.68–2.58 (m, 1 H), 2.53–2.44 (m, 1 H), 2.38-2.29 (m, 1H), 1.95-1.85 (m, 1H), 1.90 (s, 3 H), 1.23 (d, *J* = 7.1 Hz, 3 H) ppm;
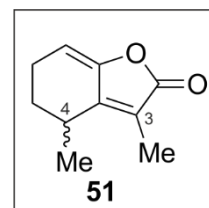
^{13}C NMR (101 MHz, CD$_3$OD): δ = 173.39 (1 C), 154.26 (1 C), 150.18 (1 C), 120.50 (1 C), 109.75 (1 C), 39.87 (1 C), 29.42 (1 C), 21.72 (1 C), 17.81 (1 C), 8.33 (1 C) ppm;

HPLC (analytical method): t_R = 11.22 min;

MSESI: *m/z* 165.00 [M + H]$^+$ (calculated for $C_{10}H_{12}O_2H$ 165.09).

IV.5.1.6 (*R*)-3,6-Dimethyl-5,6-dihydrobenzofuran-2(4H)-one (**7a**)

(+)-Menthofuran (**56**, 200 mg, 1.33 mmol, 1 eq.) was dissolved by M. Hoffmann in acetonitrile (7 mL) and 2,3-dichloro-5,6-dicyano-1,4-benzoquinone (605 mg, 2.66 mmol, 2 eq) added. The mixture was stirred for 4 h at room temperature and then filtered over a pad of celite. The residue was washed with acetonitrile. The filtrate was evaporated to dryness under reduced pressure. The resulting residue was purified by flash column chromatography (PE / EA = 5/1, R$_f$ = 0.24) to yield **7a** as a colorless oil (92 mg, 0.56 mmol; 42% yield).[282]

IV.5 (R)-Tonkafuranone and Related Compounds

^{1}H NMR (400 MHz, CDCl$_3$): δ = 5.50 (d, J = 3.3 Hz, 1 H), 2.68–2.58 (m, 1 H), 2.54–2.31 (m, 2 H), 1.77 (s, 3 H), 1.42–1.28 (m, 2 H), 1.04 (d, J = 7.1 Hz, 3 H) ppm;

^{13}C NMR (101 MHz, CDCl$_3$): δ = 171.52 (1 C), 149.26 (1 C), 148.22 (1 C), 119.83 (1 C), 114.09 (1 C), 31.08 (1 C), 29.82 (1 C), 21.83 (1 C), 21.19 (1 C), 8.55 (1 C) ppm;
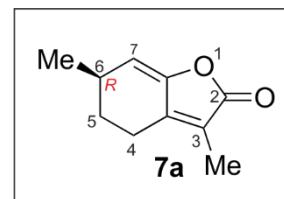
HPLC (analytical method): t_R = 11.22 min, purity = 99.3 %;

MSESI: m/z 165.00 [M+H]$^+$ (calculated for C$_{10}$H$_{12}$O$_2$H, 165.09);

$[\alpha]_D^{25}$ = 104.3 ± 0.8 (CH$_2$Cl$_2$, c = 0.32 g 100 mL^{-1}).

$[\alpha]_D^{25}$ = + 118.9 ± 4.7 (MeOH; c = 0.51 g 100 mL^{-1}).

All spectral data were in accordance with the data reported in the literature ($[\alpha]_D^{25}$ = +118.2; MeOH).[276,263,282,268]

IV.5.1.7 Isolation of (S)-Tonkafuranone (7b) from Bursera graveolens

Woody parts (about 156.4 g) of *Bursera graveolens* were ground and extracted by the author of this thesis with petroleum ether at 20–25 °C. The combined extracts were concentrated under reduced pressure to give 15.1 g of crude residue. This was submitted to flash column chromatography using silica gel as a stationary phase and a mixture of n-hexane and ethyl acetate in a gradient elution (from 95 to 60% n-hexane). Fractions containing the spot-on TLC corresponding to (S)-tonkafuranone (7b) were concentrated in vacuo, dissolved in methanol, and further purified by preparative HPLC using Methods 2 and 3 successively.[268]

$[\alpha]_D^{25}$ = −119.2 ± 4.2 (MeOH; c = 0.12 g 100 mL^{-1}).

IV.5.2 Preparative HPLC

IV.5.2.1 Method 1: The stationary phase used was a C18 Symmetry (300 × 19 mm, 7 μm) column and the mobile phases A (H$_2$O/MeCN, 9:1) and B (MeCN/H$_2$O, 9:1), containing each 0.05% TFA, with the following gradient program: at 0 min 35% of B, at 20 min 65% of B, applying a flow rate of 10 mL min^{-1} (developed by the author of this thesis).

IV.5.2.2 Method 2: As method 1 but starting with 40% of B at 0 min (developed by the author of this thesis).

IV.5.2.3 Method 3: The stationary phase used a Waters XSelect HSS PFP column (10×250 mm, 5 μm) and the mobile phases A′ (H_2O/MeOH, 9:1) and B′ (MeOH/H_2O, 9:1), each containing 0.05% TFA, with the following linear gradient program: at 0 min, 50% B′; at 20 min, 100% B′, with a flow rate of 5 mL min^{-1} (developed by the author of this thesis).

IV.5.3 Analytical HPLC Methods

For purity control of target compounds, the following conditions were used: Synergi 4U fusion RP (Synergi, Aschaffenburg, Germany), as the eluent system, water (Phase A) and methanol (Phase B), each containing 0.1% formic acid were used with a flow of 1.0 mL min^{-1} (gradient: 0 min 5% of B and 13 min 90% of B). Compounds were detected at $\lambda = 254$ nm, and target compounds were ≥ 95% pure (Analytical Method, developed in the research of Prof. M. Decker).

IV.5.4 Chiral HPLC Methods

Enantiomers were resolved using a Lux® 5-μm Cellulose-1 (250×4.6 mm) column and a mixture of *n*-hexane and isopropanol (99:1, v/v) as the mobile phase, at a flow rate of 1 mL min^{-1} (Chiral Method 1, developed by the author of this thesis).

The enantiomers of the more important and synthetically prevailing regioisomers **49** and **7** were additionally resolved on a preparative scale, using the same column but with a larger inner diameter (250×21.2 mm) and a mixture of two eluents, MeOH/H_2O (9:1) and H_2O/MeOH (9:1) at a ratio of 6:4, each containing 0.05% TFA, applying a flow rate of 20 mL min^{-1}, finally leading to pure (*R*)- and (*S*)-**49**, and to likewise pure (*R*)- and (*S*)-**7** in sufficient quantities and enantiomerically pure form for comparative bioevaluation *in vitro* (method developed by the author of this thesis).

IV.5.5 Cytotoxicity in V79 Cells

The following experiments were done by Dr. C. Kleider from the research group of Prof. L. Lehmann: Cells were cultured in Dulbecco's Modified Eagle Medium (DMEM) supplemented with 100 U mL^{-1} penicillin, 100 µg mL^{-1} streptomycin, and 10% fetal calf serum at 37 °C with 5% CO_2 in a humidified incubator.

V79 cells were seeded and grown in 24-well plates using the same culture conditions as previously applied in experiments investigating the mutagenicity of patulin (**8**). Compounds were dissolved and diluted in MeOH. Final concentrations [patulin (**8**): 0.04, 0.10, 0.26, 0.64, 1.6, 4, 10 µM; synthesized compounds: 4, 10, 26, 64, 160, 400, 1000 µM] were obtained by dilution with medium resulting in 1% (v/v) methanol. 24 h after seeding, cells were treated with

the compounds (220 μL medium per well) in triplicate for 24 h. Treatment of cells with 1% methanol served as solvent control. Subsequently, the number of viable cells was determined by electronic cell counting using a CASY Model DT as described before.[294]

Experiments were repeated independently at least twice using different batches of cells. For each independent experiment, separate aliquots of compounds were weighed, and fresh incubation solutions were prepared. Identity and concentration of solutions were verified by HPLC-UV, using a Phenomenex Luna C18 column (250×4.6 mm, 5 μm); eluents were water and acetonitrile, both with 0.1% formic acid, at a flow rate of 1 mL min^{-1}, gradient changed linearly from 35% to 65% acetonitrile during the first 20 min and was held for 3 min at 65% acetonitrile before changing back to the initial conditions.

IV.5.6 Cytotoxicity in Neuronal HT-22 Cells

This cytotoxicity was conducted in Prof. M. Decker's group by S. Gunesh: HT-22 cells were grown in Dulbecco´s Modified Eagle Medium (DMEM) supplemented with 10% (v/v) heat-inactivated fetal calf serum and 1% (v/v) penicillin-streptomycin. Cells were sub-cultured every two days and incubated at 37 °C with 5% CO_2 in a humidified incubator. Compounds were dissolved in dimethyl sulfoxide (DMSO) and diluted with medium.

An amount of 5,000 cells per well were seeded into sterile 96-well plates. A 0.1-M stock solution of the compounds was diluted with medium to 50 μM and after 24 h incubation, culture medium was removed and 100 μL of the 50 μM compound solution (highest possible concentration in this experimental setup) was added to the wells. 0.05% DMSO in DMEM served as a control. Cells were incubated for 24 h.

For quantification of cell viability, medium was removed and 3-(4,5-dimethylthiazol-2-yl)-2,5-diphenyltetrazolium bromide (MTT) stock solution (4 mg mL^{-1} in PBS) was diluted 1:10 with medium and 100 μL MTT per well was added. Cells were incubated for three h when the supernatant was removed and lysis buffer (10% sodium dodecyl sulfate) was applied. The next day (stored at room temperature, in darkness overnight), absorbance at 560 nm was determined with a multi-well plate photometer.

Literature

Literature

[1] K. J. Williams; The introduction of 'chemotherapy' using arsphenamine - The first magic bullet; *J. R. Soc. Med.* **2009**, *102*, 343–348.

[2] H. Otten; Domagk and the development of the sulphonamides; *J. Antimicrob. Chemother.* **1986**, *17*, 689–690.

[3] R. Gaynes; The discovery of penicillin - New insights after more than 75 years of clinical use; *Emerg. Infect. Dis.* **2017**, *23*, 849–853.

[4] S. Y. Tan, Y. Tatsumura; Alexander Fleming (1881–1955): Discoverer of penicillin; *Singapore Med. J.* **2015**, *56*, 366–367.

[5] J. L. Martínez, F. Baquero; Emergence and spread of antibiotic resistance: Setting a parameter space; *Upsala J. Med. Sci.* **2014**, *119*, 68–77.

[6] N. S. McClure, T. Day; A theoretical examination of the relative importance of evolution management and drug development for managing resistance; *Proc. Biol. Sci.* **2014**, *281*, 20141861.

[7] C. A. Michael, D. Dominey-Howes, M. Labbate; The antimicrobial resistance crisis: Causes, consequences, and management; *Front. Public Health* **2014**, *2*, 145.

[8] B. Bengtsson, C. Greko; Antibiotic resistance - Consequences for animal health, welfare, and food production; *Upsala J. Med. Sci.* **2014**, *119*, 96–102.

[9] R. Laxminarayan, Z. Bhutta, A. Duse, P. Jenkins, T. O'Brien, I. N. Okeke, A. Pablo-Mendez, K. P. Klugman, *Drug resistance;* The International Bank for Reconstruction and Development / The World Bank, **2006**.

[10] N. D. Friedman, E. Temkin, Y. Carmeli; The negative impact of antibiotic resistance; *Clin. Microbiol. Infect.* **2016**, *22*, 416–422.

[11] S. E. Cosgrove, Y. Carmeli; The impact of antimicrobial resistance on health and economic outcomes; *Clin. Infect. Dis.* **2003**, *36*, 1433–1437.

[12] S. Allcock, E. H. Young, M. Holmes, D. Gurdasani, G. Dougan, M. S. Sandhu, L. Solomon, M. E. Török; Antimicrobial resistance in human populations: Challenges and opportunities; *Glob. Health Epidemiol.* **2017**, *2*, e4.

[13] V. I. Band, S. W. Satola, E. M. Burd, M. M. Farley, J. T. Jacob, D. S. Weiss; Carbapenem-resistant *Klebsiella pneumoniae e*xhibiting clinically undetected colistin heteroresistance leads to treatment failure in a murine model of infection; *mBio* **2018**, *9*, e02448-17.

[14]   F. Lombardi, P. Gaia, R. Valaperta, M. Cornetta, M. R. Tejada, L. Di Girolamo, A. Moroni, F. Ramundo, A. Colombo, M. Valisi, E. Costa; Emergence of carbapenem-resistant *Klebsiella pneumoniae*: Progressive spread and four-year period of observation in a cardiac surgery division; *Biomed Res. Int.* **2015**, *2015*, 871947.

[15]   H. Sidjabat, G. R. Nimmo, T. R. Walsh, E. Binotto, A. Htin, Y. Hayashi, J. Li, R. L. Nation, N. George, D. L. Paterson; Carbapenem resistance in *Klebsiella pneumoniae* due to the New Delhi metallo-β-lactamase; *Clin. Infect. Dis.* **2011**, *52*, 481–484.

[16]   J. H. Jeon, J. H. Lee, J. J. Lee, K. S. Park, A. M. Karim, C.-R. Lee, B. C. Jeong, S. H. Lee; Structural basis for carbapenem-hydrolyzing mechanisms of carbapenemases conferring antibiotic resistance; *Int. J. Mol. Sci.* **2015**, *16*, 9654–9692.

[17]   K. M. Papp-Wallace, A. Endimiani, M. A. Taracila, R. A. Bonomo; Carbapenems: Past, present, and future; *Antimicrob. Agents Chemother.* **2011**, *55*, 4943–4960.

[18]   S. Rath, R. N. Padhy; Prevalence of fluoroquinolone resistance in *Escherichia coli* in an Indian teaching hospital and adjoining communities; *J. Taibah Uni. Med. Sci.* **2015**, *10*, 504–508.

[19]   M. Karczmarczyk, M. Martins, T. Quinn, N. Leonard, S. Fanning; Mechanisms of fluoroquinolone resistance in *Escherichia coli* isolates from food-producing animals; *Appl. Environ. Microbiol.* **2011**, *77*, 7113–7120.

[20]   M. Webber, L. J. V. Piddock; Quinolone resistance in *Escherichia coli*; *Vet. Res.* **2001**, *32*, 275–284.

[21]   T. Regnath, T. Mertes, R. Ignatius; Antimicrobial resistance of *Neisseria gonorrhoeae* isolates in south-west Germany, 2004 to 2015: Increasing minimal inhibitory concentrations of tetracycline but no resistance to third-generation cephalosporins; *Euro Surveill.* **2016**, *21*, 30335.

[22]   S. H. Park; Third-generation cephalosporin resistance in gram-negative bacteria in the community: A growing public health concern; *Korean J. Intern. Med.* **2014**, *29*, 27–30.

[23]   M. Bala, S. Sood; Cephalosporin resistance in *Neisseria gonorrhoeae*; *J. Global Infect. Dis.* **2010**, *2*, 284–290.

[24]   K. Hiramatsu, Y. Katayama, M. Matsuo, T. Sasaki, Y. Morimoto, A. Sekiguchi, T. Baba; Multi-drug-resistant *Staphylococcus aureus* and future chemotherapy; *J. Infect. Chemother.* **2014**, *20*, 593–601.

[25]   C. M. D de Maio Carrillho, J. J. Gaudereto, R. C. R. Martins, V. A. C. de Castro Lima, L. M. de Oliveira, M. R. Urbano, J. S. Perozin, A. S. Levin, S. F. Costa; Colistin-resistant

Enterobacteriaceae infections: Clinical and molecular characterization and analysis of in vitro synergy; *Diagn. Microbiol. Infect. Dis.* **2017**, *87*, 253–257.

[26]   K. J. Seung, S. Keshavjee, M. L. Rich; Multidrug-resistant tuberculosis and extensively drug-resistant tuberculosis; *Cold Spring Harb. Perspect. Med.* **2015**, *5*.

[27]   A. N. Phillips, J. Stover, V. Cambiano, F. Nakagawa, M. R. Jordan, D. Pillay, M. Doherty, P. Revill, S. Bertagnolio; Impact of HIV drug resistance on HIV/AIDS-associated mortality, new Infections, and antiretroviral therapy program costs in sub–Saharan Africa; *J. Infect. Dis.* **2017**, *215*, 1362–1365.

[28]   M. Hussain, H. D. Galvin, T. Y. Haw, A. N. Nutsford, M. Husain; Drug resistance in influenza A virus: The epidemiology and management; *Infect. Drug Resist.* **2017**, *10*, 121–134.

[29]   F. Checchi, R. Durand, S. Balkan, B. T. Vonhm, J. Z. Kollie, P. Biberson, E. Baron, J. Le Bras, J.-P. Guthmann; High *Plasmodium falciparum* resistance to chloroquine and sulfadoxine-pyrimethamine in Harper, Liberia: Results *in vivo* and analysis of point mutations; *Trans. R. Soc. Trop. Med. Hyg.* **2002**, *96*, 664–669.

[30]   T. E. Wellems, C. V. Plowe; Chloroquine-resistant malaria; *J. Infect. Dis.* **2001**, *184*, 770–776.

[31]   J.-F. Trape, G. Pison, M.-P. Preziosi, C. Enel, A. D. Du Loû, V. Delaunay, B. Samb, E. Lagarde, J.-F. Molez, F. Simondon; Impact of chloroquine resistance on malaria mortality; *C. R. Acad. Sci. III* **1998**, *321*, 689–697.

[32]   R. Abdul-Ghani, H. F. Farag, A. F. Allam; Sulfadoxine-pyrimethamine resistance in *Plasmodium falciparum*: A zoomed image at the molecular level within a geographic context; *Acta Trop.* **2013**, *125*, 163–190.

[33]   M. Imwong, K. Suwannasin, C. Kunasol, K. Sutawong, M. Mayxay, H. Rekol, F. M. Smithuis, T. M. Hlaing, K. M. Tun, R. W. van der Pluijm, R. Tripura, O. Miotto, D. Menard, M. Dhorda, N. P. J. Day, N. J. White, A. M. Dondorp; The spread of artemisinin-resistant *Plasmodium falciparum* in the Greater Mekong subregion: A molecular epidemiology observational study; *Lancet Infect. Dis.* **2017**, *17*, 491–497.

[34]   R. M. Fairhurst, A. M. Dondorp; Artemisinin-resistant *Plasmodium falciparum* malaria; in *Emerging infections 10* (Eds.: W. M. Scheld, J. M. Hughes, R. J. Whitley), American Society of Microbiology, **2016**, pp. 409–429.

[35]   Z.-R. Lun, P. E. Ferreira, L.-C. Fu; Artemisinin resistance in *Plasmodium falciparum*; *Lancet Infect. Dis.* **2014**, *14*, 450–451.

[36]   A. M. Dondorp, F. Nosten, P. Yi, D. Das, A. P. Phyo, J. Tarning, K. M. Lwin, F. Ariey, W. Hanpithakpong, S. J. Lee, P. Ringwald, K. Silamut, M. Imwong, K. Chotivanich, P. Lim, T. Herdman, S. S. An, S. Yeung, P. Singhasivanon, N. P. J. Day, N. Lindegardh, D. Socheat, N. J. White; Artemisinin resistance in *Plasmodium falciparum* malaria; *N. Engl. J. Med.* **2009**, *361*, 455–467.

[37]   D. Ménard, J. Clain, F. Ariey; Multidrug-resistant *Plasmodium falciparum* malaria in the Greater Mekong subregion; *Lancet Infect. Dis.* **2018**, *18*, 238–239.

[38]   A. Mehl, B. O. Åsvold, A. Kümmel, S. Lydersen, J. Paulsen, I. Haugan, E. Solligård, J. K. Damås, S. Harthug, T.-H. Edna; Trends in antimicrobial resistance and empiric antibiotic therapy of bloodstream infections at a general hospital in Mid-Norway: A prospective observational study; *BMC Infect. Dis.* **2017**, *17*, 116.

[39]   P. Padiyara, H. Inoue, M. Sprenger; Global governance mechanisms to address antimicrobial resistance; *Infect. Dis.: Res. Treat.* **2018**, *11*, 1-4.

[40]   G. Cheng, M. Dai, S. Ahmed, H. Hao, X. Wang, Z. Yuan; Antimicrobial drugs in fighting against antimicrobial resistance; *Front. Microbiol.* **2016**, *7*, 470.

[41]   World Health Organization, *Antimicrobial resistance. Fact Sheet*, Geneva, **2018**.

[42]   I. K. Voukeng, V. P. Beng, V. Kuete; Antibacterial activity of six medicinal Cameroonian plants against Gram-positive and Gram-negative multidrug resistant phenotypes; *BMC Complement. Altern. Med.* **2016**, *16*, 388.

[43]   A. Ponte-Sucre, J. H. Faber, T. Gulder, I. Kajahn, S. E. H. Pedersen, M. Schultheis, G. Bringmann, H. Moll; Activities of naphthylisoquinoline alkaloids and synthetic analogs against *Leishmania major*; *Antimicrob. Agents Chemother.* **2007**, *51*, 188–194.

[44]   G. Bringmann, Pokorny F.; The Naphthylisoquinoline Alkaloids; in *The Alkaloids* (Ed.: G. A. Cordell), Academic Press, New York, **1995**, pp. 127–271.

[45]   G. Bringmann, C. Günther, M. Ochse, O. Schupp, S. Tasler; Biaryls in Nature: A Multi-Facetted Class of Stereochemically, Biosynthetically, and Pharmacologically Intriguing Secondary Metabolites; in *Progress in the Chemistry of Organic Natural Products*, vol. 82 (Eds.: W. Herz, H. Falk, G. W. Kirby, R. E. Moore), Springer, Wien, **2001**, pp. 1–249.

[46]   S. R. M. Ibrahim, G. A. Mohamed; Naphthylisoquinoline alkaloids potential drug leads; *Fitoterapia* **2015**, *106*, 194–225.

[47]   Y. F. Hallock, K. P. Manfredi, J. W. Blunt, J. H. Cardellina II, M. Schaeffer, K.-P. Gulden, G. Bringmann, A. Y. Lee, J. Clardy; Korupensamines A-D, novel antimalarial alkaloids from *Ancistrocladus korupensis*; *J. Org. Chem.* **1994**, *59*, 6349–6355.

[48] G. François, G. Timperman, W. Eling, L. Aké Assi, J. Holenz, G. Bringmann; Naphthylisoquinoline alkaloids against malaria: Evaluation of the curative potentials of dioncophylline C and dioncopeltine A against *Plasmodium berghei in vivo*; *Antimicrob. Agents Chemother.* **1997**, *41*, 2533–2539.

[49] C. M. Taylor, R. E. Gereau, G. M. Walters; Revision of *Ancistrocladus* Wall. (Ancistrocladaceae); *Ann. Mo. Bot. Gard.* **2005**, *92*, 360–399.

[50] G. Heubl, F. Turini, V. Mudogo, I. Kajahn, G. Bringmann; *Ancistrocladus ileboensis* (D.R. Congo), a new liana with unique alkaloids; *Plant Ecol. Evol.* **2010**, *143*, 63–69.

[51] J. M. Dorn, M. Alpern, C. McNulty, G. W. Volcheck; Sulfonamide drug allergy; *Curr. Allergy Asthma Rep.* **2018**, *18*, 38.

[52] J. Nwokike, A. Clark, P. P. Nguyen; Medicines quality assurance to fight antimicrobial resistance; *Bull. World Health Organ.* **2018**, *96*, 135–137.

[53] E. Pisani, *Antimicrobial resistance: What does medicine quality have to do with it?;* Review Antimicrobial Resistance, **2015**.

[54] K. de With, F. Allerberger, S. Amann, P. Apfalter, H.-R. Brodt, T. Eckmanns, M. Fellhauer, H. K. Geiss, O. Janata, R. Krause, S. Lemmen, E. Meyer, H. Mittermayer, U. Porsche, E. Presterl, S. Reuter, B. Sinha, R. Strauß, A. Wechsler-Fördös, C. Wenisch, W. V. Kern; Strategies to enhance rational use of antibiotics in hospital: A guideline by the German Society for Infectious Diseases; *Infection* **2016**, *44*, 395–439.

[55] G. Jeetu, G. Anusha; Pharmacovigilance: A worldwide master key for drug safety monitoring; *J. Young Pharm.* **2010**, *2*, 315–320.

[56] P. Paul, C. Sänger-van de Griend, E. Adams, A. van Schepdael; Recent advances in the capillary electrophoresis analysis of antibiotics with capacitively coupled contactless conductivity detection; *J. Pharm. Biomed. Anal.* **2018**, *158*, 405–415.

[57] T. B. Adams, D. B. Greer, J. Doull, I. C. Munro, P. Newberne, P. S. Portoghese, R. L. Smith, B. M. Wagner, C. S. Weil, L. A. Woods, R. A. Ford; The FEMA GRAS assessment of lactones used as flavour ingredients; *Food Chem. Toxicol.* **1998**, *36*, 249–278.

[58] H. Malekinejad, J. Aghazadeh-Attari, A. Rezabakhsh, M. Sattari, B. Ghasemsoltani-Momtaz; Neurotoxicity of mycotoxins produced in vitro by *Penicillium roqueforti* isolated from maize and grass silage; *Hum. Exp. Toxicol.* **2015**, *34*, 997–1005.

[59] C. Pfenning, H. L. Esch, R. Fliege, L. Lehmann; The mycotoxin patulin reacts with DNA bases with and without previous conjugation to GSH: Implication for related α,β-unsaturated carbonyl compounds?; *Arch. Toxicol.* **2016**, *90*, 433–448.

[60] M. E. Sinka, M. J. Bangs, S. Manguin, Y. Rubio-Palis, T. Chareonviriyaphap, M. Coetzee, C. M. Mbogo, J. Hemingway, A. P. Patil, W. H. Temperley, P. W. Gething, C. W. Kabaria, T. R. Burkot, R. E. Harbach, S. I. Hay; A global map of dominant malaria vectors; *Parasit. Vectors* **2012**, *5*, 69.

[61] J. Ramirez, L. S. Garver, G. Dimopoulos; Challenges and approaches for mosquito targeted malaria control; *Curr. Mol. Med.* **2009**, *9*, 116–130.

[62] S. Antinori, L. Galimberti, L. Milazzo, M. Corbellino; Biology of human malaria plasmodia including *Plasmodium knowlesi*; *Mediterr. J. Hematol. Infect. Dis.* **2012**, *4*.

[63] B. Autino, A. Noris, R. Russo, F. Castelli; Epidemiology of malaria in endemic areas; *Mediterr. J. Hematol. Infect. Dis.* **2012**, *4*, e2012060.

[64] P. W. Gething, I. R. F. Elyazar, C. L. Moyes, D. L. Smith, K. E. Battle, C. A. Guerra, A. P. Patil, A. J. Tatem, R. E. Howes, M. F. Myers, D. B. George, P. Horby, H. F. L. Wertheim, R. N. Price, I. Müeller, J. K. Baird, S. I. Hay; A long neglected world malaria map: *Plasmodium vivax* endemicity in 2010; *PLoS Negl. Trop. Dis.* **2012**, *6*, e1814.

[65] R. E. Howes, K. E. Battle, K. N. Mendis, D. L. Smith, R. E. Cibulskis, J. K. Baird, S. I. Hay; Global epidemiology of *Plasmodium vivax*; *Am. J. Trop. Med. Hyg.* **2016**, *95*, 15–34.

[66] A. Bartoloni, L. Zammarchi; Clinical aspects of uncomplicated and severe malaria; *Mediterr. J. Hematol. Infect. Dis.* **2012**, *4*, e2012026.

[67] A. Trampuz, M. Jereb, I. Muzlovic, R. M. Prabhu; Clinical review: Severe malaria; *Crit. Care* **2003**, *7*, 315–323.

[68] D. L. Doolan, C. Dobaño, J. K. Baird; Acquired immunity to malaria; *Clin. Microbiol. Rev.* **2009**, *22*, 13-36.

[69] World Health Organization, *World Malaria Report 2017*, Geneva, **2017**.

[70] S. I. Hay, C. A. Guerra, A. J. Tatem, A. M. Noor, R. W. Snow; The global distribution and population at risk of malaria: Past, present, and future; *Lancet Infect. Dis.* **2004**, *4*, 327–336.

[71] World Health Organization, *World Malaria Report 2016*, Geneva, **2017**.

[72] A. M. van Eijk, J. Hill, A. M. Noor, R. W. Snow, F. O. ter Kuile; Prevalence of malaria infection in pregnant women compared with children for tracking malaria transmission in sub-Saharan Africa: A systematic review and meta-analysis; *Lancet Glob. Health* **2015**, *3*, e617-e628.

[73] R. González, E. Sevene, G. Jagoe, L. Slutsker, C. Menéndez; A public health paradox: The women most vulnerable to malaria are the least protected; *PLoS Med.* **2016**, *13*, e1002014.

[74] K. Raghavendra, T. K. Barik, B. P. N. Reddy, P. Sharma, A. P. Dash; Malaria vector control: From past to future; *Parasitol. Res.* **2011**, *108*, 757–779.

[75] E. Schwartz; Prophylaxis of malaria; *Mediterr. J. Hematol. Infect. Dis.* **2012**, *4*, e2012045.

[76] I. Owusu-Boateng, F. Anto; Intermittent preventive treatment of malaria in pregnancy: A cross-sectional survey to assess uptake of the new sulfadoxine-pyrimethamine five dose policy in Ghana; *Malar. J.* **2017**, *16*, 323.

[77] M. M. Meremikwu, S. Donegan, D. Sinclair, E. Esu, C. Oringanje; Intermittent preventive treatment for malaria in children living in areas with seasonal transmission; *Cochrane Database Syst. Rev.* **2012**, CD003756.

[78] World Health Organization, *Guidelines for the Treatment of Malaria*, Geneva, **2015**.

[79] R. Kunte, R. Kunwar; WHO guidelines for the treatment of malaria; *Med. J. Armed Forces India* **2011**, *67*, 376.

[80] E. Schwartz, G. Regev-Yochay; Primaquine as prophylaxis for malaria for nonimmune travelers: A comparison with mefloquine and doxycycline; *Clin. Infect. Dis.* **1999**, *29*, 1502–1506.

[81] M. Cairns, B. Cisse, C. Sokhna, C. Cames, K. Simondon, E. H. Ba, J.-F. Trape, O. Gaye, B. M. Greenwood, P. J. M. Milligan; Amodiaquine dosage and tolerability for intermittent preventive treatment to prevent malaria in children; *Antimicrob. Agents Chemother.* **2010**, *54*, 1265–1274.

[82] Q. Li, P. Weina; Artesunate: The best drug in the treatment of severe and complicated Malaria; *Pharmaceuticals* **2010**, *3*, 2322–2332.

[83] E. Esu, E. E. Effa, O. N. Opie, A. Uwaoma, M. M. Meremikwu; Artemether for severe malaria; *Cochrane Database Syst. Rev.* **2014**, CD010678.

[84] R. Ravinetto, D. Vandenbergh, C. Macé, C. Pouget, B. Renchon, J. Rigal, B. Schiavetti, J.-M. Caudron; Fighting poor-quality medicines in low- and middle-income countries: the importance of advocacy and pedagogy; *J. Pharm. Policy Pract.* **2016**, *9*, 36.

[85] L. A. Krech, L. El-Hadri, L. Evans, T. Fouche, M. Hajjou, P. Lukulay, S. Phanouvong, V. Pribluda, L. Roth; The medicines quality database: A free public resource; *Bull. World Health Organ.* **2014**, *92*, 2-2A.

[86] P. N. Newton, A. A. Amin, C. Bird, P. Passmore, G. Dukes, G. Tomson, B. Simons, R. Bate, P. J. Guerin, N. J. White; The primacy of public health considerations in defining poor quality medicines; *PLoS Med.* **2011**, *8*, e1001139.

[87] P. N. Newton, M. D. Green, F. M. Fernández; Impact of poor-quality medicines in the 'developing' world; *Trends Pharmacol. Sci.* **2010**, *31*, 99–101.

[88] World Health Organization, *WHO member state mechanism on substandard/spurious/falsely-labelled/falsified/counterfeit (SSFFC) medical products*, Geneva, **2017**.

[89] World Health Organization, *WHO surveillance and monitoring system for substandard and falsified medical products*, Geneva, **2017**.

[90] World Health Organization, *IMPACT brochure on counterfeit medicines*, Geneva, **2008**.

[91] P. N. Newton, M. D. Green, F. M. Fernández, N. P. J. Day, N. J. White; Counterfeit anti-infective drugs; *Lancet Infect. Dis.* **2006**, *6*, 602–613.

[92] Y. Akachi, F. Tarp, E. Kelley, T. Addisona, M. E. Kruk; Measuring quality-of-care in the context of sustainable development goal 3: A call for papers; *Bull. World Health Organ.* **2016**, *94*, 160-160A.

[93] J. Hanefeld, M. Khan, G. Tomson, R. Smith; Trade is central to achieving the sustainable development goals: A case study of antimicrobial resistance; *BMJ* **2017**, *358*, j3505.

[94] A. Nebot Giralt, B. Schiavetti, B. Meessen, C. Pouget, J. M. Caudron, B. Marchal, P. Massat, S. Thys, R. Ravinetto; Quality assurance of medicines supplied to low-income and middle-income countries: Poor products in shiny boxes?; *BMJ Glob. Health* **2017**, *2*, e000172.

[95] World Health Organization, *A study on the public health and socioeconomic impact of substandard and falsified medical products*, Geneva, **2017**.

[96] T. K. Mackey, B. A. Liang, P. York, T. Kubic; Counterfeit drug penetration into global legitimate medicine supply chains: A global assessment; *Am. J. Trop. Med. Hyg.* **2015**, *92*, 59–67.

[97] S. Kovacs, S. E. Hawes, S. N. Maley, E. Mosites, L. Wong, A. Stergachis; Technologies for detecting falsified and substandard drugs in low and middle-income countries; *PLoS ONE* **2014**, *9*, e90601.

[98] K. Dégardin, Y. Roggo, P. Margot; Understanding and fighting the medicine counterfeit market; *J. Pharm. Biomed. Anal.* **2014**, *87*, 167–175.

[99]   S. H. F. Scafi, C. Pasquini; Identification of counterfeit drugs using near-infrared spectroscopy; *Analyst* **2001**, *126*, 2218–2224.

[100]   S. Epstein, B. Cryer, S. Ragi, J. R. Zanchetta, J. Walliser, J. Chow, M. A. Johnson, A. E. Leyes; Disintegration/dissolution profiles of copies of Fosamax (alendronate); *Curr. Med. Res. Opin.* **2003**, *19*, 781–789.

[101]   J. K. Maurin, F. Pluciński, A. P. Mazurek, Z. Fijałek; The usefulness of simple X-ray powder diffraction analysis for counterfeit control - The Viagra® example; *J. Pharm. Biomed. Anal.* **2007**, *43*, 1514–1518.

[102]   A. A. Amin, G. O. Kokwaro; Antimalarial drug quality in Africa; *J. Clin. Pharm. Ther.* **2007**, *32*, 429–440.

[103]   S. Sengaloundeth, M. D. Green, F. M. Fernández, O. Manolin, K. Phommavong, V. Insixiengmay, C. Y. Hampton, L. Nyadong, D. C. Mildenhall, D. Hostetler, L. Khounsaknalath, L. Vongsack, S. Phompida, V. Vanisaveth, L. Syhakhang, P. N. Newton; A stratified random survey of the proportion of poor quality oral artesunate sold at medicine outlets in the Lao PDR - implications for therapeutic failure and drug resistance; *Malar. J.* **2009**, *8*, 172.

[104]   R. D. Marini, E. Rozet, M. L. A. Montes, C. Rohrbasser, S. Roht, D. Rhème, P. Bonnabry, J. Schappler, J.-L. Veuthey, P. Hubert, S. Rudaz; Reliable low-cost capillary electrophoresis device for drug quality control and counterfeit medicines; *J. Pharm. Biomed. Anal.* **2010**, *53*, 1278–1287.

[105]   P. N. Newton, M. D. Green, D. C. Mildenhall, A. Plançon, H. Nettey, L. Nyadong, D. M. Hostetler, I. Swamidoss, G. A. Harris, K. Powell, A. E. Timmermans, A. A. Amin, S. K. Opuni, S. Barbereau, C. Faurant, R. C. W. Soong, K. Faure, J. Thevanayagam, P. Fernandes, H. Kaur, B. Angus, K. Stepniewska, P. J. Guerin, F. M. Fernández; Poor quality vital anti-malarials in Africa - An urgent neglected public health priority; *Malar. J.* **2011**, *10*, 352.

[106]   F. M. Fernández, D. M. Hostetler, K. Powell, H. Kaur, M. D. Green, D. C. Mildenhall, P. N. Newton; Poor-quality drugs: Grand challenges in high throughput detection, countrywide sampling, and forensics in developing countries; *Analyst* **2011**, *136*, 3073–3082.

[107]   G. M. L. Nayyar, J. G. Breman, P. N. Newton, J. Herrington; Poor-quality antimalarial drugs in southeast Asia and sub-Saharan Africa; *Lancet Infect. Dis.* **2012**, *12*, 488–496.

[108]   M. Hajjou, Y. Qin, S. Bradby, D. Bempong, P. Lukulay; Assessment of the performance of a handheld Raman device for potential use as a screening tool in evaluating medicines quality; *J. Pharm. Biomed. Anal.* **2013**, *74*, 47–55.

[109]   R. Bate, P. Jensen, K. Hess, L. Mooney, J. Milligan; Substandard and falsified anti-tuberculosis drugs: A preliminary field analysis; *Int. J. Tuberc. Lung Dis.* **2013**, *17*, 308–311.

[110]   M. E. Monge, P. Dwivedi, M. Zhou, M. Payne, C. Harris, B. House, Y. Juggins, P. Cizmarik, P. N. Newton, F. M. Fernández, D. Jenkins; A tiered analytical approach for investigating poor quality emergency contraceptives; *PLoS ONE* **2014**, *9*, e95353.

[111]   R. Martino, M. Malet-Martino, V. Gilard, S. Balayssac; Counterfeit drugs: Analytical techniques for their identification; *Anal. Bioanal. Chem.* **2010**, *398*, 77–92.

[112]   W.-B. Zou, L.-H. Yin, S.-H. Jin; Advances in rapid drug detection technology; *J. Pharm. Biomed. Anal.* **2018**, *147*, 81–88.

[113]   H. Rebiere, M. Martin, C. Ghyselinck, P.-A. Bonnet, C. Brenier; Raman chemical imaging for spectroscopic screening and direct quantification of falsified drugs; *J. Pharm. Biomed. Anal.* **2018**, *148*, 316–323.

[114]   E. Deconinck, P.-Y. Sacré, P. Courselle, J. O. de Beer; Chromatography in the detection and characterization of illegal pharmaceutical preparations; *J. Chromatogr. Sci.* **2013**, *51*, 791–806.

[115]   F. Tagliaro, G. Manetto, F. Crivellente, F.P. Smith; A brief introduction to capillary electrophoresis; *Forensic Sci. Int.* **1998**, *92*, 75–88.

[116]   C. A. Monnig, R. T. Kennedy; Capillary electrophoresis; *Anal. Chem.* **1994**, *66*, 280–314.

[117]   G. H. Leach, *Introduction to capillary electrophoresis;* Beckman Coulter, Brea, **1991**.

[118]   M. J. Gordon, X. Huang, S. L. Pentoney, R. N. Zare; Capillary electrophoresis; *Science* **1988**, *242*, 224–228.

[119]   O. Vesterberg; History of electrophoretic methods; *J. Chromatogr. A* **1989**, *480*, 3–19.

[120]   O. Vesterberg; A short history of electrophoretic methods; *Electrophoresis* **1993**, *14*, 1243–1249.

[121]   F. Baeuml, T. Welsch; Improvement of the long-term stability of polyimide-coated fused-silica capillaries used in capillary electrophoresis and capillary electrochromatography; *J. Chromatogr. A* **2002**, *961*, 35–44.

[122]   J. L. Felhofer, L. Blanes, C. D. Garcia; Recent developments in instrumentation for capillary electrophoresis and microchip-capillary electrophoresis; *Electrophoresis* **2010**, *31*, 2469–2486.

[123]   A. Pervin, A. Alhakim, R. J. Linhardt; Separation of glycosaminoglycan-derived oligosaccharides by capillary electrophoresis using reverse polarity; *Anal. Biochem.* **1994**, *221*, 182–188.

[124]   A. A. Okemgbo, H. H. Hill, W. F. Siems; Reverse polarity capillary zone electrophoretic analysis of nitrate and nitrite in natural water samples; *Anal. Chem.* **1999**, *71*, 2725–2731.

[125]   D. L. Kirschner, M. Jaramillo, T. K. Green; Enantioseparation and stacking of Cyanobenz[*f*]isoindole-amino acids by reverse polarity capillary electrophoresis and sulfated β-cyclodextrin; *Anal. Chem.* **2007**, *79*, 736–743.

[126]   C. A. Lucy, R. S. Underhill; Characterization of the cationic surfactant induced reversal of electroosmotic flow in capillary electrophoresis; *Anal. Chem.* **1996**, *68*, 300–305.

[127]   X. Huang, M. J. Gordon, R. N. Zare; Bias in quantitative capillary zone electrophoresis caused by electrokinetic sample injection; *Anal. Chem.* **1988**, *60*, 375–377.

[128]   B. Chen, G. Chen, M. G. Bartlett; Factors influencing the electrokinetic injection of oligonucleotides in capillary gel electrophoresis when using laser-induced fluorescence detection; *Biomed. Chromatogr.* **2014**, *28*, 320–323.

[129]   H. Whatley; Basic principles and modes of capillary electrophoresis; in *Clinical and forensic applications of capillary electrophoresis*, *Pathology and laboratory medicine* (Eds.: J. R. Petersen, A. A. Mohammad), Humana Press, Totowa, **2001**, pp. 21–58.

[130]   T. Kappes, P. C. Hauser; Electrochemical detection methods in capillary electrophoresis and applications to inorganic species; *J. Chromatogr. A* **1999**, *834*, 89–101.

[131]   K. Swinney, D. J. Bornhop; Detection in capillary electrophoresis; *Electrophoresis* **2000**, *21*, 1239–1250.

[132]   S. N. Bendrysheva, M. A. Proskurnin, U. Pyell, W. Faubel; Sensitivity improvement in capillary electrophoresis using organo-aqueous separation buffers and thermal lens detection; *Anal. Bioanal. Chem.* **2006**, *385*, 1492–1503.

[133] W. F. Nirode, G. L. Devault, M. J. Sepaniak, R. O. Cole; On-column surface-enhanced Raman spectroscopy detection in capillary electrophoresis using running buffers containing silver colloidal solutions; *Anal. Chem.* **2000**, *72*, 1866–1871.

[134] J. A. Olivares, N. T. Nguyen, C. R. Yonker, R. D. Smith; On-line mass spectrometric detection for capillary zone electrophoresis; *Anal. Chem.* **1987**, *59*, 1230–1232.

[135] R. D. Smith, H. R. Udseth, J. A. Loo, B. W. Wright, G. A. Ross; Sample introduction and separation in capillary electrophoresis, and combination with mass spectrometric detection; *Talanta* **1989**, *36*, 161–169.

[136] D. A. Nedosekin, S. N. Bendrysheva, W. Faubel, M. A. Proskurnin, U. Pyell; Indirect thermal lens detection for capillary electrophoresis; *Talanta* **2007**, *71*, 1788–1794.

[137] Y. Hu, X. Li, Z. Pang; Indirect chemiluminescence detection for capillary zone electrophoresis of monoamines and catechol using luminol-$K_3[Fe(CN)_6]$ system; *J. Chromatogr. A* **2005**, *1091*, 194–198.

[138] P.-E. Mahuzier, M. S. Aurora Prado, B. J. Clark, E. R. M. Kedor-Hackmann, K. D. Altria; An introduction to the theory and application of microemulsion electrokinetic chromatography; *LCGC Europe* **2003**, *16*, 22–29.

[139] J. R. Petersen, A. O. Okorodudu, A. Mohammad, D. A. Payne; Capillary electrophoresis and its application in the clinical laboratory; *Clin. Chim. Acta* **2003**, *330*, 1–30.

[140] M. F. M. Tavares, A. V. Jager, C. L. da Silva, E. P. Moraes, E. A. Pereira, E. C. de Lima, F. N. Fonseca, F. G. Tonin, G. A. Micke, M. R. Santos, M. A. L. de Oliveira, M. L. L. de Moraes, M. H. van Kampen, N. M. Fujiya; Applications of capillary electrophoresis to the analysis of compounds of clinical, forensic, cosmetological, environmental, nutritional and pharmaceutical importance; *J. Braz. Chem. Soc.* **2003**, *14*, 281–290.

[141] J. Kraly, M. A. Fazal, R. M. Schoenherr, R. Bonn, M. M. Harwood, E. Turner, M. Jones, N. J. Dovichi; Bioanalytical applications of capillary electrophoresis; *Anal. Chem.* **2006**, *78*, 4097–4110.

[142] S. R. Rabel, J. F. Stobaugh; Applications of capillary electrophoresis in pharmaceutical analysis; *Pharm. Res.* **1993**, *10*, 171–186.

[143] L. Suntornsuk; Capillary electrophoresis in pharmaceutical analysis: a survey on recent applications; *J. Chromatogr. Sci.* **2007**, *45*, 559–577.

[144] G. Bringmann; The Naphthylisoquinoline Alkaloids; in *The Alkaloids*, vol. 29 (Ed.: A. Brossi), Academic Press, New York, **1986**, pp. 141–184.

Literature

[145]   J. F. Walker, Y. Yang, M. J. Moore, J. Mikenas, A. Timoneda, S. F. Brockington, S. A. Smith; Widespread paleopolyploidy, gene tree conflict, and recalcitrant relationships among the carnivorous Caryophyllales; *Am. J. Bot.* **2017**, *104*, 858–867.

[146]   G. Bringmann, F. Pokorny, M. Wenzel, K. Wurm, C. Schneider; Labelled precursors for biosynthetic studies on naphthylisoquinoline alkaloids; *J. Label. Compd. Radiopharm.* **1997**, *39*, 29–38.

[147]   G. Bringmann, J. Mutanyatta-Comar, M. Greb, S. Rüdenauer, T. F. Noll, A. Irmer; Biosynthesis of naphthylisoquinoline alkaloids: synthesis and incorporation of an advanced $^{13}C_2$-labeled isoquinoline precursor; *Tetrahedron* **2007**, *63*, 1755–1761.

[148]   G. Bringmann, D. Feineis; Stress-related polyketide metabolism of Dioncophyllaceae and Ancistrocladaceae; *J. Exp. Bot.* **2001**, *52*, 2015–2022.

[149]   G. Bringmann, G. François, L. Aké Assi, J. Schlauer; The Alkaloids of *Triphyophyllum peltatum* (Dioncophyllaceae); *Chimia* **1998**, *52*, 18–28.

[150]   G. Bringmann, F. Pokorny, M. Stäblein, M. Schäffer, L. Aké Assi; Ancistrobrevine C from *Ancistrocladus abbreviatus*: The first mixed 'Ancistrocladaceae/Dioncophyllaceae-type' naphthylisoquinoline alkaloid; *Phytochemistry* **1993**, *33*, 1511–1515.

[151]   G. Bringmann, R. Zagst, H. Reuscher, L. Aké Assi; Ancistrobrevine B, the first naphthylisoquinoline alkaloid with A 5,8'-coupling site, and related compounds from *Ancistrocladus abbreviatus*; *Phytochemistry* **1992**, *31*, 4011–4014.

[152]   G. Bringmann, M. Dreyer, J. H. Faber, P. W. Dalsgaard, D. Staerk, J. W. Jaroszewski, H. Ndangalasi, F. Mbago, R. Brun, M. Reichert, K. Maksimenka, S. B. Christensen; Ancistrotanzanine A, the first 5,3'-coupled naphthylisoquinoline alkaloid, and two further, 5,8'-linked related compounds from the newly described species *Ancistrocladus tanzaniensis*; *J. Nat. Prod.* **2003**, *66*, 1159–1165.

[153]   G. Bringmann, M. Dreyer, M. Michel, F. S. K. Tayman, R. Brun; Ancistroheynine B and two further 7,3'-coupled naphthylisoquinoline alkaloids from *Ancistrocladus heyneanus* Wall.; *Phytochemistry* **2004**, *65*, 2903–2907.

[154]   G. Bringmann, G. Zhang, T. Ölschläger, A. Stich, J. Wu, M. Chatterjee, R. Brun; Highly selective antiplasmodial naphthylisoquinoline alkaloids from *Ancistrocladus tectorius*; *Phytochemistry* **2013**, *91*, 220–228.

[155]   G. Bringmann, R. Seupel, D. Feineis, M. Xu, G. Zhang, M. Kaiser, R. Brun, E.-J. Seo, T. Efferth; Antileukemic ancistrobenomine B and related 5,1'-coupled naphthylisoquinoline alkaloids from the Chinese liana *Ancistrocladus tectorius*; *Fitoterapia* **2017**, *121*, 76–85.

[156]   G. Bringmann, C. Günther, W. Saeb, J. Mies, R. Brun, L. Aké Assi; 8-O-Methyldioncophyllinol B and revised structures of other 7,6'-coupled naphthylisoquinoline alkaloids from *Triphyophyllum peltatum* (Dioncophyllaceae); *Phytochemistry* **2000**, *54*, 337–346.

[157]   G. Bringmann, I. Kajahn, M. Reichert, S. E. H. Pedersen, J. H. Faber, T. Gulder, R. Brun, S. B. Christensen, A. Ponte-Sucre, H. Moll, G. Heubl, V. Mudogo; Ancistrocladinium A and B, the first *N,C*-coupled naphthyldihydroisoquinoline alkaloids, from a Congolese *Ancistrocladus* species; *J. Org. Chem.* **2006**, *71*, 9348–9356.

[158]   G. Bringmann, B. Hertlein-Amslinger, I. Kajahn, M. Dreyer, R. Brun, H. Moll, A. Stich, K. Ndjoko Ioset, W. Schmitz, L. H. Ngoc; Phenolic analogs of the *N,C*-coupled naphthylisoquinoline alkaloid ancistrocladinium A, from *Ancistrocladus cochinchinensis* (Ancistrocladaceae), with improved antiprotozoal activities; *Phytochemistry* **2011**, *72*, 89–93.

[159]   L.-K. Yang, R. P. Glover, K. Yoganathan, J. P. Sarnaik, A. J. Godbole, D. D. Soejarto, A. D. Buss, M. S. Butler; Ancisheynine, a novel naphthylisoquinolinium alkaloid from *Ancistrocladus heyneanus*; *Tetrahedron Lett.* **2003**, *44*, 5827–5829.

[160]   Y. F. Hallock, J. H. Cardellina II, M. Schäffer, G. Bringmann, G. François, M. R. Boyd; Korundamine A, a novel HIV-inhibitory and antimalarial "hybrid" naphthylisoquinoline alkaloid heterodimer from *Ancistrocladus korupensis*; *Bioorg. Med. Chem. Lett.* **1998**, *8*, 1729–1734.

[161]   G. Bringmann, M. Wohlfarth, H. Rischer, J. Schlauer, R. Brun; Extract screening by HPLC coupled to MS–MS, NMR, and CD: A dimeric and three monomeric naphthylisoquinoline alkaloids from *Ancistrocladus griffithii*; *Phytochemistry* **2002**, *61*, 195–204.

[162]   M. Xu, T. Bruhn, B. Hertlein, R. Brun, A. Stich, J. Wu, G. Bringmann; Shuangancistrotectorines A-E, dimeric naphthylisoquinoline alkaloids with three chiral biaryl axes from the Chinese plant *Ancistrocladus tectorius*; *Chem. - Eur. J.* **2010**, *16*, 4206–4216.

[163] G. Bringmann, G. Zhang, T. Büttner, G. Bauckmann, T. Kupfer, H. Braunschweig, R. Brun, V. Mudogo; Jozimine A$_2$: The first dimeric Dioncophyllaceae-type naphthylisoquinoline alkaloid, with three chiral axes and high antiplasmodial activity; *Chem. - Eur. J.* **2013**, *19*, 916–923.

[164] G. Bringmann, B. K. Lombe, C. Steinert, K. Ndjoko Ioset, R. Brun, F. Turini, G. Heubl, V. Mudogo; Mbandakamines A and B, unsymmetrically coupled dimeric naphthylisoquinoline alkaloids, from a Congolese *Ancistrocladus* species; *Org. Lett.* **2013**, *15*, 2590–2593.

[165] M. Meininger, R. Stowasser, P. M. Jakob, H. Schneider, D. Koppler, G. Bringmann, U. Zimmermann, A. Haase; Nuclear magnetic resonance microscopy of *Ancistrocladus heyneanus*; *Protoplasma* **1997**, *198*, 210–217.

[166] E. Urlaub, J. Popp, W. Kiefer, G. Bringmann, D. Koppler, H. Schneider, U. Zimmermann, B. Schrader; FT-Raman investigation of alkaloids in the liana *Ancistrocladus heyneanus*; *Biospectroscopy* **1998**, *4*, 113–120.

[167] G. Bringmann, M. Rückert, J. Schlauer, M. Herderich; Acetogenic isoquinoline alkaloids: CXII. Separation and identification of dimeric naphthylisoquinoline alkaloids by liquid chromatography coupled to electrospray ionization mass spectrometry; *J. Chromatogr. A* **1998**, *810*, 231–236.

[168] G. Bringmann, K. Messer, M. Wohlfarth, J. Kraus, K. Dumbuya, M. Rückert; HPLC-CD online coupling in combination with HPLC-NMR and HPLC-MS/MS for the determination of the full absolute stereostructure of new metabolites in plant extracts; *Anal. Chem.* **1999**, *71*, 2678–2686.

[169] G. Bringmann, T. A. M. Gulder, M. Reichert, T. Gulder; The online assignment of the absolute configuration of natural products: HPLC-CD in combination with quantum chemical CD calculations; *Chirality* **2008**, *20*, 628–642.

[170] G. Bringmann, F. Teltschik, M. Schäffer, R. Haller, S. Bär, S. A. Robertson, M. A. Isahakia; Ancistrobertsonine A and related naphthylisoquinoline alkaloids from *Ancistrocladus robertsoniorum*; *Phytochemistry* **1998**, *47*, 31–35.

[171] W. D. Conway; Counter-current chromatography: Simple process and confusing terminology; *J. Chromatogr. A* **2011**, *1218*, 6015–6023.

[172] G. Bringmann, T. Geuder, M. Rübenacker, R. Zagst; A facile degradation procedure for determination of absolute configuration in 1,3-dimethyltetra- and dihydroisoquinolines; *Phytochemistry* **1991**, *30*, 2067–2070.

[173]   G. Bringmann, R. God, M. Schäffer; An improved degradation procedure for determination of the absolute configuration in chiral isoquinoline and β-carboline derivatives; *Phytochemistry* **1996**, *43*, 1393–1403.

[174]   G. Bringmann, R. Zagst, B. Schöner, H. Busse, M. Hemmerling, C. Burschka; Structure of the naphthyl isoquinoline alkaloid dioncophylline A; *Acta Crystallogr. C Cryst. Struct. Commun.* **1991**, *47*, 1703–1705.

[175]   G. Bringmann, D. Koppler, D. Scheutzow, A. Porzel; Determination of configuration at the biaryl axes of naphthylisoquinoline alkaloids by long-range NOE effects; *Magn. Reson. Chem.* **1997**, *35*, 297–301.

[176]   G. Bringmann, K.-P. Gulden, H. Busse, J. Fleischhauer, B. Kramer, E. Zobel; Circular dichroism of naphthyltetrahydroisoquinoline alkaloids: Calculation of CD spectra by semiempirical methods; *Tetrahedron* **1993**, *49*, 3305–3312.

[177]   X.-C. Li, D. Ferreira, Y. Ding; Determination of absolute configuration of natural products: Theoretical calculation of electronic circular dichroism as a tool; *Curr. Org. Chem.* **2010**, *14*, 1678–1697.

[178]   P. Chau, I. R. Czuba, M. A. Rizzacasa, G. Bringmann, K.-P. Gulden, M. Schäffer; Convergent synthesis of naphthylisoquinoline alkaloids: Total synthesis of (+)- O - methylancistrocline; *J. Org. Chem.* **1996**, *61*, 7101–7105.

[179]   G. Bringmann, T. Gulder, B. Hertlein, Y. Hemberger, F. Meyer; Total synthesis of the *N*,*C*-coupled naphthylisoquinoline alkaloids ancistrocladinium A and B and related analogues; *J. Am. Chem. Soc.* **2010**, *132*, 1151–1158.

[180]   G. Bringmann, J. Holenz, L. Aké Assi, C. Zhao, K. Hostettmann; Molluscicidal activity of naphthylisoquinoline alkaloids from *Triphyophyllum* and *Ancistrocladus* species; *Planta Med.* **1996**, *62*, 556–557.

[181]   G. Bringmann, J. Holenz, L. Aké Assi, K. Hostettmann; Molluscicidal activity (*Biomphalaria glabrata*) of dioncophylline A: Structure-activity investigations; *Planta Med.* **1998**, *64*, 485–486.

[182]   G. François, M. van Looveren, G. Timperman, B. Chimanuka, L. Aké Assi, J. Holenz, G. Bringmann; Larvicidal activity of the naphthylisoquinoline alkaloid dioncophylline A against the malaria vector *Anopheles stephensi*; *J. Ethnopharmacol.* **1996**, *54*, 125–130.

[183]   G. Bringmann, S. Gramatzki, C. Grimm, P. Proksch; Feeding deterrency and growth retarding activity of the naphthylisoquinoline alkaloid dioncophylline A against *Spodoptera littoralis*; *Phytochemistry* **1992**, *31*, 3821–3825.

[184]   G. Bringmann, J. Holenz, B. Wiesen, B. W. Nugroho, P. Proksch; Dioncophylline A as a growth-retarding agent against the herbivorous insect *Spodoptera littoralis*: Structure-activity relationships; *J. Nat. Prod.* **1997**, *60*, 342–347.

[185]   G. Bringmann, F. Teltschik, M. Michel, S. Busemann, M. Rückert, R. Haller, S. Bär, S.A. Robertson, R. Kaminsky; Ancistrobertsonines B, C, and D as well as 1,2-didehydroancistrobertsonine D from *Ancistrocladus robertsoniorum*; *Phytochemistry* **1999**, *52*, 321–332.

[186]   G. Bringmann, J. Spuziak, J. H. Faber, T. Gulder, I. Kajahn, M. Dreyer, G. Heubl, R. Brun, V. Mudogo; Six naphthylisoquinoline alkaloids and a related benzopyranone from a Congolese *Ancistrocladus* species related to *Ancistrocladus congolensis*; *Phytochemistry* **2008**, *69*, 1065–1075.

[187]   D. T. Tshitenge, D. Feineis, V. Mudogo, M. Kaiser, R. Brun, G. Bringmann; Antiplasmodial ealapasamines A-C, 'mixed' naphthylisoquinoline dimers from the Central African liana *Ancistrocladus ealaensis*; *Sci. Rep.* **2017**, *7*, 5767.

[188]   B. K. Lombe, D. Feineis, V. Mudogo, R. Brun, S. Awale, G. Bringmann; Michellamines A_6 and A_7, and further mono- and dimeric naphthylisoquinoline alkaloids from a Congolese *Ancistrocladus* liana and their antiausterity activities against pancreatic cancer cells; *RSC Adv.* **2018**, *8*, 5243–5254.

[189]   J. Li, R. Seupel, D. Feineis, V. Mudogo, M. Kaiser, R. Brun, D. Brünnert, M. Chatterjee, E.-J. Seo, T. Efferth, G. Bringmann; Dioncophyllines C_2, D_2, and F and related naphthylisoquinoline alkaloids from the Congolese liana *Ancistrocladus ileboensis* with potent activities against *Plasmodium falciparum* and against multiple myeloma and leukemia cell lines; *J. Nat. Prod.* **2017**, *80*, 443–458.

[190]   Y. F. Hallock, K. P. Manfredi, J.-R. Dai, J. H. Cardellina II, R. J. Gulakowski, J.a. B. McMahon, M. Schäffer, M. Stahl, K.-P. Gulden, G. Bringmann, G. François, M. R. Boyd; Michellamines D-F, new HIV-inhibitory dimeric naphthylisoquinoline alkaloids, and korupensamine E, a new antimalarial monomer, from *Ancistrocladus korupensis*; *J. Nat. Prod.* **1997**, *60*, 677–683.

[191]   G. Bringmann, C. Steinert, D. Feineis, V. Mudogo, J. Betzin, C. Scheller; HIV-inhibitory michellamine-type dimeric naphthylisoquinoline alkaloids from the Central African liana *Ancistrocladus congolensis*; *Phytochemistry* **2016**, *128*, 71–81.

[192]   Programme National de Lutte contre le Paludisme, *Rapport annuel des activités de lutte contre le paludisme*, Kinshasa, **2017**.

[193] Programme National de Lutte contre le Paludisme, *Guide technique de prévention et prise en charge du paludisme;* Ministère de la Santé Publique, RD Congo, Kinshasa, **2012**.

[194] ACTwatch, *DRC 2015 outlet survey findings in Katanga and Kinshasa*, ACTwatch Research Brief, Washington DC, USA, **2017**.

[195] World Health Organization, *Survey of the quality of selected antimalarial medicines circulating in six countries of sub-Saharan Africa*, Geneva, **2011**.

[196] J.-P. Mufusama, K. Ndjoko Ioset, D. Feineis, L. Hoellein, U. Holzgrabe, G. Bringmann; Quality of the antimalarial medicine artemether - lumefantrine in eight cities of the Democratic Republic of the Congo; *Drug Test. Anal.* **2018**, *10*, 1599–1606.

[197] M. A. Atemnkeng, B. Chimanuka, J. Plaizier-Vercammen; Quality evaluation of chloroquine, quinine, sulfadoxine-pyrimethamine and proguanil formulations sold on the market in East Congo DR; *J. Clin. Pharm. Ther.* **2007**, *32*, 123–132.

[198] M. A. Atemnkeng, K. de Cock, J. Plaizier-Vercammen; Quality control of active ingredients in artemisinin-derivative antimalarials within Kenya and DR Congo; *Trop. Med. Int. Health* **2007**, *12*, 68–74.

[199] M. C. Gaudiano, A. Di Maggio, E. Cocchieri, E. Antoniella, P. Bertocchi, S. Alimonti, L. Valvo; Medicines informal market in Congo, Burundi and Angola: Counterfeit and substandard antimalarials; *Malar. J.* **2007**, *6*, 22.

[200] S. Mziray, K. Mwamwitwa, S. Kisoma, S. Augustine, A. Fimbo, D. Hipolite, H. Sillo, E. Kaale; Post marketing surveillance of anti-malarial medicines in Tanzania; *Pharmaceut. Reg. Affairs* **2017**, *6*, 1000191.

[201] F. Khuluza, S. Kigera, L. Heide; Low prevalence of substandard and falsified antimalarial and antibiotic medicines in public and faith-based health facilities of Southern Malawi; *Am. J. Trop. Med. Hyg.* **2017**, *96*, 1124–1135.

[202] P. N. Newton, S. J. Lee, C. Goodman, F. M. Fernández, S. Yeung, S. Phanouvong, H. Kaur, A. A. Amin, C. J. M. Whitty, G. O. Kokwaro, N. Lindegårdh, P. Lukulay, L. J. White, N. P. J. Day, M. D. Green, N. J. White; Guidelines for field surveys of the quality of medicines: a proposal; *PLoS Med.* **2009**, *6*, e52.

[203] World Health Organization, *Guidelines on the conduct of surveys of the quality of medicines*, Geneva, **2016**.

[204] K. Dégardin, Y. Roggo; Counterfeit analysis strategy illustrated by a case study; *Drug Test. Anal.* **2016**, *8*, 388–397.

[205] A. Yemoa, V. Habyalimana, J. K. Mbinze, V. Crickboom, B. Muhigirwa, A. Ngoya, P.-Y. Sacré, F. Gbaguidi, J. Quetin-Leclercq, P. Hubert, R. D. Marini; Detection of poor quality artemisinin-based combination therapy (ACT) medicines marketed in Benin using simple and advanced analytical techniques; *Curr. Drug Saf.* **2017**, *12*, 178–186.

[206] J. S. Batson, D. K. Bempong, P. H. Lukulay, N. Ranieri, R. D. Satzger, L. Verbois; Assessment of the effectiveness of the CD3+ tool to detect counterfeit and substandard anti-malarials; *Malar. J.* **2016**, *15*, 119.

[207] H. Kaur, E. L. Allan, I. Mamadu, Z. Hall, O. Ibe, M. El Sherbiny, A. van Wyk, S. Yeung, I. Swamidoss, M. D. Green, P. Dwivedi, M. J. Culzoni, S. Clarke, D. Schellenberg, F. M. Fernández, O. Onwujekwe; Quality of artemisinin-based combination formulations for malaria treatment: Prevalence and risk factors for poor quality medicines in public facilities and private sector drug outlets in Enugu, Nigeria; *PLoS ONE* **2015**, *10*, e0125577.

[208] P. N. Newton, P. Tabernero, P. Dwivedi, M. J. Culzoni, M. E. Monge, I. Swamidoss, D. Mildenhall, M. D. Green, R. W. O. Jähnke, M. d. S. de Oliveira, J. Simao, N. J. White, F. M. Fernández; Falsified medicines in Africa: All talk, no action; *Lancet Glob. Health* **2014**, *2*, e509-e510.

[209] World Health Organization, *Drug alert N° 130*: Falsified batches of Coartem recently circulating in Cameroon, Geneva, **2013**.

[210] Santé tropicale au Cameroun, *Revue de presse du 20/11/2013*, **2013**.

[211] M. Lalani, F. E. Kitutu, S. E. Clarke, H. Kaur; Anti-malarial medicine quality field studies and surveys: A systematic review of screening technologies used and reporting of findings; *Malar. J.* **2017**, *16*, 197.

[212] A. Petersen, N. Held, L. Heide; Surveillance for falsified and substandard medicines in Africa and Asia by local organizations using the low-cost GPHF Minilab; *PLoS ONE* **2017**, *12*, e0184165.

[213] F. Khuluza, S. Kigera, R. W. O. Jähnke, L. Heide; Use of thin-layer chromatography to detect counterfeit sulfadoxine/pyrimethamine tablets with the wrong active ingredient in Malawi; *Malar. J.* **2016**, *15*, 215.

[214] B. J. Visser, J. Meerveld-Gerrits, D. Kroon, J. Mougoula, R. Vingerling, E. Bache, J. Boersma, M. van Vugt, S. T. Agnandji, H. Kaur, M. P. Grobusch; Assessing the quality of anti-malarial drugs from Gabonese pharmacies using the MiniLab®: A field study; *Malar. J.* **2015**, *14*, 273.

[215] World Health Organization, *The International Pharmacopoeia*, Geneva, **2017**.

[216] International Council for Harmonization, *Guideline Q3B(R2)*: Impurities in new drug products; International Council for Harmonization, Geneva, **2006**.

[217] K. V. V. P. Rao, A. Rani, A. V. R. Reddy, C. H. Bharathi, R. Dandala, A. Naidu; Isolation, structural elucidation and characterization of impurities in Cefdinir; *J. Pharm. Biomed. Anal.* **2007**, *43*, 1476–1482.

[218] R. Holm, D. P. Elder; Analytical advances in pharmaceutical impurity profiling; *Eur. J. Pharm. Sci.* **2016**, *87*, 118–135.

[219] K. Vandercruyssen, M. D'Hondt, V. Vergote, H. Jansen, C. Burvenich, B. de Spiegeleer; LC-UV/MS quality analytics of paediatric artemether formulations; *J. Pharm. Anal.* **2014**, *4*, 37–52.

[220] N. T. Ho, D. Desai, M. H. Zaman; Rapid and specific drug quality testing assay for artemisinin and its derivatives using a luminescent reaction and novel microfluidic technology; *Am. J. Trop. Med. Hyg.* **2015**, *92*, 24–30.

[221] M. Verbeken, S. Suleman, B. Baert, E. Vangheluwe, S. van Dorpe, C. Burvenich, L. Duchateau, F. H. Jansen, B. de Spiegeleer; Stability-indicating HPLC-DAD/UV-ESI/MS impurity profiling of the anti-malarial drug lumefantrine; *Malar. J.* **2011**, *10*, 51.

[222] Z. Hall, E. L. Allan, D. A. van Schalkwyk, A. van Wyk, H. Kaur; Degradation of artemisinin-based combination therapies under tropical conditions; *Am. J. Trop. Med. Hyg.* **2016**, *94*, 993–1001.

[223] ACT consortium drug quality project team and the Impact study team; Quality of artemisinin-containing antimalarials in Tanzania's private Sector - Results from a nationally representative outlet Survey; *Am. J. Trop. Med. Hyg.* **2015**, *92*, 75–86.

[224] M. Tivura, I. Asante, A. van Wyk, S. Gyaase, N. Malik, E. Mahama, D. M. Hostetler, F. M. Fernandez, K. P. Asante, H. Kaur, S. Owusu-Agyei; Quality of artemisinin-based combination therapy for malaria found in Ghanaian markets and public health implications of their use; *BMC Pharmacol. Toxicol.* **2016**, *17*, 48.

[225] B. Schiavetti, E. Wynendaele, B. de Spiegeleer, G. J. Mbinze, N. Kalenda, R. Marini, V. Melotte, E. Hasker, B. Meessen, R. Ravinetto, J. van der Elst, D. Mutolo Ngeleka; The quality of medicines used in children and supplied by private pharmaceutical wholesalers in Kinshasa, Democratic Republic of Congo: A prospective survey; *Am. J. Trop. Med. Hyg.* **2018**, *98*, 894–903.

[226] P. Tabernero, F. M. Fernández, M. D. Green, P. J. Guerin, P. N. Newton; Mind the gaps - The epidemiology of poor-quality anti-malarials in the malarious world - Analysis of the WorldWide Antimalarial Resistance Network database; *Malar. J.* **2014**, *13*, 139.

[227] L. Hoellein, E. Kaale, Y. H. Mwalwisi, M. H. Schulze, U. Holzgrabe; Routine quality control of medicines in developing countries: Analytical challenges, regulatory infrastructures and the prevalence of counterfeit medicines in Tanzania; *Trends Anal. Chem.* **2016**, *76*, 60–70.

[228] P. G. Kremsner, S. Krishna; Antimalarial combinations; *Lancet* **2004**, *364*, 285–294.

[229] S. B. Sirima, A. Gansané; Artesunate-amodiaquine for the treatment of uncomplicated malaria; *Expert Opin. Invest. Drugs* **2007**, *16*, 1079–1085.

[230] J. H. Burckhalter, F. H. Tendick, E. M. Jones, P. A. Jones, W. F. Holcomb, A. L. Rawlins; Aminoalkylphenols as antimalarials (heterocyclic-amino)-α-amino-o-cresols; the Synthesis of Camoquin; *J. Am. Chem. Soc.* **1948**, *70*, 1363–1373.

[231] X.-Q. Li, A. Björkman, T. B. Andersson, M. Ridderström, C. M. Masimirembwa; Amodiaquine clearance and its metabolism to *N*-desethylamodiaquine is mediated by CYP2C8: A new high affinity and turnover enzyme-specific probe substrate; *J. Pharmacol. Exp. Ther.* **2002**, *300*, 399–407.

[232] L. Hoellein, U. Holzgrabe; Development of simplified HPLC methods for the detection of counterfeit antimalarials in resource-restraint environments; *J. Pharm. Biomed. Anal.* **2014**, *98*, 434–445.

[233] C. Rohrbasser, D. Rhême, S. Décastel, S. Roth, M. d. L. A. Montes, J.-L. Veuthey, S. Rudaz; A new capillary electrophoresis device with deep UV detector based on LED technology; *Chimia* **2009**, *63*, 890–891.

[234] International Council for Harmonization, *Guideline Q2(R1)*: Validation of analytical procedures: Text and Methodology, Geneva, **2006**.

[235] J.-P. Mufusama, L. Hoellein, D. Feineis, U. Holzgrabe, G. Bringmann; Capillary zone electrophoresis for the determination of amodiaquine and three of its synthetic impurities in pharmaceutical formulations; *Electrophoresis* **2018**, *39*, 2530–2539.

[236] N.'C. C. Amin, M.-D. Blanchin, M. Aké, J. Montels, H. Fabre; Capillary electrophoresis for the assay of fixed-dose combination tablets of artesunate and amodiaquine; *Malar. J.* **2012**, *11*, 149.

[237] C. Lamalle, R. D. Marini, B. Debrus, P. Lebrun, J. Crommen, P. Hubert, A.-C. Servais, M. Fillet; Development of a generic micellar electrokinetic chromatography method for the separation of 15 antimalarial drugs as a tool to detect medicine counterfeiting; *Electrophoresis* **2012**, *33*, 1669–1678.

[238] Q. Zhang, Y. F. Li, C. Z. Huang; Quality control of piperaquine in pharmaceutical formulations by capillary zone electrophoresis; *Talanta* **2008**, *76*, 44–48.

[239] G. Geetha, K. Raju, B. Vigmesh Kumar, M. Gnana Raja; Analytical method validation: An updated review; *Int. J. Adv. Pharm. Biol. Chem.* **2012**, *1*, 64–71.

[240] S. C. Mitchell, P. Carmichael, R. Waring; Aminophenols; in *Encyclopedia of chemical technology* (Eds.: R. E. Kirk, D. F. Othmer), Wiley, New York, NY, **2003**, p. 3081.

[241] H. Rischer, G. Heubl, H. Meimberg, M. Dreyer, H. A. Hadi, G. Bringmann; *Ancistrocladus benomensis* (Ancistrocladaceae): A new species from Peninsular Malaysia; *Blumea* **2005**, *50*, 357–365.

[242] F. G. Turini, C. Steinert, G. Heubl, G. Bringmann, B. K. Lombe, V. Mudogo, H. Meimberg; Microsatellites facilitate species delimitation in Congolese *Ancistrocladus* (Ancistrocladaceae), a genus with pharmacologically potent naphthylisoquinoline alkaloids; *Taxon* **2014**, *63*, 329–341.

[243] J.-P. Mufusama, D. Feineis, V. Mudogo, M. Kaiser, R. Brun, G. Bringmann; Antiprotozoal dimeric naphthylisoquinolines, mbandakamines B_3 and B_4 , and related 5,8'-coupled monomeric alkaloids, ikelacongolines A-D, from a Congolese *Ancistrocladus* liana; *RSC Adv.* **2019**, *9*, 12034–12046.

[244] G. Bringmann, C. Günther, W. Saeb, J. Mies, A. Wickramasinghe, V. Mudogo, R. Brun; Ancistrolikokines A-C: New 5,8'-coupled naphthylisoquinoline alkaloids from *Ancistrocladus likoko*; *J. Nat. Prod.* **2000**, *63*, 1333–1337.

[245] G. Bringmann, K. Messer, R. Brun, V. Mudogo; Ancistrocongolines A-D, new naphthylisoquinoline alkaloids from *Ancistrocladus congolensis*; *J. Nat. Prod.* **2002**, *65*, 1096–1101.

[246] D. T. Tshitenge, PhD thesis, University of Würzburg, **2017**.

[247]   B. K. Lombe, T. Bruhn, D. Feineis, V. Mudogo, R. Brun, G. Bringmann; Antiprotozoal spirombandakamines A_1 and A_2, fused naphthylisoquinoline dimers from a Congolese *Ancistrocladus* plant; *Org. Lett.* **2017**, *19*, 6740–6743.

[248]   S. Fayez, D. Feineis, V. Mudogo, E.-J. Seo, T. Efferth, G. Bringmann; Ancistrolikokine I and further 5,8'-coupled naphthylisoquinoline alkaloids from the Congolese liana *Ancistrocladus likoko* and their cytotoxic activities against drug-sensitive and multidrug resistant human leukemia cells; *Fitoterapia* **2018**, *129*, 114–125.

[249]   S. Fayez, D. Feineis, V. Mudogo, S. Awale, G. Bringmann; Ancistrolikokines E-H and related 5,8′-coupled naphthylisoquinoline alkaloids from the Congolese liana *Ancistrocladus likoko* with antiausterity activities against PANC-1 human pancreatic cancer cells; *RSC Adv.* **2017**, *7*, 53740–53751.

[250]   S. M. Kavatsurwa, B. K. Lombe, D. Feineis, D. F. Dibwe, V. Maharaj, S. Awale, G. Bringmann; Ancistroyafungines A-D, 5,8'- and 5,1'-coupled naphthylisoquinoline alkaloids from a Congolese *Ancistrocladus* species, with antiausterity activities against human PANC-1 pancreatic cancer cells; *Fitoterapia* **2018**, *130*, 6–16.

[251]   B. K. Lombe, T. Bruhn, D. Feineis, V. Mudogo, R. Brun, G. Bringmann; Cyclombandakamines A_1 and A_2, oxygen-bridged naphthylisoquinoline dimers from a Congolese *Ancistrocladus* liana; *Org. Lett.* **2017**, *19*, 1342–1345.

[252]   B. K. Lombe, D. Feineis, V. Mudogo, R. Brun, S. Awale, G. Bringmann; Michellamines A_6 and A_7 , and further mono- and dimeric naphthylisoquinoline alkaloids from a Congolese *Ancistrocladus* liana and their antiausterity activities against pancreatic cancer cells; *RSC Adv.* **2018**, *8*, 5243–5254.

[253]   D. T. Tshitenge, D. Feineis, V. Mudogo, M. Kaiser, R. Brun, E.-J. Seo, T. Efferth, G. Bringmann; Mbandakamine-type naphthylisoquinoline dimers and related alkaloids from the Central African liana *Ancistrocladus ealaensis* with antiparasitic and antileukemic activities; *J. Nat. Prod.* **2018**, *81*, 918–933.

[254]   J. Li, R. Seupel, T. Bruhn, D. Feineis, M. Kaiser, R. Brun, V. Mudogo, S. Awale, G. Bringmann; Jozilebomines A and B, naphthylisoquinoline dimers from the Congolese liana *Ancistrocladus ileboensis*, with antiausterity activities against the PANC-1 human pancreatic cancer cell line; *J. Nat. Prod.* **2017**, *80*, 2807–2817.

[255]   E. Izumi, T. Ueda-Nakamura, B. P. Dias Filho, V. F. Veiga Júnior, C. V. Nakamura; Natural products and Chagas' disease: A review of plant compounds studied for activity against *Trypanosoma cruzi*; *Nat. Prod. Rep.* **2011**, *28*, 809–823.

[256]   M. Salem, K. Werbovetz; Natural products from plants as drug candidates and lead compounds against leishmaniasis and trypanosomiasis; *Curr. Med. Chem.* **2006**, *13*, 2571–2598.

[257]   G. Bringmann, W. Saeb, D. Koppler, G. François; Jozimine A ('dimeric' dioncophylline A), a non-natural michellamine analog with high antimalarial activity; *Tetrahedron* **1996**, *52*, 13409–13418.

[258]   G. Bringmann, W. Saeb, M. Wohlfarth, K. Messer, R. Brun; Jozipeltine A, a novel, unnatural dimer of the highly hydroxylated naphthylisoquinoline alkaloid dioncopeltine A; *Tetrahedron* **2000**, *56*, 5871–5875.

[259]   G. Bringmann, S. Tasler; Oxidative aryl coupling reactions: A biomimetic approach to configurationally unstable or axially chiral biaryl natural products and related bioactive compounds; *Tetrahedron* **2001**, *57*, 331–343.

[260]   K. Izuishi, K. Kato, T. Ogura, T. Kinoshita, H. Esumi; Remarkable tolerance of tumor cells to nutrient deprivation: Possible new biochemical target for cancer therapy; *Cancer Res.* **2000**, *60*, 6201–6207.

[261]   S. Awale, J. Lu, S. K. Kalauni, Y. Kurashima, Y. Tezuka, S. Kadota, H. Esumi; Identification of arctigenin as an antitumor agent having the ability to eliminate the tolerance of cancer cells to nutrient starvation; *Cancer Res.* **2006**, *66*, 1751–1757.

[262]   S. Awale, D. F. Dibwe, C. Balachandran, S. Fayez, D. Feineis, B. K. Lombe, G. Bringmann; Ancistrolikokine E_3, a 5,8'-coupled naphthylisoquinoline alkaloid, eliminates the tolerance of cancer cells to nutrition starvation by inhibition of the Akt/mTOR/Autophagy signaling pathway; *J. Nat. Prod.* **2018**, *81*, 2282–2291.

[263]   C. Yukawa, H. Iwabuchi, S. Komemushi, A. Sawabe; Mono- and sesquiterpenoids of the volatile oil of *Bursera graveolens*; *Flavour Fragr. J.* **2005**, *20*, 653–658.

[264]   M. A. Hawrył, K. Skalicka-Woźniak, R. Świeboda, M. Niemiec, K. Stępak, M. Waksmundzka-Hajnos, A. Hawryl, G. Szymczak; GC-MS fingerprints of mint essential oils; *Open Chem.* **2015**, *13*, 1326–1332.

[265]   R. B. Woodward, R. H. Eastman; The autoxidation of menthofuran; *J. Am. Chem. Soc.* **1950**, *72*, 399–403.

[266]   E. Frérot, A. Bagnoud, C. Vuilleumier; Menthofurolactone: A new *p*-menthane lactone in *Mentha piperita* L.: Analysis, synthesis and olfactory properties; *Flavour Fragr. J.* **2002**, *17*, 218–226.

[267] R. Näf, A. Velluz; Phenols and lactones in Italo-Mitcham peppermint oil *Mentha piperita* L.; *Flavour Fragr. J.* **1998**, *13*, 203–208.

[268] C. Yukawa, H. Iwabuchi; Terpenoids in volatile oil from *Bursera graveolens*; *J. Oleo Sci.* **2003**, *52*, 483–489.

[269] C. Pfenning, H. L. Esch, R. Fliege, L. Lehmann; The mycotoxin patulin reacts with DNA bases with and without previous conjugation to GSH: Implication for related α,β-unsaturated carbonyl compounds?; *Arch. Toxicol.* **2016**, *90*, 433–448.

[270] R. Fliege, M. Metzler; Electrophilic properties of patulin. *N*-acetylcysteine and glutathione adducts; *Chem. Res. Toxicol.* **2000**, *13*, 373–381.

[271] M. M. Moake, O. I. Padilla-Zakour, R. W. Worobo; Comprehensive review of patulin control methods in foods; *Comp. Rev. Food Sci. Food Saf.* **2005**, *4*, 8–21.

[272] H. Malekinejad, J. Aghazadeh-Attari, A. Rezabakhsh, M. Sattari, B. Ghasemsoltani-Momtaz; Neurotoxicity of mycotoxins produced in vitro by *Penicillium roqueforti* isolated from maize and grass silage; *Hum. Exp. Toxicol.* **2015**, *34*, 997–1005.

[273] E. Song, C. Su, J. Fu, X. Xia, S. Yang, C. Xiao, B. Lu, H. Chen, Z. Sun, S. Wu, Y. Song; Selenium supplementation shows protective effects against patulin-induced brain damage in mice via increases in GSH-related enzyme activity and expression; *Life Sci.* **2014**, *109*, 37–43.

[274] M. Sabater-Vilar, R. F. M. Maas, H. de Bosschere, R. Ducatelle, J. Fink-Gremmels; Patulin produced by an *Aspergillus clavatus* isolated from feed containing malting residues associated with a lethal neurotoxicosis in cattle; *Mycopathologia* **2004**, *158*, 419–426.

[275] M. Hoffmann, J.-P. Mufusama, C. Kleider, S. Gunesch, B. Rothmund, L. Lehmann, G. Bringmann, M. Decker; (*R*)-Tonkafuranone and related compounds: Improved synthesis, stereochemical purity in nature, and bioactivities of the pure enantiomers; *Flavour Fragr. J.* **2019**, *34*, 329–338.

[276] K. Takahashi, T. Someya, S. Muraki, T. Yoshida; A new keto-alcohol, (−)-mintlactone, (+)-*iso*mintlactone and minor components in peppermint oil; *Agric. Biol. Chem.* **1980**, *44*, 1535–1543.

[277] L. Baiocchi, M. Bonanomi, M. Giannangeli, G. Picconi; Aromatization of aliphatic compounds; IV 1 . On the aromatization of some dihydrobenzofuranones; *Synthesis* **1979**, *1979*, 434–436.

[278] M. Giannangeli, L. Baiocchi; Aromatization of aliphatic compounds: Benzofuranones, indoles and oxindoles; *J. Heterocycl. Chem.* **1982**, *19*, 891–895.

[279] W. K. Goh, D. S. Black, N. Kumar; Synthesis of novel 7-substituted 5,6-dihydroindol-2-ones via a Suzuki–Miyaura cross-coupling strategy; *Tetrahedron Lett.* **2007**, *48*, 9008–9011.

[280] H. Wyss, L. Révész, R. Scheffold; 1,6-Additionen an 3-Methyl-5-methyliden-2-(5 H)-furanon-Derivate; *Helv. Chim. Acta* **1981**, *64*, 2272–2278.

[281] C. Barba, G. Santa-María, M. Herraiz, R. M. Martínez; Direct enantiomeric analysis of Mentha essential oils; *Food Chem.* **2013**, *141*, 542–547.

[282] M. de Lucia, F. Mainieri, L. Verotta, M. Maffei, L. Panzella, O. Crescenzi, A. Napolitano, V. Barone, G. Appendino, M. d'Ischia; Nitration versus nitrosation chemistry of menthofuran: Remarkable fragmentation and dimerization pathways and expeditious entry into dehydromenthofurolactone; *J. Org. Chem.* **2007**, *72*, 10123–10129.

[283] G. Bringmann, S. Tasler, H. Endress, J. Kraus, K. Messer, M. Wohlfarth, W. Lobin; Murrastifoline-F: First total synthesis, atropo-enantiomer resolution, and stereoanalysis of an axially chiral *N*,C-coupled biaryl alkaloid; *J. Am. Chem. Soc.* **2001**, *123*, 2703–2711.

[284] D. M. Schumacher, M. Metzler, L. Lehmann; Mutagenicity of the mycotoxin patulin in cultured Chinese hamster V79 cells, and its modulation by intracellular glutathione; *Arch. Toxicol.* **2005**, *79*, 110–121.

[285] S. Morrison, J. J. Sosnoff, K. S. Heffernan, S. Y. Jae, B. Fernhall; Aging, hypertension and physiological tremor: The contribution of the cardioballistic impulse to tremorgenesis in older adults; *J. Neurol. Sci.* **2013**, *326*, 68–74.

[286] R. Fliege, M. Metzler; Electrophilic properties of patulin. Adduct structures and reaction pathways with 4-bromothiophenol and other model nucleophiles; *Chem. Res. Toxicol.* **2000**, *13*, 363–372.

[287] T. Bruhn, A. Schaumlöffel, Y. Hemberger, G. Bringmann; SpecDis: quantifying the comparison of calculated and experimental electronic circular dichroism spectra; *Chirality* **2013**, *25*, 243–249.

[288] R. Fliege, M. Metzler; The mycotoxin patulin induces intra- and intermolecular protein crosslinks in vitro involving cysteine, lysine, and histidine side chains, and α-amino groups; *Chem.-Biol. Interact.* **1999**, *123*, 85–103.

[289]   H. Glatt, I. Gemperlein, G. Turchi, H. Heinritz, J. Doehmer, F. Oesch; Search for cell culture systems with diverse xenobiotic-metabolizing activities and their use in toxicological studies; *Mol. Toxicol.* **1987-1988**, *1*, 313–334.

[290]   V. Habyalimana, J. K. Mbinze, N. K. Tshilombo, A. Dispas, A. Y. Loconon, P.-Y. Sacré, J. Widart, P. de Tullio, S. Counerotte, J.-L. K. Ntokamunda, E. Ziemons, P. Hubert, R. D. Marini; Analytical tools and strategic approach to detect poor-quality medicines, identify unknown components, and timely alerts for appropriate measures: Case study of antimalarial medicines; *Am. J. Anal. Chem.* **2015**, *6*, 977–994.

[291]   I. Orhan, B. Sener, M. Kaiser, R. Brun, D. Tasdemir; Inhibitory activity of marine sponge-derived natural products against parasitic protozoa; *Mar. Drugs* **2010**, *8*, 47–58.

[292]   J. Li, R. Seupel, T. Bruhn, D. Feineis, M. Kaiser, R. Brun, V. Mudogo, S. Awale, G. Bringmann; Jozilebomines A and B, naphthylisoquinoline dimers from the Congolese liana *Ancistrocladus ileboensis*, with antiausterity activities against the PANC-1 human pancreatic cancer cell line; *J. Nat. Prod.* **2017**, *80*, 2807–2817.

[293]   W. K. Goh, D. S. Black, N. Kumar; Synthesis of novel 7-substituted 5,6-dihydroindol-2-ones via a Suzuki–Miyaura cross-coupling strategy; *Tetrahedron Lett.* **2007**, *48*, 9008–9011.

[294]   A. Scheffler, A. E. Albrecht, H. L. Esch, L. Lehmann; Mutagenic potential of the isoflavone irilone in cultured V79 cells; *Toxicol. Lett.* **2015**, *234*, 81–91.

Acknowledgements

Acknowledgements

I would like herewith to thank everyone who had contributed in a way or another to help having completed the present work.

May Professor G. Bringmann, my main supervisor, find here all my gratitude for his infinite support and mentoring all along my study.

To Professor U. Holzgrabe, my second supervisor, I am grateful for the nice collaboration and for allowing me to carry out parts of the experiments in her research group, taking advantage of her know-how in pharmaceutical analysis.

To Professor K. Ndjoko Ioset, my third supervisor, thank you for being there from the beginning of this journey.

May Dr. D. Feineis receive special thanks for her unlimited support during my doctoral study.

For the financial funding, I would like to thank the German Academic Exchange Service (DAAD) and the *Else Kröner-Fresenius-Stiftung* through the Excellence Scholarship Program BEBUC (www.foerderverein-uni-kinshasa.de).

To the Faculty of Pharmaceutical Sciences at the University of Kinshasa and its academic staff, Professors J. Ndelo, J. Lami, J. Mbinze, P. Kalenda, P. Memvanga, P. Mutwale, P. Tshisekedi, D. Mana, N. Ngombe, T. Kimbeni, J.-M. Liesse, K. Takaisi, K. Mesia, thank you for the encouragements and for allowing me to be on study leave all this time.

I would like to appreciate support and assistance from numerous people, including Dr. A. Zillenbiller, S. Pöhlmann, C. Wolf, Prof. H. Mavoko, Dr. L. Hoellein, Dr. J. Wahl, Dr. M. Zilker, Dr. D. Ilko, Dr. Y. Mwalwisi, Dr. H. Rasheed, Dr. J. Skaf, D. Volpato, M. Volpp, Dr. M. Grüne, P. Altenberger, Dr. M. Büchner, J. Adelmann, M. Michel, A. Sailer, and K. Gottschalk.

The tonkafuranone project would not have been possible without the fruitful collaboration with Prof. M. Decker, Prof. L. Lehmann, Dr. C. Kleider, M. Hoffmann, B. Rothmund, and S. Gunesch and the help of L. Schlund, Y. Lan Pham, and A. Rosa.

For the naphthylisoquinoline project, I am thankful for the nice cooperation with Professors V. Mudogo, M. Kaiser, R. Brun, and S. Awale.

For the wonderful moments spent together, thanks to all people met during my stay in Würzburg, Prof Y. Manzanza, P. Manzanza, S. Busha, V. Fungula, F. Fungula, J. Kaba, G. Bambi, J. Monsenepwo, D. Mumbanika, F. Bangelesa, T. Bishola, Pastor N. Mangani, Pastor Tembo, S. Fami, D. de Souza, T. Yilu, L. Fouefack, M. Vitale, M. Nzambi, and B. Kamneng.

For the nice working atmosphere and collaboration, thanks to former and current members of the research group Bringmann, B. K. Lombe, S. Fayez, W. Shamburger, L. Wittmann, S. Mianda, S. Muyisa, J. Wendrich, Dr. J. Maier, C. Froschgeiser, Prof. D. T. Tshitenge, Dr. C. Schies, Dr. R. Seupel, S. Schmitt, M. Schraut, Dr. J. Li, Dr. T. Bruhn, Dr. A. Gehrold, Dr. F. Witterauf, Dr. C. Steinert, Dr. A. Irmer, and Dr. G. Zhang.

For the encouragement and attention, I would like to thank all my siblings, Dodo, Freddy, Yvette, Maguy, Rita, André, and Léonard; my family-in-law, Henriette, Fortune, Marco, Szvy, Kiese, and Syntiche; my wife, Conchita, and my newly born son, Tröster.